

FUNGICIDE RESISTANCE IN GRAPEVINE POWDERY AND DOWNY MILDEWS:
GEOGRAPHIC DISTRIBUTION, MOLECULAR DETECTION METHODS, AND GENE
EXPRESSION RESPONSES TO SUBLETHAL FUNGICIDE DOSES

By

Nancy Sharma

A DISSERTATION

Submitted to
Michigan State University
in partial fulfillment of the requirements
for the degree of

Plant Pathology- Doctor of Philosophy

2024

ABSTRACT

Grape powdery mildew and downy mildew, caused by *Erysiphe necator* and *Plasmopara viticola*, respectively, are considered as major threats to grape production worldwide. Growers rely heavily on various contact and systemic fungicides. However, repeated fungicide applications have led to widespread fungicide resistance. This dissertation explores the prevalence and geographic distribution of fungicide resistance in *Plasmopara viticola* populations in the eastern United States and Canada. It also focuses on developing rapid detection tools for identifying QoI (Quinone oxide inhibitors) resistance in *E. necator* and CAA (Carboxylic Acid Amides) resistance in *P. viticola* populations. Additionally, this research explores the impact of sublethal doses of powdery mildew-specific fungicides (cyflufenamid, flutianil, metrafenone, and quinoxifen) on *E. necator* conidial germination and assesses associated changes in gene expression.

The G143A mutation in the cytochrome b gene is commonly associated with QoI resistance in *E. necator* populations in the field. A peptide nucleic acid-locked nucleic acid mediated loop-mediated isothermal amplification (PNA-LNA-LAMP) assay was developed to detect the G143A mutation, achieving 100% specificity and sensitivity in distinguishing QoI-sensitive and resistant isolates. The assay demonstrated rapid detection capabilities, completing tests in under 30 minutes. This diagnostic tool is faster and more cost-effective than the TaqMan assay, as it does not require expensive equipment. In the second part, a spore germination assay assessed the effects of sub-lethal doses of specialized fungicides—cyflufenamid, flutianil, metrafenone, quinoxifen, and trifloxystrobin—on *E. necator*. While flutianil, quinoxifen and trifloxystrobin effectively inhibited conidial germination, cyflufenamid and metrafenone showed no inhibitory effects, even at high concentrations (100 ppm). Transcriptomic analyses of

flutianil, quinoxyfen and trifloxystrobin revealed that all of these fungicides induced distinct gene expression profiles in *E. necator*. Flutianil, quinoxyfen, and trifloxystrobin treatments upregulated genes involved in respiration, including pathways of the electron transport chain, glycolysis, and the Krebs cycle. Specific genes such as Cytochrome P450 monooxygenase, Maltose permease MAL31, and NADP-dependent oxidoreductase RED1 were upregulated. Exposure to quinoxyfen resulted in decreased expression of protein kinase genes, indicating disruption in signal transduction. In contrast, flutianil treatment led to increased expression of sugar transporters and chitinase, possibly indicating increased energy requirements and cell wall remodeling. Additionally, overexpression of multidrug transporters (MFS transporters and ABC drug transporters) in quinoxyfen and flutianil treatments indicated an elevated risk of developing fungicide resistance.

The final section addresses fungicide resistance in *P. viticola* populations, with a focus on QoI, CAA, Quinone inside inhibitors (QiIs), and Quinone inside and outside inhibitor, stigmatellin binding mode (QioSI, FRAC 45) fungicides. A total of 658 samples were sequenced of *CesA3* and *Cytb* genes, along with ITS1 region analysis was conducted. Three prevalent clades: *aestivalis*, *vinifera*, and *riparia* were identified. QoI resistance was widespread among *aestivalis* and *vinifera* clades. The G143A mutation was not specific to any particular clade. Mixed-genotype samples were identified in *P. viticola* clades *vinifera* and *riparia* clades from Michigan, New York, and Wisconsin. No mutations associated with QiI and QioSI resistance were detected in the eastern United States and Canada. A TaqMan probe-based assay developed for detecting the G1105S mutation associated with CAA fungicide resistance effectively distinguishing resistant genotypes in both leaf and air samples. These findings are valuable for implementing effective fungicide resistance management strategies in grape cultivation.

Copyright by
NANCY SHARMA
2024

I dedicate this dissertation to the
Gurinder Singh Dhillon, Sharma's and Chahal's of my loving family.

ACKNOWLEDGEMENTS

First and foremost, I would like to express my heartfelt gratitude to my advisor, Dr. Timothy D. Miles, for his invaluable guidance, encouragement, and support throughout this journey. I am deeply appreciative of his trust in me, his mentorship, and his ever readiness to help me reach my career aspirations. I sincerely appreciate the invaluable feedback and support from my committee members, Dr. Mary Hausbeck, Dr. Martin Chilvers and Dr. Rachel Naegele, throughout this journey. Special thanks to Dr. Shinhan Shiu for his invaluable feedback and suggestions in my research. I am thankful to Dr. Kerri Neugebauer especially for hearing me out, when I thought nothing will work. I am also grateful to my lab colleagues and research aides: Dr. Joel Abbey, Dr. Safa Alzohairy, Shay Szymanski, Ross Hatlen, Lexi Heger, Samantha Thompson, Sukhdeep Singh as well as Roger Sysak. I extend my heartfelt thanks to my friends: Sukhdeep Singh, Mohit Mahey, Lovepreet Singh Chahal and Dr. Prabhjot Kaur for their emotional support and science talks. Lastly, I extend my heartfelt thanks to my husband, Dr. Karandeep Singh Chahal, who has been on by my side like a rock in happy and sad/good and bad days (my constant cheerleader and a best friend who can do anything to make me smile!!) and my parents (Rattanjit Kumar, Meenakshi (**THIS IS FOR YOU AMMI AND DADDY!!!**) and Jasdev Singh, Sukhwinder Kaur) and brothers (Mohit Sharma; Jaspreet Singh Chahal) for their emotional support and encouragement, which played a crucial role in the completion of my Ph.D.

TABLE OF CONTENTS

CHAPTER 1: COMPREHENSIVE REVIEW OF FUNGICIDE RESISTANCE IN GRAPES: DOWNY MILDEW, POWDERY MILDEW, BOTRYTIS BUNCH ROT.....	1
LITERATURE CITED.....	36
CHAPTER 2: DEVELOPMENT OF A PNA-LNA-LAMP ASSAY TO DETECT A SNP ASSOCIATED WITH QOI RESISTANCE IN <i>ERYSIPHE NECATOR</i>	51
LITERATURE CITED.....	92
CHAPTER 3: SUB-LETHAL DOSE EXPOSURE OF CYFLUFENAMID, FLUTIANIL, QUINOXYFEN AND METRAFENONE: EFFECTS ON SPORE GERMINATION AND GENE EXPRESSION IN THE GRAPE POWDERY MILDEW PATHOGEN	97
LITERATURE CITED.....	140
CHAPTER 4: PREVALENCE OF MUTATIONS ASSOCIATED WITH QOI, QII, QIOSI AND CAA FUNGICIDE RESISTANCE WITHIN <i>PLASMOPARA VITICOLA</i> IN NORTH AMERICA AND A TOOL TO DETECT CAA RESISTANT ISOLATES	144
LITERATURE CITED.....	185
CONCLUSION AND FUTURE DIRECTIONS.....	191
APPENDIX A: MANAGING GRAPEVINE DOWNY MILDEW	193
APPENDIX B: OTHER PUBLISHED PEER-REVIEWED ARTICLES DURING PH.D. PROGRAM.....	203

CHAPTER 1: COMPREHENSIVE REVIEW OF FUNGICIDE RESISTANCE IN GRAPES: DOWNY MILDEW, POWDERY MILDEW, BOTRYTIS BUNCH ROT

Abstract

Powdery mildew caused by *Erysiphe necator*, downy mildew caused by *Plasmopara viticola*, and botrytis bunch rot caused by *Botrytis cinerea* are among the most devastating diseases affecting grapevines. These pathogens can cause severe damage to both foliage and fruit. Several multi-sites and site-specific fungicides are widely used to manage these diseases effectively. However, the repeated application of single-site fungicides poses a high risk of resistance development in the targeted pathogen populations. A lack of knowledge regarding pathogen biology and fungicide modes of action further exacerbates this risk. This review aims to provide a comprehensive analysis of fungicide resistance in grapevine pathogens, including *E. necator*, *P. viticola* and *B. cinerea*. Additionally, we explore current and emerging diagnostic tools for monitoring resistance and examine technological advancements that could aid in effective fungicide resistance management strategies.

Introduction

Grape (*Vitis* spp.) production ranks second in the fruit production, with a utilized fruit production value exceeding \$ 6.8 billion US, cultivated on over 891,000 bearing acres in the United States (NASS 2023). In the United States, grapes are usually produced as wine grapes, juice grapes, table, and raisin grapes. However, most of this acreage is planted with the grape species *Vitis vinifera*, which is particularly consumed for wine production (Oliver et al. 2024). This cultivar is famous for its great wine qualities, however susceptible to most major diseases of grapes affecting foliage and fruits. Also, unlike other fruit tree crops, it is common in wine industry to consider older grapevines as nonpareil due to their superior wine quality (Riffle et al.

2022). Older grapevines tend to have potential of greater root depths, yield and wine quality due to larger concentration of carbohydrate reserve compared to younger grapevines (Riffle et al. 2022). However, older vineyards cultivations have higher risk of issues including virus infections (Ezzili 1992), and damage from pests (Nicol et al. 1999, Benheim et al. 2012), trunk diseases (Kaplan et al. 2016), and requirement of constant replanting of the dead grapevines. The older vineyard cultivations harbor survival structures for various pathogens, acting as reservoir for diseases, requiring highly effective disease management practices throughout the season.

Canopy management practices also effect disease and pest pressure in vineyards. Trellising and pruning are commonly used to alter the canopy structure of the grapevines to improve the productivity and fruit quality. Vine vigor and canopy size is the primary consideration while selecting the trellis system. Several other site-specific factors such as rootstock, soil-type, growing region and climate that can affect vine vigor are also considered while selecting the trellis system and vineyard design. More vigorous cultivars require a more extensive trellis system than less vigorous cultivar. Some of the commonly used trellis systems include Two-wire vertical trellis, Vertical-shoot-positioned trellis (VSP), Y-trellis, single curtain with vertically divided foliage, vertically divided double curtain, Wye-trellis and Lyre- trellis. These trellis systems can affect the crop architecture and ultimately influence vine microclimate (Cahoon 1991). Hence, the trellis systems that reduces the crop density can play a vital role in the grape disease management by improve canopy air movement, reduced leaf wetness and relative humidity, greater sun exposure, and better spray deposition efficiency (English et al. 1989, 1990, Wright 2001). For instance, a study conducted in Brazil showed that VSP trellis system had reduced disease intensity for grape downy mildew caused by *Plasmopara viticola* and Botrytis bunch rot caused *Botrytis cinerea*, Y-trellis system had higher intensity for both

diseases (de Bem et al. 2015). Therefore, integrated pest management using these cultural practices along with chemical control is practiced in the vineyards to get sustainable disease management.

Due to high susceptibility of *V. vinifera* to major grape diseases including grape powdery mildew, downy mildew and botrytis bunch rot, fungicides applications are required for disease management. The history of fungicides with grapes is tied long back in 1882 in France when Millardet discovered that the grapevines sprayed with mixture of copper sulfate and lime effectively controlled manage grape downy mildew (Morton and Staub 2008). Up until the 1940s, the chemical disease control mainly relied upon the use of inorganic chemicals that were mostly prepared by the users. For example, sulphur was used at high rate (10 to 20 kb a.i/ha) to control powdery mildew on grapes (Morton and Staub 2008). Numerous new fungicide chemistry classes such as Dithiocarbamates (1941-1961), Aromatic hydrocarbons (1944), Phthalimide (1952), Fentin (1954), Antibiotic (1955-1965), Triazine (1955), Benzimidazoles (1964-1970), Phthalonitrile (1964), Morpholine (1965-1969), and Carboxanilide (1966) were introduced from 1940 to 1970 (Horsfall 1975; Morton and Staub 2008). The introduction of dithiocarbamates and phthalimides showed a greater improvement over previously used inorganic fungicides in terms of efficacy, less toxicity and feasibility. This trend reflected in the drastic reduction in the amount of fungicide use rates in the US from 300 million lbs in 1944 to 150 lbs in 1971 (Gianessi and Reigner 2006; Morton and Staub 2008). Then, the era of modern fungicides (since 1970) began with introduction of fungicides such as Benzimidazole, Morpholine, Imidazoles, Pyrimidines, Triazoles, Anilides, Strobilurins, Phenylpyrroles etc. These systemic fungicides had low use rates, broad spectrum activity against several pathogens, systemic activity against post infection, extended spray intervals. Although these qualities are

popular among growers, but systemic fungicides are also prone to misuse such as curative applications, consecutive applications of same fungicide class or low spray coverage, leading to development of fungicide resistance.

Before 1960s, inorganic fungicides were used to control diseases that affected many targets and are often called multi-site inhibitors. This property helped in maintenance of fungicidal efficacy for longer periods even after many years of introduction in the market. However, the fungicide resistance incidence has increased greatly after the introduction of the systemic fungicides as these fungicides mainly targets at single site of the pathogens (Brent and Hollomon 2007; Yin et al. 2023). Fungicide resistance refers to the heritable genetic change in a fungus that leads to reduction in the sensitivity of a fungus to a particular chemical/fungicide (Delp and Dekker 1985). This means that pathogen is able to grow in the presence of the chemical at the concentrations that it would not be normally able to grow. Fungicide resistance is a result of evolutionary changes within pathogen population that occur under fungicide stress selection. These evolutionary shifts can either hinder or benefit the pathogen's ability to survive, grow and reproduce (Yin et al. 2023). The evolutionary beneficial adaptations can lead to increased prevalence of these traits in subsequent generations, ultimately affecting the fungicide efficacy over time.

The threat of development of fungicide resistance is taken as a major consideration while designing fungicide use strategies. Pesticide industries put greater efforts to conduct research on various aspects including mode of action, risk of resistance, monitoring for baseline sensitivity in field settings etc. (Morton and Staub 2008). Fungicide use strategies are made based on the results in order to reduce the risk of resistance build-up or worse, and further loss of efficacy of the complete fungicide class to the pathogen. Often cross-resistance in pathogens has been

reported in various fungicide products from different pesticide manufacturers (Morton and Staub 2008). This has led to collaboration among pesticide manufacturers to form a Fungicide Resistance Action Committee (FRAC). FRAC produces monographs on yearly basis by grouping the market available fungicides based on various resistance aspects. These monographs are published in order to improve the understanding of resistance risk in different fungicide groups and also provides recommendation for preventing, delaying or reducing build-up of fungicide resistance in pathogen populations.

To date, occurrence of fungicide resistance has been attributed to the four main common molecular mechanisms including (1) mutations in the fungicide target can reduce the fungicide's ability to bind to its target protein; (2) upregulation of ATP-binding cassette (ABC) or major facilitator superfamily (MFS) transporters, which drive efflux pumps, also contributes to resistance; (3) overexpression or duplication of the target gene can result in an increased amount of the target protein; (4) epigenetic modifications, including chromatin or histone changes, can modify gene expression, helping pathogen adapt to fungicide stress (Deising et al. 2008; Yin et al. 2023). Additionally, fungicide detoxification or metabolism, and other unknown factors can also help in development of fungicide resistance (Yin et al. 2023).

Vitis vinifera is highly vulnerable to many diseases, therefore fungicide application is estimated to be responsible for around 95% of the harvestable grape yield to maintain acceptable fruit quality market standards (Gianessi and Reigner 2006; Oliver et al. 2024). The effective management of major diseases of grapevines such as grape powdery mildew (caused by *Erysiphe necator* Schwein), downy mildew, botrytis bunch rot and other foliar and fruit fungal diseases requires numerous prophylactic applications of fungicides in most growing regions otherwise serious yield losses may occur (Gadoury et al. 2012). These frequent fungicide applications with

lack of understanding of pathogen biology or fungicide activity by the applicators can lead to enhanced chances of risk of development of fungicide resistance. The objective of this review is to provide the comprehensive understanding of fungicide resistance in major grapevine diseases including powdery mildew, downy mildew and Botrytis bunch rot (Table 1.1). In addition, we summarize the scope of the fungicide resistance monitoring using existing and potential diagnostic tools, and advancement in technology that can potentially help fungicide resistance management.

Grapevine powdery mildew

Grapevine powdery mildew is a widespread and severe disease affecting both cultivated and wild grapevines globally, resulting in significant yield losses (Gadoury et al. 2012). The disease is caused by an obligate biotrophic fungus *Erysiphe necator* Schwein (formerly *Uncinula necator* Schwein., anamorph *Oidium tuckeri* Berk.). Typical symptoms of powdery mildew appear as white, circular patches on the plant's surface, which later develop a characteristic powdery texture. This pathogen can infect all green plant tissues, including leaves, shoots, flowers, and grape clusters (Fig. 1.1). However, the most economical damage happens when infections occur in the flowers and berries (Calonnec et al. 2004; Gadoury et al. 2012). Early and severe infections can lead to flower drop, reducing the number of berries per cluster. Additionally, infected berries often stop growing, causing them to split and become more susceptible to other pathogens. Beyond direct damage to the fruit, the infection also interferes with photosynthesis, lowering sugar and anthocyanin levels in the grapes, reducing juice color, and increasing acidity and levels of phenylacetic and acetic acids. This combination of factors results in lower-quality wine, with diminished taste and appearance (Calonnec et al. 2004; Gadoury et al. 2001; Stummer et al. 2003; Rantsiou et al. 2020).

Management of grapevine powdery mildew is difficult due to the fact that majority of the cultivated grapevines belong to *V. vinifera* which has no resistance to *E. necator*. Although some non-vinifera or transgenic vine options are available for growers but market preference for conventional *V. vinifera* varieties does not make sense for growers to adopt them (Fuller et al. 2014). The situation gets more complicated as *E. necator* can reproduce sexually, and this disease is polycyclic, have a shorter disease cycle, wind-dispersion of spores making it more difficult to control if not managed timely. The only effective option for powdery mildew control is intensive fungicide applications in preventive manner, even then sometimes poor disease control has been observed due to improper alignment of timing between fungicide application and fruit susceptibility (Ficke et al. 2002). Furthermore, frequent, and widespread use of fungicides increases the risk of resistance emerging in *E. necator* populations. The cost of managing grapevine powdery mildew can reach as much as 37% of the gross production value in areas where the disease poses a significant threat (Fuller et al. 2014). Following paragraphs provides brief description about the most important fungicide classes used for grape powdery mildew and their fungicide resistance status.

Sulphur

Sulfur is the most widely used pesticide in viticulture, applied across conventional, organic, and biodynamic farming practices (Neill et al. 2015). This inorganic fungicide has a multisite mode of action, therefore, have a very low risk of development of resistance. In organic farming practices, sulphur is the only choice for managing grape powdery mildew (Neill et al. 2015). In conventional farming setup, sulphur is either used as alone treatment or in a tank mixing with other active ingredients, mostly single-site. The process of tank mixing sulphur with other fungicides helps as management strategy for reducing the risk of resistance in single-site

fungicides. However, sulphur is a protectant fungicide and may require high application rate and weekly application intervals. Excessive sulphur applications can have several negative impacts including the large amount of water needed for application, increased insect and mite problems, association with hydrogen sulfide formation during fermentation or wine aging, phytotoxicity risk of grapevines at higher temperatures (Neill et al. 2015; Thomas et al. 1993; Walton et al. 2007; Warneke et al. 2022).

Demethylation inhibitors

Demethylation inhibitors (DMIs) also known as sterol biosynthesis inhibitors are considered as one of the most successful fungicide classes for grape powdery mildew. DMIs target cytochrome P450 C14 α -demethylase (CYP51) in the ergosterol production pathway and are classified under FRAC group 3. The DMIs were introduced in the 1970s and currently seven different DMI fungicides are widely used in viticulture (FRAC 2024). DMI fungicides significantly compromise membrane integrity and function causing disruption in fungal growth (Jones et al. 2014). DMI fungicides binds to the heme iron of CYP51 via a nitrogen atom, blocking oxygen from binding and transferring to lanosterol's C14-methyl group. This process stops lanosterol C-14 demethylation process (Ziogas and Malandrakis 2015). Although DMI fungicides have site-specific mechanism, but DMI fungicide resistance tends to be quantitative and is likely controlled by multiple genes. Consequently, these fungicides have generally maintained their effectiveness even after being used in the market for years (Ziogas and Malandrakis 2015). However, reports of shift in sensitivity to DMIs due to its repeated and extensive usage has been observed in various countries including Australia, Chile, Europe, India, South Africa, and United States (Deyle et al. 1997; Hall et al. 2016; Halleen et al. 2000; Frenkel et al. 2015; Gubler et al. 1996).

Resistance mechanisms to DMIs include point mutations in the CYP51 gene, overexpression of efflux pumps and/or overexpression of CYP51 gene, and copy-number variations of CYP51 gene (Ziogas and Malandrakis 2015). The presence of A495T mutation at CYP51 gene resulting in the Y136F amino acid substitution conferring DMI resistance in *E. necator* was first reported in 1997 (Deyle et al. 1997). Additionally, another mutation, A1119C has been associated with CYP51 overexpression and azole resistance in *E. necator*. Although this mutation does not change amino acid sequence, but it could possibly influence mRNA stability or be linked to another, unknown mutation in the promoter region that causes overexpression (Deyle et al. 1997; Kunova et al. 2021). Moreover, a combination of the Y136F mutation and CYP51 copy-number variation has been linked to DMI resistance in *E. necator*, suggesting that having extra copies of a fungicide-tolerant allele confers an advantage in resistance development (Jones et al. 2014; Kunova et al. 2021). Interestingly polygenic nature of DMI resistance has been controversial (Dyer et al. 2000; Kunova et al. 2021; Peever et al. 1992). In other pathogens, it has been hypothesized that in addition to a major resistance gene, other genetic factors may play a role in increased resistance but only when the primary resistance gene is already present (Dyer et al. 2000; Kunova et al. 2021). More detailed research is needed to better understand these interactions and fill existing knowledge gaps for *E. necator*.

Quinone outside inhibitors (QoIs, FRAC 11)

Quinone outside inhibitors (QoI, FRAC 11) also commonly known as strobilurins are one of the most commonly used fungicides for management of grape powdery mildew. These fungicides were originally derived from natural compounds like strobilurin A and oudemansin A (Hirooka et al. 2013; Jeschke et al. 2019; Kunova et al. 2021). These compounds are produced by certain basidiomycetes and were optimized to improve light stability and reduce toxicity to

mammals (Kunova et al. 2021). Azoxystrobin and kresoxim-methyl were the first QoI products introduced in the market in 1996 (FRAC 2024). Currently, 18 different products are registered in different crops (FRAC 2024).

QoIs operate by targeting mitochondrial respiration in a broad range of fungi, including Ascomycetes, Basidiomycetes, Deuteromycetes, and Oomycetes. The QoI fungicides specifically bind to the quinol oxidation site (Qo site) of cytochrome b in the inner mitochondrial membrane. This blocks electron transfer to cytochrome c1 and ultimately stops the production of adenosine-5'-triphosphate (ATP) (Balba 2007). As a result, these fungicides are particularly effective in plant pathogens by disturbing energy-dependent processes like spore germination and zoospore mobility (Barlett et al. 2002; Miles et al. 2012).

Unfortunately, the first instance of reduced field sensitivity to azoxystrobin in populations of *Mycosphaerella fijiensis* was reported in a year after the market launch of QoI fungicides (Sierotzki et al. 2000). Five years after launch, QoI resistance was reported in *E. necator* in the United States (Baudoin et al. 2008; Wilcox et al. 2003). Later, repetitive applications, extensive use and single-site mode of action of the QoI fungicides led to rapid emergence of resistance in various pathogens (Kunova et al. 2021; Miles et al. 2012; Sharma et al. 2023). The G143A mutation conferring to an amino acid substitution from glycine to alanine in the cytochrome b (CYTB) gene is the most common cause of resistance in pathogens including *E. necator* (Corio-Costet 2015; Gisi et al. 2002; Grasso et al. 2006; Kim et al. 2003). This mutation can cause a significant resistance factor (RF) greater than 1000 (Rallo et al. 2014). Overall, at least 11 point mutations in the CYTB gene have been associated with resistance to QoI fungicides in various pathogens, but in plant-pathogenic fungi, the G143A, F129L, and G137R mutations, along with activation of the alternative oxidation (AOX) pathway, are the

primary mechanisms of resistance (Miles et al. 2012; Rallo et al. 2014). In the United States, *E. necator* resistance has been reported in states of the eastern United States (Baudoin et al. 2008; Miles et al. 2021). Resistance to QoI fungicides has now become widespread across grape growing region in various countries, including the U.S., Europe, and Australia (Baudoin et al. 2008; Dufour et al. 2011; Miles et al. 2012; Wick et al. 2013).

Cyflufenamid (FRAC U06)

Cyflufenamid is a newer benzamidoxime fungicide and was approved for use in Japan and EU in 2002 and 2005, respectively (Kunova et al. 2021). Later, it was registered for management of powdery mildew in the United States in 2012. It has proven to be highly effective both as a preventive and curative treatment against powdery mildew on cereals, specialty crops, cucurbit crops, cherries, hops as well as brown rot on stone fruits (Dietz and Winter 2019; Sano et al. 2007). Cyflufenamid is also known for its ability to move in the vapor phase and penetrate plant tissue with translaminar activity (Dietz et al. 2019).

While its specific biochemical mode of action has yet to be identified, it is currently classified under FRAC U06 (FRAC 2024a). Haramoto et al. 2006 found that cyflufenamid does not prevent spore germination or appressorium development in *Blumeria graminis* f. sp. *tritici* but instead strongly inhibits the formation of haustoria, thereby stopping the further growth of the fungus. a few years after market launch, resistance to this fungicide was reported in cucurbit powdery mildew in Japan in 2006 (Frac 2024b). Later resistance was reported to *Podosphora xanthii* in Italy in 2014 and the United States in 2018 (Pirondi et al. 2014; McGrath and Sexton 2018). However, to date, no resistance has been detected in grapevine powdery mildew.

Cyflufenamid is currently considered as a vital tool for powdery mildew management along with resistant management programs in grapes.

Azanaphthalenes (FRAC 13)

Azanaphthalenes are a group of fungicides with activity restricted to fungi from the *Erysiphaceae* family. Two active compounds, proquinazid and quinoxifen are approved for powdery mildew management (FRAC, 2024). While quinoxifen was withdrawn from the European Union (EU) market in March 2020, proquinazid remains authorized for use (Kunova et al., 2021). However, quinoxifen is still used in the United States. Although the precise mechanism of action remains unclear, azanaphthalenes are known to disrupt signal transduction and serine esterase functions (Wheeler et al., 2003; Lee et al., 2008). These fungicides are mainly considered protectants and have a localized systemic activity along with redistribution through vapor. These fungicides are known for their ability to stop early development of powdery mildew by halting spore germination and appressorium formation. Moreover, it has been observed that proquinazid can express defense-related genes in *Arabidopsis thaliana* by activating pathways related to ethylene signaling, phytoalexin production, reactive oxygen species (ROS) generation, and pathogenesis-related genes.

The *Erysiphe necator* isolates with EC50 values over 100 mg/L had been identified showing greater resistance to quinoxifen in Europe (Genet and Jaworska 2009). Moreover, potential cross-resistance between resistance to quinoxifen and proquinazid has also been identified across Europe (FRAC 2024). In field trials conducted in western New York during 2010 and 2011, a reduced efficacy of quinoxifen in controlling *E. necator* was associated with suspected resistance to quinoxifen (Wilcox and Riegel 2012a, 2012b, 2012c). Furthermore, Feng et al. (2018) found high quinoxifen resistance in *E. necator* field isolates in leaf disc assays, but despite this, quinoxifen remained highly effective in three-year field trials conducted in Virginia.

Aryl-phenyl ketones (FRAC 50)

Aryl-phenyl ketones (FRAC 50) are relatively newer category of fungicides, mainly used to control powdery mildew. This fungicide class includes two main fungicides: metrafenone, which was first registered in the EU in 2007, and pyriofenone was registered in 2014 (Kunova et al. 2021). The exact mechanism of this fungicide class is not entirely understood. However, studies on cereal powdery mildews suggest these fungicides may disrupt the actin cytoskeleton and affect hyphal morphogenesis, polarized growth, and cell polarity (Opalski 2005; Schmitt et al. 2006; Kunova et al. 2021). Resistance to these fungicides began emerging shortly after their introduction. Resistance has been reported in *B. graminis* f. sp. *tritici* to metrafenone in 2010, in *E. necator* to metrafenone in 2016 and in *P. xanthii* to *Pyriofenone* in 2020 (Felsenstein et al. 2010; Kunova et al. 2016; Miyamoto et al. 2020). In *E. necator*, both moderate and high levels of resistance have been detected. Isolates with high resistance to metrafenone can grow and produce spores even at 1250 mg/L (Kunova et al. 2016). Cross resistance has been observed to pyriofenone in various European countries, though their prevalence and distribution can vary (Graft 2017).

Cyano-methylene thiazolidine (FRAC U13)

Flutianil, another newer fungicide used to control powdery mildew is the only fungicide classified in this group. This fungicide was first launched in the market in 2013. In *P. xanthii*, this fungicide has proven to be highly effective with strong residual and translaminar activity, as well as resistance to being washed away by rain (Kimura et al. 2020). Additionally, it demonstrates curative effects to manage *P. xanthii* on *cucumbers*, even at the remarkably low concentration of 10 mg/L (Kimura et al. 2020). The exact mode of action of this fungicide is still unknown, however, morphological experiments conducted on *B. graminis* f. sp. *hordei*, revealed that Flutianil do not interfere with the initial infection stages such as conidial bursting, primary

or appressorial germination, appressorium formation, or hook development (Kimura et al. 2020). It seems that Flutianil effectively blocks the formation of haustoria and inhibits subsequent fungal progression (Kimura et al. 2020). Additionally, flutianil also disrupts nutrient absorption through haustoria and preventing further elongation of the secondary hyphae (Kimura et al. 2020). Furthermore, it was found that flutianil affects the extra-haustorial matrix and the fungal cell wall by making them less distinct (Kimura et al. 2021). Interestingly, this fungicide does not significantly impact the genes critical for the survival of *B. graminis* (Kimura et al. 2021). However, it alters the expression of specific genes, including multiple effector genes and three sugar transporter genes, most of which are predominantly active within haustoria (Kimura et al. 2021). The resistance to Flutianil has been reported in field isolates of *P. xanthii* in cucumbers in Japan in 2020 (Miyamoto et al. 2020). No report of resistance to *E. necator* has been found yet. This fungicide plays a very critical role in resistance management strategies for grape powdery mildew. Therefore, flutianil should be used critically to reduce the chances of fungicide resistance in *E. necator*.

Grapevine downy mildew

Grape downy mildew, caused by an oomycete *Plasmopara viticola*, is a highly destructive and widespread disease. This disease commonly occurs in viticultural areas with relatively humid areas where summer and spring rainfall occurs at temperatures >10°C (Ash 2000). Downy mildew is a one of major diseases of grapes in the eastern United States and Canada due to suitable weather conditions and *V. vinifera* based viticulture cultivation (Sharma et al. 2022). This obligate pathogen can affect all green grapevine tissues. Initial foliar symptoms are characterized by circular, oily-looking green to yellow spots. Under favorable conditions, these spots can multiply and merge, resulting in larger leaf areas covered under spots. White,

fuzzy sporangia may also form on the underside of infected leaves or other plant parts (Fig. 1.1). As the disease advances, the affected areas turn brown as the tissue dies. In cases of severe infection, premature leaf drop may occur. Infected flower clusters can dry out entirely and get colonized with white sporangia. Young, infected clusters get dull green or reddish-brown colored and eventually, these clusters also get colonized with white sporangia (Sharma et al. 2023).

Managing grape downy mildew is as challenging as controlling grapevine powdery mildew, primarily because most cultivated grapevine varieties, *V. vinifera*, also lack resistance to *P. viticola*. This pathogen is a season-long issue for viticulture in the eastern North America, and that makes it even more challenging. This is a polycyclic disease and can turn into epidemic rapidly under optimal environmental conditions (Hu and Fiola 2023). The highly effective cycle of asexual reproduction by sporangia drives the rapid spread of *P. viticola* (Islam et al. 2011). In general, 7 to 8 fungicide applications are usually applied in warm and humid conditions to avoid losses due to downy mildew infestation (Hu and Fiola 2023). The most common site-specific fungicides used to manage grape downy mildew and associated fungicide resistance are briefly discussed below.

QoI fungicides (FRAC 11)

The mode of action of QoI fungicides have been discussed in detail in grape powdery mildew section. Famoxadone and Fenamidone are the two main active ingredients of QoI fungicides that are effective in managing grape downy mildew. However, repetitive and prophylactic applications of these fungicides have led to resistance in *P. viticola*, as well. The resistance mechanism to QoI fungicides is similar to *E. necator* and higher level of resistance mainly occurs due to G143A amino acid change in cyt b gene (Chen et al. 2007; Gisi et al. 2002). Furthermore, another SNP resulting in a phenylalanine to leucine substitution (F129L) at

codon 129 has been found in *P. viticola* field populations in France, though its occurrence is rare, with a frequency of less than 2% (Sierotzki et al. 2005). The emergence of QoI resistance in *P. viticola* in various European countries since 2000 (Baudoin et al. 2008; Gisi et al. 2002). The first confirmation of QoI resistance in the United States was first detected in Virginia and North Carolina in 2008 (Baudoin et al. 2008). Since then, widespread QoI resistance in *P. viticola* populations has been reported in many states of the eastern United States and Canada (Sharma et al. 2024). Moreover, QoI resistance in *P. viticola* populations has spread to various grape growing countries including Japan, Brazil, India, China and several European countries (Baudoin et al. 2008; Gisi et al. 2002; Sierotzki et al. 2005; Colcol 2008; Toffolatti et al. 2007). Similar to *E. necator* and *P. viticola*, QoI resistance has also been reported in *B. cinerea* in grapes. Due to this widespread spread QoI resistance worldwide, it is important to use this fungicide efficiently by applying resistant management strategies and avoid control failures in the field conditions.

Carboxylic acid amides (FRAC 40)

Carboxylic acid amides are one of the most extensively used to manage grape downy mildew worldwide (Gisi and Sierotzki 2015). Dimethomorph, a CAA fungicide has been utilized to control grapes and cucurbit downy mildew since the late 1980s. Currently, mandipropamid and dimethomorph are two active ingredients of Carboxylic acid amides (CAAs) fungicides that effectively control *P. viticola*. The molecular mechanism of CAA fungicides is inhibiting cell wall biosynthesis by targeting cellulose synthase 3 (CesA3) gene (Gisi et al. 2007; Blum et al. 2010). These fungicides are classified as low to medium risk for resistance (FRAC 2024). Fungicide resistance to dimethomorph in *P. viticola* was first noticed in France in 1994 but did not affect field efficacy at that time (Sierotzki et al. 2011).

Resistance to CAA fungicides in *P. viticola* has been traced to a single nucleotide polymorphism (SNP) that leads to an amino acid change at codon 1105 from glycine to serine, and less frequently to valine, in the PvCesA3 gene (Blum et al. 2010). Interestingly, CAA fungicide resistance in *P. viticola* is controlled by recessive nuclear gene, meaning both alleles are required to possess resistant phenotype (Blum et al. 2010). Resistance to CAA fungicides in *P. viticola* populations have been reported in various grape-growing regions, including Europe, India, Japan, China, Brazil, as well as Virginia and North Carolina in the United States (Aoki et al., 2013; Blum et al., 2010; Feng and Baudoin, 2018; Santos et al., 2020; Sawant et al., 2017; Zhang et al., 2017). In a recent survey conducted in the eastern United States and Canada, first occurrence of CAA fungicide resistance in the Michigan, Georgia, New York, Wisconsin and Ontario has been reported (Sharma et al. 2024). Likewise, CAA fungicide resistance has been also identified in other oomycetes, such as *Phytophthora capsici*, *P. infestans*, and *Pseudoperonospora cubensis* (Blum et al., 2012). Increased CAA fungicide resistance in *P. viticola* is an alarming situation and therefore recommended resistance management strategies for CAA fungicides should be practiced to avoid loss of efficacy of this important fungicide class (Sharm et al. 2022).

Quinone inside inhibitors (FRAC 21)

Cyazofamid is an active ingredient in Quinone inside inhibitors (QiIs) that has an activity against *P. viticola* in grapes. The molecular mechanism of this fungicide class is inhibiting mitochondrial respirations of the pathogen. QiI fungicides binds to cytochrome bc1 at Quinone inside (Qi) site and disrupt complex III (Cherad 2023; Sharma et al. 2024). In general, QiI fungicides stops the quinol reduction in the QiI site (Cherrad et al. 2023). Fungicides in FRAC group 21 are regarded as having a moderate to high risk for developing resistance (FRAC 2024).

This elevated risk means that pathogens can more easily adapt to these fungicides over time, reducing their long-term effectiveness. Reports of resistance to QiI fungicides are rare but have been linked to specific mutations in the Cyt b gene (Cherrad et al. 2018; Cherrad et al. 2023). This involves an amino acid shift from leucine to serine at codon 201. Another change, two insertions of two amino acids occurs between codons 203 and 204 (E203-DE-V204, or E203-VE-V204) in the Qi site has also been associated with QiI fungicide resistance in *P. viticola* (Cherrad et al. 2018; Cherrad et al. 2023). The reports of QiI resistance have only been observed in France in 2018 so far, however, no QiI fungicide resistance was found in a recent survey conducted in the eastern United States and Canada (Cherrad et al. 2018; Cherrad et al. 2023; Sharma et al. 2024). For grape powdery mildew management, QiI fungicides act as a promising option.

Quinone inside outside inhibitor (FRAC 45)

Ametoctracadin, an active ingredient classified under Quinone inside outside inhibitor (QioSI) is an effective fungicide that used to control *P. viticola* populations in field. The mode of action of this fungicide also involves targeting both the Qi and Qo sites of complex III, interacting through a stigmatellin-like binding mechanism to disrupt mitochondrial respiration (Cherrad 2023). Due to its site-specific activity of the fungicides, FRAC has considered FRAC 45 fungicides as medium to high risk in chances of resistance development in pathogens. Few reports of QioSI fungicide resistance have been observed in France in 2018 and India in 2023 (Cherrad et al. 2018; Cherrad et al. 2023; Fontaine et al. 2019; Sagar et al. 2023). Resistance to QioSI fungicides has been attributed to an amino acid shift at codon 35 from serine to leucine (S34L) at Cyt b gene. So far, this QioSI fungicide resistance is not widespread and has not been detected in the eastern United States and Canada (Sharma et al. 2024). However, there are high

chances of resistance development in this fungicide class, therefore continuous monitoring is important to increase the longevity of fungicide efficacy in fields.

Phenylamides (FRAC 4)

Phenylamides (PAs) are among the earliest classes of fungicides designed to target oomycete pathogens, with many fungicides introduced since 1977 (Gisi et al. 2015). These fungicides provide long-lasting preventive effects, systemic movement within plants and curative effects against pathogens (Gisi et al. 2015). Since 1970, metalaxyl and metalaxyl-M (mefenoxam) are the active ingredients that are used against *P. viticola* in grape downy management worldwide (Hermann et al. 2019; Wicks et al. 2005). The mode of action of metalaxyl-M is to inhibit ribosomal RNA polymerase in *P. viticola* (FRAC 2024). First metalaxyl fungicide resistance in *P. viticola* was reported in France in 1981 (Clerjeau and Simone 1982). Later in 2004, widespread metalaxyl resistance was observed in 92% of 813 vineyard samples collected in South Africa (Fourie 2004). The metalaxyl fungicides resistance has now been reported in Australia, France, Italy, India, China and Japan (Corio-costet 2015; Ghule et al. 2020; Wick et al. 2005; Sun et al. 2010). Interestingly, the exact resistance mechanism to this fungicide group is still unknown.

Botrytis bunch rot

Botrytis bunch rot, which is caused by the fungus *Botrytis cinerea* Pers. represents a significant disease threat to grapevines in temperate climates and leads to major economic losses around the world (Ficke et al. 2002; Hartman and Kaiser 2008). The pathogen initially infects blossoms during bloom but stays dormant, likely lingering in the fruit receptacles, until the berries ripening stage (Gindro et al. 2005; Holz et al. 2003; McClellan and Hewitt 1973; Viret et al. 2004). As the fruit matures, *B. cinerea* can invade through damaged or cracked areas and

infect berries. Later berries rot severely and get colonized with conidial masses (Fig. 1.2). Conidia are dispersed by wind and leads to new infections (Hartman and Kaiser 2008; Holz et al. 2003; McClellan and Hewitt 1973; Puhl and Treutter 2008; Weber and Hahn 2011). Managing Botrytis bunch rot requires integrated pest management strategies involving cultural practices. The most important cultural control practices involve managing grapevine canopy in a manner to improve maximum air flow. However, when warm (15 to 20 C) and wet (>90% humidity) weather conditions are available, management relies on chemical control.

Various site-specific synthetic fungicides with distinct mechanisms of action are employed to manage *B. cinerea* on grapes (Leroux et al. 2002b; Saito et al. 2019). Some of important fungicide classes labelled for managing Botrytis bunch rot in grapes include benzimidazoles (FRAC 1), dicarboximides (FRAC 2), succinate dehydrogenase inhibitors (SDHIs; FRAC 7), anilinopyrimidines (FRAC 9), QoIs (FRAC 11), phenylpyrroles (FRAC 12), and hydroxyanilides (FRAC 17). In *B. cinerea*, fungicide resistance has been reported in most of these important fungicide classes and are discussed briefly in the below paragraphs.

Benzimidazoles (FRAC 1)

Methyl benzimidazole carbamates (MBCs) fungicides were first launched in the late 1960s and are effective against various plant pathogens including *B. cinerea*. The mode of action of benzimidazole fungicide by binding to β -tubulin that causes protein to unfold locally and inhibits polymerization of microtubules (Leroux et al. 1999). This leads to disruption in germ-tube elongation and mycelial growth. Resistance to benzimidazoles has been attributed to multiple point mutations in the β -tubulin gene BctubA in *B. cinerea* field populations. Three amino acid changes including substitution of glutamic acid with alanine (E198A), valine (E198V), or lysine (E198K) at codon 198, and another amino acid substitution from

phenylalanine is replaced by tyrosine at codon 200 are considered responsible for development of MBC fungicide resistance (Banno et al. 2008; Yarden and Katan 1993). The MBC fungicide resistance has been already detected in *B. cinerea* in greenhouse vegetables, grapes, strawberries and blueberries. Moreover, resistance to Thiabendazole (FRAC 1) has also been reported in *B. cinerea* in grapes in the United States (Alzohairy et al. 2021).

Dicarboximides (FRAC 2)

Iprodione is the active ingredient that is commonly used to control gray mold in various fruits and vegetable crops. The exact mode of action of dicarboximides is unclear, however, research studies indicate that dicarboximide fungicides primarily act by disrupting the phosphorylation of the high osmolarity glycerol 1 (Hog1) mitogen-activated protein kinase (MAPK), which is regulated by group III HisK and its associated downstream kinases (Fillinger et al. 2012). Resistance to Frac 2 in *B. cinerea* has been attributed to point mutations in Bos1, with substitutions at codon I365 (I365S, I365N, or I365R) being the most common mutations (Oshima et al. 2006). Additionally, the Q369P mutation along with the N373S mutation was also observed in *B. cinerea* isolates with moderate resistance to procymidone, another active ingredient in FRAC 2 fungicide class (Adnan et al. 2018).

Succinate dehydrogenase inhibitors (FRAC 7)

Boscalid is the main active ingredient of Succinate dehydrogenase inhibitors (SDHIs) fungicides that is used to manage *B. cinerea* populations. This fungicide class is known to block the activity of the succinate dehydrogenase (SDH) enzyme and in consequence, mitochondrial respiration stops (Kim and Xiao 2011). Overall, SDHI fungicides are effective against plant pathogens by preventing germination of spores and development of germ tubes (Leroux et al. 2010). The SDHI fungicide resistance in *B. cinerea* has been reported on several fruit crops

including strawberry, kiwifruit, apple and grapes (Bardas et al. 2010; Kim and Xiao 2010; Leroch et al. 2011). Moreover, this fungicide class is also effective on control powdery mildew in grapes, however, SDHI resistance has also been found in *E. necator* populations (Alzohairy et al. 2021). Mutations occurring in the Sdh subunits SdhB, SdhC and SdhD are known to cause resistance in SDHI fungicides. The SDHI fungicide resistance is primarily associated with SNPs occurring at codon 225, 230 or 272 at SdhB subunit, leading to P225L/F/T, N230I, or H272L/R/Y amino acid shifts (Leroux et al. 2010). Lalève et al. 2014 found that P225F/L and H272L substitutions are linked with the highest levels of boscalid fungicide resistance. Different H272 mutations in the SdhB subunit affects SDHI sensitivity of different active ingredients in distinct ways. For instance, the H272L amino acid substitution causes reduced sensitivity to all SDHI fungicides, while the H272Y amino acid substitution causes hypersensitivity to fluopyram (Lalève et al. 2014). Boscalid fungicides are registered for gray mold control by more than 70 pesticide companies and therefore, are used extensively in many crops (Shao et al. 2020). It is very important that growers should consider resistance management strategies for reducing the risk of SDHI resistance (FRAC 2024). Moreover, careful examination of the pesticide labels before designing the spray program for the season is a must.

Anilinopyrimidines (FRAC 9), phenylpyrroles (FRAC 12), and keto reductase inhibitors (FRAC 17)

These three fungicide classes are actively used to manage gray mold in several crops including grapes. The most used active ingredients of FRAC 9, 12 and 17 that has inhibitory activities against *B. cinerea* include cyprodinil, fludioxonil and fenhexamid, respectively. AP fungicide class (FRAC 9) function by preventing methionine biosynthesis and suppressing the release of cell wall-degrading enzymes that are essential for the infection process of *B. cinerea*.

On other hand, Fludioxonil (PP fungicide, FRAC 12) is known to target Bos1- and MAPK-dependent osmoregulation pathway causing hyperosmolarity, which results in glycerol accumulation and prevents fungal growth (Kojima et al. 2004; Vignutelli et al. 2002). The fenhexamid (FRAC 17) fungicide acts by preventing sterol biosynthesis, especially ergosterol, which is an important component for integrity of fungal membrane. Interestingly, fungicide resistance in FRAC 9,12 and 17 has been already reported in *B. cinerea* isolates in several crops including grapes (Alzohairy et al. 2021). Fungicide resistance mechanism in AP fungicides (FRAC 9) is not clearly understood. Mutations in nine distinct genes in *B. cinerea* isolates has been linked to AP fungicide resistance. All of these identified genes are required in mitochondrial metabolism (Mosbach et al. 2017). In case of fludioxonil (PP fungicide, FRAC 12), several point mutations in Bos1 including I365N, S426P, G538R, A1259T, R319K, V336M, D337N, V346I, A350S, G311R, G265D, N609T, G545E, I365S, T1267A, S531G, T565N, F127S, R319K, V336M, D337N, V346I, A350S, Q369P, and G262S+Q369P+N373S has been reported causing resistance in field isolates (Sang et al. 2018). It was found these mutations in Bos1 decreased fludioxonil's binding affinity to BcOS1. Similarly, varying level of fenhexamid resistance (FRAC 17) in *B. cinerea* have been associated with several point mutations in the *erg27* genes (Albertini and Leroux 2004; Esterio et al. 2011; Fillinger et al. 2008; Grabke et al. 2013; Leroux et al. 2002a). The HydR3+ *B. cinerea* isolates exhibiting a high to moderate resistance to fenhexamid have shown amino acid changes at codons 63 (T63I), 412 (F412S/I/V/C), and 496 (T496R) (Albertini and Leroux 2004; Fillinger et al. 2008; Grabke et al. 2013). In contrast, HydR3– isolates displays weak to moderate resistance, showing F26S, L195F, V309M, A314V, S336C, N369D, L400F, L400S, P238S, I199L, and Y408S amino acid substitution, as well as a deletion at P298 (Esterio et al. 2011; Fillinger et al. 2008).

Multiple resistance in B. cinerea

Multiple resistance in pathogens is a serious concern and refers to when a pathogen population has loss/reduced sensitivity to multiple fungicides belonging to chemical classes with different mode of action. Interestingly, multiple resistance to several fungicide classes have been observed in field isolates in *B. cinerea* populations in various fruit crops such as strawberries, blueberries, mandarins and grapes (Amiri et al. 2013; Alzohairy et al. 2021; Chen et al. 2016; Fernández-Ortuño et al. 2015; Saito et al. 2016, 2019; Saito and Xiao 2018). Multiple fungicide resistance has also been identified in *B. cinerea* populations in vineyards across China, Germany, Italy and United States (Leroch et al. 2011; Rupp et al. 2017; De Miccolis Angelini et al. 2014; Panebianco et al. 2015). In table grapes, multiple fungicide resistance to cyprodinil, fenhexamid, boscalid and pyraclostrobin has been detected in *B. cinerea* in California (Saito and Xiao 2018). Isolates with multiple fungicide resistance to boscalid, pyraclostrobin, thiabendazole, fenhexamid, cyprodinil, and iprodione were found as most predominant multiple fungicide resistance phenotype in Michigan. It was also found that frequency of multiple resistance in *B. cinerea* isolates increased over years in Michigan vineyards indicating the practice of repetitive use and higher number of applications of same fungicides (Alzohairy et al. 2021). Sequencing of target genes associated with fungicides has demonstrated that multiple fungicide resistance in *B. cinerea* arises due to the buildup of mutations in the respective fungicide target genes (Adnan et al. 2018; Shao et al. 2021; Yin et al. 2015). This situation seems alarming; therefore, growers need to be precautionous especially using fungicides with high level of resistance. Moreover, growers should provide special care while choosing premixture fungicides with two modes of action based on the presence of multiple fungicide resistance populations in their vineyards.

Multi-drug resistance in B. cinerea populations

Multi-drug resistance (MDR) is another mechanism than target site modifications that can cause resistance to structurally unrelated fungicides. In most of the cases, overexpression of efflux transporters present in the plasma membrane can drive MDR in plant pathogens. The ABC transporters (ATP-binding Cassette superfamily) and MFS transporters (Major Facilitator Superfamily) are the primary families of efflux transporters that have been linked to MDR mechanism in fungi including *B. cinerea*. Interestingly, MDR has been detected in *B. cinerea* isolates in the French vineyards in the mid-1990s (Shao et al. 2021). Four distinct MDR strains including MDR1, MDR1h, MDR2 and MDR3 have been identified in *B. cinerea* isolates. These strains differ in their range and degree of fungicide resistance and are associated with the overexpression of drug efflux transporters encoded by the *atrB* and *mfsM2* genes (Kretschmer et al., 2009; Mernke et al., 2011; Leroch et al., 2013). The MDR1 phenotype possess point mutations along with 3-bp deletion at position 497 in the gene coding for the transcriptional regulator *Mrr1*, leading to over expression of *AtrB* gene (Leroch et al. 2013). However, the MDR2 phenotypes are known to have rearrangements in the *MfsM2* promoter, causing continuous *MfsM2* expression. The MDR1 phenotype that contain both genetic alterations due to the natural hybridization of MDR1 and MDR2, displaying highest level and broad spectrum MDR (Kretschmer et al. 2009; Hanh 2014; Shao et al. 2021). Managing MDR is challenging with conventional resistance management strategies, such as alternating fungicides or using mixtures. Therefore, constant monitoring to understand the composition of *B. cinerea* populations regarding MDR frequencies is essential for implementing effective resistance management strategies.

Fitness cost associated with fungicide resistance

The development of fungicide resistance poses a significant challenge in disease management. While fungicide resistance offers a selective advantage in the presence of fungicides, mutations that confer resistance can also lead to fitness costs, creating an evolutionary trade-off. These fitness costs may arise due to functional limitations of the mutating target site or from the diversion of energy from growth and reproduction to processes like overexpression or active transport mechanisms required for resistance. Fitness costs that can greatly impact the survival of resistant strains are evident in several traits, including reduced mycelial growth, increased osmotic or oxidative stress, lower aggressiveness and spore production, a more limited optimal temperature range, reduced production of sexual fruiting bodies, viability challenges and poor competitive fitness with other microbes present in field settings etc. Interestingly, fitness penalties and resistance stability can vary between species and may also depend on the specific fungicide. For instance, studies have shown that QoI-resistant *E. necator* isolates were even more competitive than their sensitive counterparts (Rallo et al. 2014), however, continuous transfers of QoI-resistant *P. viticola* populations in the absence of fungicide pressure resulted in a reduction of resistance or even a complete restoration of sensitivity (Genet et al. 2006). Moreover, different mutations causing resistance to same fungicides may have different fitness capabilities (Hawkins et al. 2018). For example, in *B. cinerea*, populations with the E198A mutation remained stable following the discontinuation of MBC fungicides (FRAC 1), whereas the *B. cinerea* isolates with F200Y mutation declined, potentially because of fitness penalties (Walker et al. 2013; Hawkins et al. 2018). Variable results in fitness costs between field isolates and lab mutants in *B. cinerea* has been also observed. A study conducted on lab mutants with *sdhB*-H272R, *sdhB*-H272Y, *sdhB*-H272L,

sdhB-P225F, and sdhB-N230I mutations reported no significant fitness costs in terms of growth and sporulation, sclerotia production, or osmotic sensitivity (Amiri et al. 2014). In contrast, another study indicated that sensitive strains outcompeted field isolates with mutations H272R/Y/L, N230I, and P225F in most planta competition tests, with most resistant isolates exhibiting diminished fitness. Although H272R was found to be less fitness compromised than the other resistant strains, it showed greater sensitivity to oxidative stress (Veloukas et al. 2014; Hawkins et al 2018). Conversely to fitness cost, sometimes fungicide resistance may also cause fitness advantage over sensitive populations. Fitness advantages have been noted in QoI-resistant *E. necator* populations, which can establish colonies more efficiently and release inoculum sooner in cooler temperatures, especially at the start of the season, compared to susceptible populations (Newbold 2021).

Understanding fitness costs associated with fungicide resistance can enhance the precision of resistance risk assessments (Holloman 2015). Ignoring these fitness costs may result in inflated resistance risk estimates. For instance, mechanisms identified in laboratory mutants that carry significant fitness costs might have minimal relevance especially in field settings (Grimmer et al. 2014; Hawkins et al. 2018). Testing fitness cost associated with lab mutants can enhance predictions about which resistance mechanisms are more likely to develop in field settings. This will enable proactive identification of what to monitor and guide the early development of molecular diagnostics tools (Hawkins et al. 2018).

A better knowledge of fitness costs might help in designing better fungicide resistance management strategies. The success of many resistance management practices depends on the fitness costs of resistant strains during periods when spraying is halted (Hawkins et al. 2018). Fungicide resistance in mutants that have associated fitness costs can be reversed by using

strategies that involve timing gaps between sprays, alternating fungicide modes of action, or employing spatial mosaics/refugia. Furthermore, complex models are required for resistance management strategies that incorporate different selection coefficients adjusted for local prevalence as fitness costs may also vary according to the environmental conditions or pathogen life stages (Billard et al. 2012; Raposo et al. 2000; Hawkins et al. 2018).

Diagnostics for fungicide resistance

Detection of fungicide resistance in plant pathogens using conventional methods including testing spore germination or mycelial growth using discriminatory doses. These are usually straightforward methods and enable the tracking of sensitivity changes and resistance levels, regardless of the underlying resistance mechanisms. However, these methods are time consuming and laborious which restricts the number of isolates that can be tested. Traditional methods necessitate isolating pathogens that bring complexities of poor germination or loss of pathogenicity, culture maintenance, issues of in-planta culturing of obligate pathogens etc. To overcome these issues, a significant progress has been done in developing molecular techniques for detecting and tracking the fungicide resistance of plant pathogens. In the cases where resistance mechanism is known, several nucleic acid detection techniques have been developed in *E. necator*, *B. cinerea* and *P. viticola* in grapes. QoI resistance based on G143A mutation is well studied, three tests are available to monitor QoI resistance in *P. viticola* (Gisi et al. 2002; Chen et al. 2007; Corio-Costet et al. 2011). Similarly, SYBR Green-based quantitative Polymerase Chain Reaction (qPCR) assays have been developed to detect A-143 allele in *E. necator* (Baudoin et al. 2008; Dufour et al. 2011; Miles et al. 2012). However, they can generate false positives and cannot simultaneously distinguish between A-143 and G-143 alleles in a single reaction, increasing detection costs (Miles et al. 2012). Furthermore, allele-specific

TaqMan probe and digital-droplet PCR-based assays have also been designed to detect QoI resistance in *E. necator*. These methods can be applied at any developmental stage of pathogens. Adaptability, rapidity, specificity, sensitivity, reliability, reproducibility, and ability to detect multiple alleles make TaqMan probe based qPCR tools popular choice. Another molecular diagnostic tool, RNase-H-dependent polymerase chain amplification reaction (rhAMP) assays has been also utilized for allelic discrimination of P225F/H mutation associated with fluopyram-boscalid resistance in *B. cinerea* populations. The rhAMP assays were found to be more flexibility in designing, have better allelic discrimination, more affordable compared to TaqMan assays (Alzohariry et al. 2021). These assays, however, require expensive equipment and trained operators, making them impractical for point-of-care use by growers. In contrast, isothermal amplification techniques bypass the need for costly, complex equipment or intensive labor. Isothermal techniques like loop-mediated isothermal amplification (LAMP) offer point-of-care detection for SNP based fungicide resistance. LAMP assays are highly specific, efficient, and rapid, with amplification completed in under 30 minutes (Notomi et al. 2000). LAMP reactions can be monitored visually with affordable equipment like block heaters or water baths, or fluorometrically using portable devices such as Genie II (OptiGene Ltd., U.K.) or T16-ISO Axxin (Axxin, U.S.A.), making it a strong candidate for point-of-care diagnostics (Notomi et al. 2000). LAMP has been also employed to detect H272R mutation conferring SDHI-resistance of *B. cinerea* (Fan et al. 2018). Similarly, PNA-LNA-LAMP assay has been designed for QoI resistance in *E. necator* (Sharma et al. 2023). While isothermal assays are promising choice for point-of-care detection, their sensitivity and specificity still require refinement for in-field use (Sharma et al. 2023). Recently, several CRISPR-Cas-based detection platforms have been developed for detection of human and animal pathogens, offering high specificity, sensitivity,

and accuracy. In medical science, a CRISPR-Cas12b system combined with RPA has also been shown to effectively detect the 3232A>G mutation in the BRCA1 gene, associated with breast cancer (Teng et al. 2019). To enhance the specificity and sensitivity of LAMP assay, incorporating CRISPR-Cas detection systems could be a viable strategy (Li et al. 2018; Pang et al. 2020; Sharma et al. 2023). Hence, the advancement in the sector of molecular diagnostics have revolutionized the rapid fungicide resistance detection and guide growers in taking in-season decision making.

Advances that might help with fungicide resistance

Risk of fungicide resistance can be reduced by using more sustainable agricultural practices. One of the guiding principles is that control interventions should be aligned based on field monitoring and pathogen thresholds, guiding decisions about fungicide dosage, application timing, and frequency (Lázaro et al. 2021). In sustainable agricultural practices, decision support systems (DSS) have been introduced as tools to significantly reduce the frequency of fungicide applications (Lázaro et al. 2021). Unlike traditional fungicide schedules based on calendar, DSSs enable growers to time their treatments based on actual or predicted disease risk, ensuring fungicides are applied only when required (Lázaro et al. 2021). By the year 2030, the European Green Deal targets a 50% reduction in their chemical pesticide use (Lázaro et al. 2021). Studies have found that with the use of DSS tools, fungicide applications can be cut by over half, all while reducing disease incidence and maintaining the effective disease management (Lázaro et al. 2021). This approach will lower the frequency of fungicide applications, extend the intervals between treatments, and offer a better opportunity to rotate different modes of action within a season, ultimately reducing the selection pressure on resistant populations (Lázaro et al. 2021).

Therefore, DSS tools should be used to conduct informed disease management while limiting the risk of fungicide resistance development.

Using disease prediction models to forecast disease outbreak is essential for making timely decisions regarding crop protection. Independent observations of diseases are often compared with predictions of empirical and mechanistic models for further validation (Lázaro et al. 2021). Thorough assessment is essential to establish the prediction model's reliability and its applicability in diverse situations to avoid disease management failures (Lázaro et al. 2021). A recent study demonstrated that employing machine learning algorithms, LASSO, random forest, and gradient boosting, for decision-making in fungicide applications can reduce the number of treatments by 50% for grape downy mildew in Bordeaux vineyards (Chen et al. 2020). Similarly, another study found C5.0 algorithm can be very effective in predicting symptom presence of botrytis bunch rot, downy mildew and powdery mildew in grapes (Volpi et al. 2021). Furthermore, precision agriculture tools such as using proximal colour imaging and infrared imagery has been developed to detect in-field disease like grape downy mildew (Abdelghafour et al. 2020; Zia-khan et al. 2022). However, factors like look-alike diseases, abiotic stress, influence of sun direction etc. are needed to be further investigated before applying these techniques for large-scale in-field disease management strategies.

Agricultural extension efforts play very crucial role in communication information about efficient resistant management strategies to growers (Lowder et al. 2024). It has been found the growers highly value the extension information that is provided through personal connections involving one to one information discussion with professionals and extension agents (Lowder et al. 2024). Moreover, engaging influential individuals, outreach professionals can effectively disseminate information and promote changes in opinions or behaviors throughout the region

(Lowder et al. 2024). Taking these social behaviors into account can greatly enhance the effectiveness of information dissemination related to managing fungicide resistance risks.

Conclusion and future direction

Growers are advised to rotate fungicides with diverse modes of action and be cautious when applying fungicides mixtures containing different FRAC codes that prone to multiple fungicide resistance. DSS informed spray schedules, proper fungicide dosage and strategic resistance management throughout the season can effectively suppress the development of fungicide resistance in the grape powdery mildew, downy mildew and botrytis bunch rot. Several novel chemical compounds such as pyrisoxazole, compound IV-9, tetramycin and RNA-based fungicides should be explored as new generation solution for management of botrytis bunch rot. Continuous fungicide resistance monitoring of newer released fungicides for powdery mildew such as cyflufenamid, metrafenone, quinoxifen and flutianil should be conducted in vineyards to avoid accumulation of resistance. Identifying genotypes of resistant pathogen populations and underlying resistance mechanisms will also aid in developing molecular diagnostic tools for rapid resistance detection. Moreover, growers should implement the resistance management strategies recommended by FRAC for each fungicide. This will also extend the effectiveness of existing fungicides, ensuring control of grape diseases.

Acknowledgments

Michigan State University is situated on the ancestral, traditional, and contemporary lands of the Anishinaabe, including the Three Fires Confederacy of the Ojibwe, Odawa, and Potawatomi peoples. These lands were ceded in the 1819 Treaty of Saginaw. We recognize the ongoing presence of Indigenous peoples and their enduring connection to this land.

Figures

Figure 1.1. Grape powdery mildew (GPM), and downy mildew (GDM): A) Typical GPM symptoms on upper side of leaf; B) *E. necator* conidial chains and conidiophores under microscope; C) Chasmothecia on infected leaf (photos A,C by Timothy Miles, MSU); D) Typical GDM symptoms on upper side of leaf; E) *P. viticola* sporulation on lower side of leaf; F) Sporulation on affected berries (photo F taken by Jacquelyn Perkins, MSU).

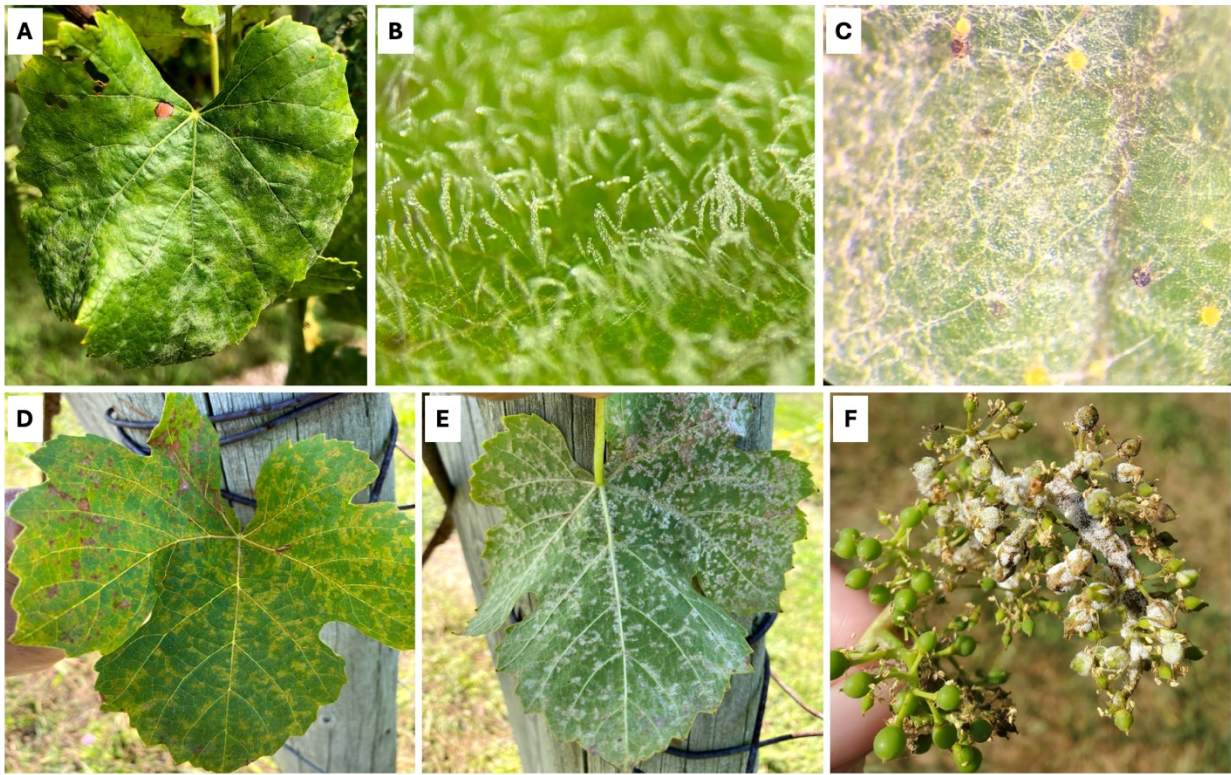
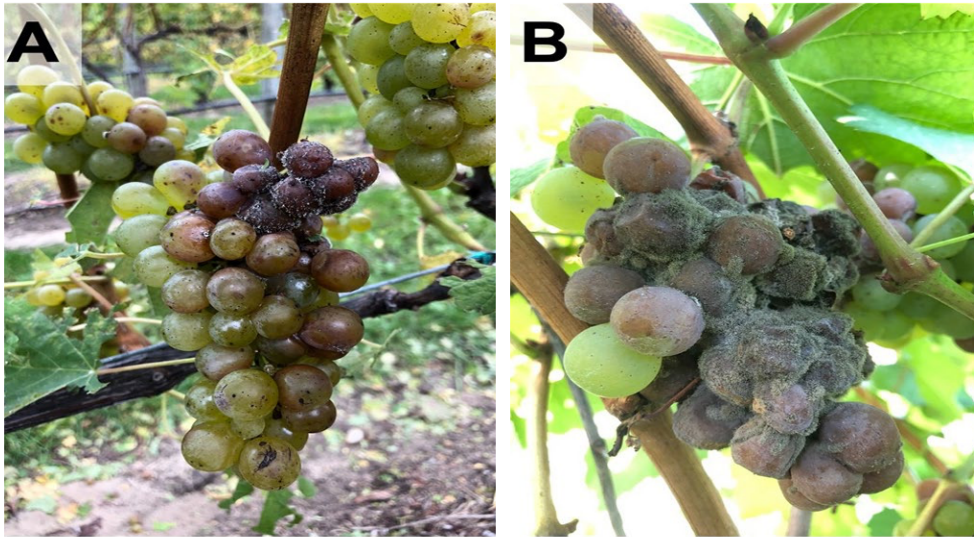


Figure 1.2. Botrytis bunch rot symptoms: A) typical symptoms of Botrytis bunch rot infection on berries of Riesling cultivar, B) Typical symptoms of Botrytis bunch rot infection on grape berries of Vignoles cultivar (photos A, B by Safa Alzohairy).



Tables

Table 1.1. Active ingredients within FRAC 7, 11, 21, 40 and 45 and known fungicide resistance in *Erysiphe necator*, *Plasmopara viticola*, and *Botrytis cinerea*.

Active Ingredient	FRAC Code	Target Site	Molecular Mechanisms
Thiabendazole	1	Microtubuline polymerization	Specific mechanism unclear yet
Iprodione	2	DNA & RNA synthesis during the spore germination	point mutations in Bos1, drug efflux pump activity
Boscalid and Fluopyram	7	Succinate dehydrogenase enzyme activity	H272R/Y amino acid change in SDHb gene in <i>B. cinerea</i> and <i>P. viticola</i>
Cyprodinil	9	Methionine biosynthesis	Resistance mechanism is unclear yet
Azoxystrobin	11	Cytochrome bc1 at Qo site	G143A mutation in Cyt b gene in <i>E. necator</i> and <i>P. viticola</i>
Fenamidone	12	Bos1 and MAPK-dependent osmoregulation pathway	Several point mutations at Bos1 in <i>B. cinerea</i>
Fludoxonil	12		
Fenhexamid	17	Ergosterol biosynthesis pathway	F412S/I/V amino acid change in Erg27 gene in <i>B. cinerea</i>
Cyazofamid	21	cytochrome bc1 at Qi site	Insertion in Cyt b gene (i.e., E203-DE-V204) in <i>P. viticola</i>
Dimethomorph and Mandipropamid	40	cellulose synthase activity	G1105S amino acid change in cesA3 gene in <i>P. viticola</i>
Ametoctradin	45	cytochrome bc1 at Qo site, stigmatellin-binding subsite	S34L amino acid change Cyt b gene in <i>P. viticola</i>

LITERATURE CITED

- Abdelghafour, F., Keresztes, B., Germain, C., and Da Costa, J.P. 2020. In field detection of downy mildew symptoms with proximal colour imaging. *Sensors* 20:4380.
- Adnan, M., Hamada, M.S., Li, G.Q., and Luo, C.X. 2018. Detection and molecular characterization of resistance to the dicarboximide and benzamide fungicides in *Botrytis cinerea* from tomato in Hubei Province, China. *Plant Dis.* 102:1299-1306.
- Albert, G., Thomas, A., and G hne, M. 1991. Fungicidal activity of dimethomorph on different stages in the life cycle of *Phytophthora infestans* and *Plasmopara viticola*. In: The 3rd International Conference on Plant Diseases, Bordeaux. Bordeaux, France: ANPP, 887–94.
- Albertini, C., and Leroux, P. 2004. A *Botrytis cinerea* putative 3-keto reductase gene (ERG27) that is homologous to the mammalian 17 -hydroxysteroid dehydrogenase type 7 gene (17 -HSD7). *Eur. J. Plant Pathol.* 110:723-733.
- Alzohairy, S.A., Gillett, J., Saito, S., Naegele, R.N., Xiao, C.L., and Miles, T.D. 2021. Fungicide resistance profiles of *Botrytis cinerea* isolates from Michigan vineyards and development of a TaqMan assay for detection of fenhexamid resistance. *Plant Dis.* 105:285-294.
- Amiri, A., Heath, S.M., and Peres, N.A. 2013. Phenotypic characterization of multifungicide resistance in *Botrytis cinerea* isolates from strawberry fields in Florida. *Plant Dis.* 97:393-401.
- Amiri, A., Heath, S.M., and Peres, N.A. 2014. Resistance to fluopyram, fluxapyroxad, and penthiopyrad in *Botrytis cinerea* from strawberry. *Plant Dis.* 98:532–39.
- Aoki, Y., Hada, Y., and Suzuki, S. 2013. Development of a multiplex allele-specific primer PCR assay for simultaneous detection of QoI and CAA fungicide resistance alleles in *Plasmopara viticola* populations. *Pest Manag. Sci.* 69:268-273.
- Bardas, G.A., Veloukas, T., Koutita, O., and Karaoglanidis, G.S. 2010. Multiple resistance of *Botrytis cinerea* from kiwifruit to SDHIs, QoIs and fungicides of other chemical groups. *Pest Manag. Sci.* 66:967-973.
- Balba, H. 2007. Review of strobilurin fungicide chemicals. *J. Environ. Sci. Health Part B* 42:441–451.
- Banno, S., Fukumori, F., Ichiishi, A., Okada, K., Uekusa, H., Kimura, M., and Fujimura, M. 2008. Genotyping of benzimidazole-resistant and dicarboximide-resistant mutations in *Botrytis cinerea* using real-time polymerase chain reaction assays. *Phytopathology* 98:397-404.

- Bartlett, D.W., Clough, J.M., Godwin, J.R., Hall, A.A., Hamer, M., and Parr-Dobrzanski, B. 2002. The strobilurin fungicides. *Pest Manag. Sci.* 58:649–662.
- Baudoin, A., Olaya, G., Delmotte, F., Colcol, J.F., and Sierotzki, H. 2008. QoI resistance of *Plasmopara viticola* and *Erysiphe necator* in the mid-Atlantic United States. *Plant Health Prog.* 9:25.
- Benheim, D., Rochfort, S., Robertson, E., Potter, I.D., and Powell, K.S. 2012. Grape phylloxera (*Daktulosphaira vitifoliae*) – a review of potential detection and alternative management options. *Appl. Biol.* 161:91-115.
- Billard, A., Fillinger, S., Leroux, P., Lachaise, H., Beffa, R., and Debieu, D. 2012. Strong resistance to the fungicide fenhexamid entails a fitness cost in *Botrytis cinerea*, as shown by comparisons of isogenic strains. *Pest Manag. Sci.* 68:684–91.
- Blum, M., Waldner, M., and Gisi, U. 2010. A single point mutation in the novel PvCesA3 gene confers resistance to the carboxylic acid amide fungicide mandipropamid in *Plasmopara viticola*. *Fungal Genet. Biol.* 47:499–510.
- Blum, M., Gamper, H.A., Waldner, M., Sierotzki, H., and Gisi, U. 2012. The cellulose synthase 3 (CesA3) gene of oomycetes: structure, phylogeny and influence on sensitivity to carboxylic acid amide (CAA) fungicides. *Fungal Biol.* 116:529-542.
- Brent, J.B. and Hollomon, D.W. 2007. Fungicide resistance in crop pathogens: How can it be managed? Fungicide Resistance Action Committee.
- Cahoon, G.A. 1991. Cultural practices in relation to insect and disease management. In: *Proc. of the Ohio Grape-Wine Short Course*. Hort. Dept. Series 62:4-11.
- Calonnec, A., Cartolaro, P., Poupot, C., Dubourdieu, D., and Darriet. 2004. Effects of *Uncinula necator* on the yield and quality of grapes (*Vitis vinifera*) and wine. *Plant Pathol.* 53:434–445.
- Chen, M., Brun, F., Raynal, M., and Makowski, D. 2020. Forecasting severe grape downy mildew attacks using machine learning. *PLoS One.* 15. e0230254.
- Chen, S.N., Luo, C.X., Hu, M.J., and Schnabel, G. 2016. Fitness and competitive ability of *Botrytis cinerea* isolates with resistance to multiple chemical classes of fungicides. *Phytopathology.* 106:997-1005.
- Chen, W.J., Delmotte, F., Richard-Cervera, S., Douence, L., Greif, C., and Corio-Costet, M.F. 2007. At least two origins of fungicide resistance in grapevine downy mildew populations. *Appl. Environ. Microbiol.* 73:5162–5172.
- Cherrad, S., Hernandez, C., Steva, H., and Vacher, S. 2018. Resistance of *Plasmopara viticola* to complex III inhibitors: a point on the phenotypic and genotypic characterization of

- strains. 12e Conférence Internationale sur les Maladies des Plantes, 11 et 12 décembre 2018, Tours, France: 449–459.
- Cherrad, S., Gillet, B., Dellinger, J., Bellaton, L., Roux, P., Hernandez, C., Steva, H., Perrier, L., Vacher, S., and Hughes, S. 2023. New insights from short and long reads sequencing to explore cytochrome b variants in *Plasmopara viticola* populations collected from vineyards and related to resistance to complex III inhibitors. PLoS One. 18. e0268385.
- Clerjeau, M. and Simone, J. 1982. Apparition en France de souches de *Plasmopara viticola* résistantes aux fongicides de la famille des anilides (métalaxyl, milfuram). Le Progrès Agricole et Viticole 99:59–61.
- Colcol, J.F., Rallos, L., and Baudoin, A. 2012. Sensitivity of *Erysiphe necator* to demethylation inhibitor fungicides in Virginia. Plant Dis. 96:111–116.
- Corio-Costet, M.-F. 2015. Monitoring resistance in obligate pathogens by bioassays relating to field use: Grapevine powdery and downy mildews. Pages 251–279 in: Fungicide Resistance in Plant Pathogens: Principles and a Guide to Practical Management. H. Ishii and D.W. Hollomon, eds. Springer Japan, Tokyo, Japan.
- Corio-Costet, M.-F., Dufour, M.-C., Cigna, J., Abadie, P., and Chen, W.J. 2011. Diversity and fitness of *Plasmopara viticola* isolates resistant to QoI fungicides. Eur. J. Plant Pathol. 129:315–329.
- Chen, W.J., Delmotte, F., Richard-Cervera, S., Douence, L., Greif, C., and Corio-Costet, M.F. 2007. At least two origins of fungicide resistance in grapevine downy mildew populations. Appl. Microbiol. Biotechnol. 73:5162–5172.
- de Bem, B.P., Bogo, A., Everhart, S., Casa, R.T., Gonçalves, M.J., Marcon Filho, J.L., and da Cunha, I.C. 2015. Effect of Y-trellis and vertical shoot positioning training systems on downy mildew and botrytis bunch rot of grape in highlands of southern Brazil. Scientia Horticulturae 185:162–166.
- Deising, H.B., Reimann, S., and Pascholati, S.F. 2008. Mechanisms and significance of fungicide resistance. Braz. J. Microbiol. 39:286–295.
- Delp, C. and Dekker, J. 1985. Fungicide resistance: Definitions and use of terms. EPPO Bull. 15:333–335.
- Délye, C., Laigret, F., and Corio-Costet, M.F. 1997. A mutation in the 14 alpha-demethylase gene of *Uncinula necator* that correlates with resistance to a sterol biosynthesis inhibitor. Appl. Environ. Microbiol. 63:2966–2970.
- Dietz, J. and Winter, C. 2019. Modern Crop Protection Compounds. Wiley-VCH Verlag GmbH & Co. KGaA; Weinheim, Germany. Recently introduced powdery mildew fungicides: 933–947.

- De Miccolis Angelini, R.M., Rotolo, C., Masiello, M., Gerin, D., Pollastro, S., and Fretra, F. 2014. Occurrence of fungicide resistance in populations of *Botryotinia fuckeliana* (*Botrytis cinerea*) on table grape and strawberry in southern Italy. *Pest Manag. Sci.* 70:1785-1796.
- Dufour, M.-C., Fontaine, S., Montarry, J., and Corio-Costet, M.-F. 2011. Assessment of fungicide resistance and pathogen diversity in *Erysiphe necator* using quantitative real-time PCR assays. *Pest Manage. Sci.* 67:60-69.
- Dyer, P.S., Hansen, J., Delaney, A., and Lucas, J.A. 2000. Genetic control of resistance to the sterol 14 α -demethylase inhibitor fungicide prochloraz in the cereal eyespot pathogen *Tapesia yallundae*. *Appl. Environ. Microbiol.* 66:4599.
- English, J.T., Thomas, C.S., Marois, J.J., and Gubler, W.D. 1989. Microclimates of grapevine canopies associated with leaf removal and control of *Botrytis* bunch rot. *Phytopathology.* 79:395-401.
- English, J.T., Bledsoe, A.M., Marois, J.J., and Gubler, W.D. 1990. Influence of grapevine canopy management on evaporative potential in the fruit zone. *Am. J. Enol. Vitic.* 41:859-864.
- Esterio, M., Muñoz, G., Ramos, C., Cofré, G., Estévez, R., Salinas, A., and Auger, J. 2011. Characterization of *Botrytis cinerea* isolates present in Thompson seedless table grapes in the Central Valley of Chile. *Plant Dis.* 95:683-690.
- Ezzili, B. 1992. Effect of vine age on the evolution of the number of flower buds of *Alicante Grenache noir* grown in El Khanguet (Tunisia) [fruit set, flower abscission]. *Bulletin de l'OIV* 65:161-176.
- Fan, F., Yin, W.X., Li, G.Q., Lin, Y., and Luo, C.X. 2018. Development of a LAMP method for detecting SDHI fungicide resistance in *Botrytis cinerea*. *Plant Dis.* 102:1612-1618.
- Feng, X. and Baudoin, A. 2018. First report of carboxylic acid amide fungicide resistance in *Plasmopara viticola* (grapevine downy mildew) in North America. *Plant Health Prog.* 19:139.
- Felsenstein, F., Semar, M., and Stammli, G. 2010. Sensitivity of wheat powdery mildew (*Blumeria graminis* f. sp. *tritici*) towards metrafenone. *Gesunde Pflanz.* 62:29–33.
- Fernández-Ortuño, D., Grabke, A., Li, X., and Schnabel, G. 2015. Independent emergence of resistance to seven chemical classes of fungicides in *Botrytis cinerea*. *Phytopathology.* 105:424-432.
- Ficke, A., Gadoury, D.M., and Seem, R.C. 2002. Ontogenic resistance and plant disease management: A case study of grape powdery mildew. *Phytopathology.* 92:671-675.

- Fillinger, S., Leroux, P., Auclair, C., Barreau, C., Al Hajj, C., and Debieu, D. 2008. Genetic analysis of fenhexamid-resistant field isolates of the phytopathogenic fungus *Botrytis cinerea*. *Antimicrob. Agents Chemother.* 52:3933-3940.
- Fillinger, S., Ajouz, S., Nicot, P.C., Leroux, P., and Bardin, M. 2012. Functional and structural comparison of pyrrolnitrin- and iprodione-induced modifications in the class III histidine-kinase Bos1 of *Botrytis cinerea*. *PLoS One.* 7. e42520
- Fourie, P.H. 2004. Metalaxyl sensitivity status of downy mildew populations in Western Cape vineyards. *South African J. Enol. Vitic.* 25:19–22.
- Fuller, K.B., Alston, J.M., and Sambucci, O.S. 2014. The value of powdery mildew resistance in grapes: evidence from California. *Wine Econ. Policy* 3:90-107.
- FRAC. 2024. FRAC Code List ©: Fungal Control Agents Sorted by Cross Resistance Pattern and Mode of Action.
- FRAC. FRAC List of Plant Pathogenic Organisms Resistant to Disease Control Agents.
- Fontaine, S., Remuson, F., Caddoux, L., and Barrès, B. 2019. Investigation of the sensitivity of *Plasmopara viticola* to amisulbrom and ametoctradin in French vineyards using bioassays and molecular tools. *Pest Manage. Sci.* 75:2115–2123.
- Frenkel, O., Cadle-Davidson, L., Wilcox, W.F., and Milgroom, M.G. 2015. Mechanisms of resistance to an azole fungicide in the grapevine powdery mildew fungus, *Erysiphe necator*. *Phytopathology.* 105:370–377.
- Gadoury, D.M., Seem, R.C., Ficke, A., and Wilcox, W.F. 2001. The epidemiology of powdery mildew on Concord grapes. *Phytopathology.* 91:948–955.
- Gadoury, D.M., Cadle-Davidson, L., Wilcox, W.F., Dry, I.B., Seem, R.C., and Milgroom, M.G. 2012. Grapevine powdery mildew (*Erysiphe necator*): A fascinating system for the study of the biology, ecology, and epidemiology of an obligate biotroph. *Mol. Plant Pathol.* 13:1–16.
- Genet, J.L., Jaworska, G., and Deparis, F. 2006. Effect of dose rate and mixtures of fungicides on selection for QoI resistance in populations of *Plasmopara viticola*. *Pest Manage. Sci.* 62:188-194.
- Genet, J.L. and Jaworska, G. 2009. Baseline sensitivity to proquinazid in *Blumeria graminis* f. sp. *tritici* and *Erysiphe necator* and cross-resistance with other fungicides. *Pest Manage. Sci.* 65:878–884.
- Gianessi, L. and Reigner, N. 2006. The importance of fungicides in U.S. crop production. *Outlook on Pest Manage.* 10:209-213.

- Gindro, K., Pezet, R., Viret, O., and Richter, H. 2005. Development of a rapid and highly sensitive direct-PCR assay to detect a single conidium of *Botrytis cinerea* Pers.: Fr in vitro and quiescent forms in planta. *Vitis* 44:139-142.
- Gisi, U., Sierotzki, H., Cook, A., and McCaffery, A. 2002. Mechanisms influencing the evolution of resistance to Qo inhibitor fungicides. *Pest Manage. Sci.* 58:859-867.
- Gisi, U. and Sierotzki, H. 2015. Oomycete fungicides: phenylamides, quinone outside inhibitors, and carboxylic acid amides. In: Ishii, H. and Hollomon, D.W. (Eds.) *Fungicide Resistance in Plant Pathogens*. Tokyo, Japan: Springer, pp. 145–174.
- Gisi, U., Waldner, M., Kraus, N., Dubuis, P.H., and Sierotzki, H. 2007. Inheritance of resistance to carboxylic acid amide (CAA) fungicides in *Plasmopara viticola*. *Plant Pathol.* 56:199–208.
- Ghule, M.R., Sawant, I.S., Sawant, S.D., and Saha, S. 2020. Resistance of *Plasmopara viticola* to multiple fungicides in vineyards of Maharashtra, India. *J. Environ. Biol.* 41(5):1026-1033.
- Grabke, A., Fernández-Ortuño, D., and Schnabel, G. 2013. Fenhexamid resistance in *Botrytis cinerea* from strawberry fields in the Carolinas is associated with four target gene mutations. *Plant Dis.* 97:271-276.
- Gubler, W.D., Ypema, H.L., Ouimette, D.G., and Bettiga, L.J. 1996. Occurrence of resistance in *Uncinula necator* to triadimefon, myclobutanil, and fenarimol in California grapevines. *Plant Dis.* 80:902–909.
- Graf, S. 2017. Characterisation of Metrafenone and succinate dehydrogenase inhibitor resistant isolates of the grapevine powdery mildew *Erysiphe necator*. Ph.D. Thesis. Technische Universität Kaiserslautern; Kaiserslautern, Germany.
- Grasso, V., Palermo, S., Sierotzki, H., Garibaldi, A., and Gisi, U. 2006. Cytochrome b gene structure and consequences for resistance to Qo inhibitor fungicides in plant pathogens. *Pest Manage. Sci.* 62:465-472.
- Grimmer, M.K., van den Bosch, F., Powers, S.J., and Paveley, N.D. 2014. Evaluation of a matrix to calculate fungicide resistance risk. *Pest Manage. Sci.* 70:1008–1016.
- Halleen, F., Holz, G., and Pringle, K.L. 2000. Resistance in *Uncinula necator* to triazole fungicides in South African grapevines. *South Afr. J. Enol. Vitic.* 21:71–80.
- Hall, B., McKay, S., Lopez, F., Harper, L., Savocchia, S., Borneman, A., and Herderich, M. 2016. Fungicide resistance in Australian viticulture. In: Deising, H.B., Fraaije, B., Mehl, A., Oerke, E.C., Sierotzki, H., and Stammer, G. (Eds.) *Modern Fungicides and Antifungal Compounds*. Volume VIII. Deutsche Phytomedizinische Gesellschaft; Braunschweig, Germany, pp. 181–186.

- Hahn, M. 2014. The rising threat of fungicide resistance in plant pathogenic fungi: *Botrytis* as a case study. *J. Chem. Biol.* 7:133-141.
- Haramoto, M., Yamanaka, H., Sano, H., Sano, S., and Otani, H. 2006. Fungicidal activities of cyflufenamid against various plant-pathogenic fungi. *J. Pestic. Sci.* 31:95–101.
- Hartman, J.R. and Kaiser, C.A. 2008. Fruit rots of grape. Plant Pathology Fact Sheet. University of Kentucky College of Agriculture, Lexington, KY.
- Hawkins, N.J. and Fraaije, B.A. 2018. Fitness penalties in the evolution of fungicide resistance. *Annu. Rev. Phytopathol.* 56:339-360.
- Hermann, D.C., McKenzie, D., Cohen, Y., and Gisi, U. 2019. Chapter 6: Phenylamides: market trends and resistance evolution for important oomycete pathogens more than 35 years after the first product introduction (FRAC code 4). In: Hermann, D.C., McKenzie, D., Cohen, Y., and Gisi, U. (Eds.) *Fungicide Resistance in North America*, 2nd ed. The American Phytopathological Society, St. Paul, MN, USA, pp. 69–84.
- Hirooka, T. and Ishii, H. 2013. Chemical control of plant diseases. *J. Gen. Plant Pathol.* 79:390–401.
- Hollomon, D.W. 2015. Fungicide resistance: facing the challenge. *Plant Prot. Sci.* 51:170–176.
- Horsfall, J.G. 1975. Fungi and fungicides: The story of a nonconformist. *Annu. Rev. Phytopathol.* 13:1-14.
- Holz, G., Gütschow, M., Coertze, S., and Calitz, F.J. 2003. Occurrence of *Botrytis cinerea* and subsequent disease expression at different positions on leaves and bunches of grape. *Plant Dis.* 87:351-358.
- Hu, M. and Fiola, J. 2023. Downy mildew management. University of Maryland Extension. Available online: <https://extension.umd.edu/resource/downy-mildew-management/>. Accessed online: 09/18/2024.
- Ishii, H. 2015. Stability of resistance. In: *Fungicide Resistance in Plant Pathogens*, pp. 35-48. Springer Japan, Tokyo Osaka, Japan.
- Islam, M.T., von Tiedemann, A., and Laatsch, H. 2011. Protein kinase C is likely to be involved in zoosporogenesis and maintenance of flagellar motility in the peronosporomycete zoospores. *Mol. Plant-Microbe Interact.* 24:938–947.
- Jones, L., Riaz, S., Morales-Cruz, A., Amrine, K.C., McGuire, B., Gubler, W.D., Walker, M.A., and Cantu, D. 2014. Adaptive genomic structural variation in the grape powdery mildew pathogen, *Erysiphe necator*. *BMC Genom.* 15:1081.

- Jeschke, P., Witschel, M., Krämer, W., Schirmer, U., and Earley, F. 2019. Modern Crop Protection Compounds. Wiley-VCH Verlag GmbH & Co. KGaA; Weinheim, Germany: Fungicides acting on oxidative phosphorylation, pp. 609–747.
- Kaplan, J., Travadon, R., Cooper, M., Hillis, V., Lubell, M., and Baumgartner, K. 2016. Identifying economic hurdles to early adoption of preventive practices: The case of trunk diseases in California winegrape vineyards. *Wine Econ. Policy* 5:127-141.
- Kim, Y.S., Dixon, E.W., Vincelli, P., and Farman, M.L. 2003. Field resistance to strobilurin (QoI) fungicides in *Pyricularia grisea* caused by mutations in the mitochondrial cytochrome b gene. *Phytopathology*. 93:891-900.
- Kim, Y.K., and Xiao, C.L. 2011. Stability and fitness of pyraclostrobin- and boscalid-resistant phenotypes in field isolates of *Botrytis cinerea* from apple. *Phytopathology*. 101:1385-1391.
- Kimura, S., Komura, T., Yamaoka, N., and Oka, H. 2020. Biological properties of flutianil as a novel fungicide against powdery mildew. *J. Pestic. Sci.* 45:206-215.
- Kimura, S., Shibata, Y., Oi, T., Kawakita, K., and Takemoto, D. 2021. Effect of flutianil on the morphology and gene expression of powdery mildew. *J. Pestic. Sci.* 46:206-213.
- Kojima, K., Takano, Y., Yoshimi, A., Tanaka, C., Kikuchi, T., and Okuno, T. 2004. Fungicide activity through activation of a fungal signaling pathway. *Mol. Microbiol.* 53:1785-1796.
- Kretschmer, M., Leroch, M., Mosbach, A., Walker, A.S., Fillinger, S., Mernke, D., et al. 2009. Fungicide-driven evolution and molecular basis of multidrug resistance in field populations of the grey mould fungus *Botrytis cinerea*. *PLoS Pathog.* 5. e1000696.
- Kunova, A., Pizzatti, C., Bonaldi, M., and Cortesi, P. 2016. Metrafenone resistance in a population of *Erysiphe necator* in northern Italy. *Pest Manage. Sci.* 72:398–404.
- Kunova, A., Pizzatti, C., Saracchi, M., Pasquali, M., and Cortesi, P. 2021. Grapevine powdery mildew: Fungicides for its management and advances in molecular detection of markers associated with resistance. *Microorganisms* 9:1541.
- Lalève, A., Gamet, S., Walker, A.-S., Debieu, D., Toquin, V., and Fillinger, S. 2014. Site-directed mutagenesis of the P225, N230, and H272 residues of succinate dehydrogenase subunit B from *Botrytis cinerea* highlights different roles in enzyme activity and inhibitor binding. *Environ. Microbiol.* 16:2253-2266.
- Lázaro, E., Makowski, D., and Vicent, A. 2021. Decision support systems halve fungicide use compared to calendar-based strategies without increasing disease risk. *Commun. Earth Environ.* 2:224.

- Leroch, M., Kretschmer, M., and Hahn, M. 2011. Fungicide resistance phenotypes of *Botrytis cinerea* isolates from commercial vineyards in South West Germany. *J. Phytopathol.* 159:63-65.
- Leroch, M., Plesken, C., Weber, R.W.S., Kauff, F., Scalliet, G., and Hahn, M. 2013. Gray mold populations in German strawberry fields are resistant to multiple fungicides and dominated by a novel clade closely related to *Botrytis cinerea*. *Appl. Environ. Microbiol.* 79:159–167.
- Leroux, P., Chapeland, F., Desbrosses, D., and Gredt, M. 1999. Patterns of cross-resistance to fungicides in *Botryotinia fuckeliana* (*Botrytis cinerea*) isolates from French vineyards. *Crop Protect.* 18:687-697.
- Leroux, P., Fritz, R., Debieu, D., Albertini, C., Lanen, C., Bach, J., Gredt, M., and Chapeland, F. 2002. Mechanisms of resistance to fungicides in field strains of *Botrytis cinerea*. *Pest Manag. Sci.* 58:876-888.
- Leroux, P., Gredt, M., Leroch, M., and Walker, A.-S. 2010. Exploring mechanisms of resistance to respiratory inhibitors in field strains of *Botrytis cinerea*, the causal agent of gray mold. *Appl. Environ. Microbiol.* 76:6615-6630.
- Li, L., Li, S., Wu, N., Wu, J., Wang, G., Zhao, G., and Wang, J. 2018. HOLMESv2: A CRISPR-Cas12b-assisted platform for nucleic acid detection and DNA methylation quantitation. *ACS Synth. Biol.* 10:2228–2237.
- Lowder, S.R., Moyer, M.M., Cooper, M.L., Pscheidt, J.W., and Mahaffee, W.F. 2024. Information transfer among grape producers in the western United States on pest and disease management. *PhytoFrontiers™: PHYTOFR-07.*
- McClellan, W.D., and Hewitt, W.B. 1973. Early Botrytis rot of grapes: Time of infection and latency of *Botrytis cinerea* Pers. in *Vitis vinifera* L. *Phytopathology* 63:1151-1157.
- McGrath, M.T., and Sexton, Z.F. 2018. Poor control of cucurbit powdery mildew associated with first detection of resistance to cyflufenamid in the causal agent, *Podosphaera xanthii*, in the United States. *Plant Health Prog.* 19:222–223.
- Mernke, D., Dahm, S., Walker, A.S., Lalève, A., Fillinger, S., Leroch, M., et al. 2011. Two promoter rearrangements in a drug efflux transporter gene are responsible for the appearance and spread of multidrug resistance phenotype MDR2 in *Botrytis cinerea* isolates in French and German vineyards. *Phytopathology* 101:1176–1183.
- Morton, A. and Staub, T. 2008. A short history of fungicides. APSnet Features. <https://www.apsnet.org/edcenter/apsnetfeatures/Pages/Fungicides.aspx>

- Mosbach, A., Edel, D., Farmer, A.D., Widdison, S., Barchietto, T., Dietrich, R.A., Corran, A., and Scalliet, G. 2017. Anilinopyrimidine resistance in *Botrytis cinerea* is linked to mitochondria function. *Front. Microbiol.* 8:2361.
- Miles, L.A., Miles, T.D., Kirk, W.W., and Schilder, A.M.C. 2012. Strobilurin (QoI) resistance in populations of *Erysiphe necator* on grapes in Michigan. *Plant Dis.* 96:1621-1628.
- Miyamoto, T., Hayashi, K., and Ogawara, T. 2020. First report of the occurrence of multiple resistance to flutianil and pyriofenone in field isolates of *Podosphaera xanthii*, the causal fungus of cucumber powdery mildew. *Eur. J. Plant Pathol.* 156:953–963.
- Nicol, J.M., Stirling, G.R., Rose, B.J., May, P., and Van Heeswijck, R. 1999. Impact of nematodes on grapevine growth and productivity: Current knowledge and future directions, with special reference to Australian viticulture. *Aust. J. Grape Wine Res.* 5:109-127.
- Neill, T., Livesay, A., Albrecht, A., and Mahaffee, W.F. 2015. Seeking the right level of sulfur to fight powdery mildew on grapes. OSU Extension Service. Available online: <https://extension.oregonstate.edu/crop-production/wine-grapes/seeking-right-level-sulfur-fight-powdery-mildew-grapes>
- Newbold, C.L. 2021. Is resistance futile: Examining fitness costs associated with QoI resistance in *E. necator*. MS Thesis. Oregon State University.
- Oliver, C., Cooper, M., Ivey, M.L., Brannen, P., Miles, T., Lowder, S., Mahaffee, W., and Moyer, M.M. 2024. Fungicide use patterns in select United States wine grape production regions. *Plant Dis.* 108:104-112.
- Opalski, K. 2005. Cell polarity in plant defense and fungal pathogenesis in the interaction of barley with powdery mildew fungi. Ph.D. Thesis. Justus-Liebig-University Giessen, Giessen, Germany.
- Oshima, M., Banno, S., Okada, K., Takeuchi, T., Kimura, M., Ichiishi, A., Yamaguchi, I., and Fujimura, M. 2006. Survey of mutations of a histidine kinase gene BcOS1 in dicarboximide-resistant field isolates of *Botrytis cinerea*. *J. Gen. Plant Pathol.* 72:65-73.
- Panebianco, A., Castello, I., Cirvilleri, G., Perrone, G., Epifani, F., Ferrara, M., Polizzi, G., Walters, D.R., and Vitale, A. 2015. Detection of *Botrytis cinerea* field isolates with multiple fungicide resistance from table grape in Sicily. *Crop Protect.* 77:65-73.
- Pang, B., Xu, J., Liu, Y., Peng, H., Feng, W., Cao, Y., Wu, J., Xiao, H., Pabbaraju, K., Tipples, G., Joyce, M.A., Saffran, H.A., Tyrrell, D.L., Zhang, H., and Le, X.C. 2020. Isothermal amplification and ambient visualization in a single tube for the detection of SARS-CoV-2 using loop-mediated amplification and CRISPR technology. *Anal. Chem.* 92:16204–16212.

- Peever, T.L., and Milgroom, M.G. 1992. Inheritance of triadimenol resistance in *Pyrenophora teres*. *Phytopathology* 82:821. doi: 10.1094/Phyto-82-821.
- Pirondi, A., Nanni, I.M., Brunelli, A., and Collina, M. 2014. First report of resistance to cyflufenamid in *Podosphaera xanthii*, the causal agent of powdery mildew, from melon and zucchini fields in Italy. *Plant Dis.* 98:1581.
- Puhl, I., and Treutter, D. 2008. Ontogenetic variation of catechin biosynthesis as basis for infection and quiescence of *Botrytis cinerea* in developing strawberry fruits. *J. Plant Dis. Prot.* 115:247-251.
- Rallos, L.E.E., Johnson, N.G., Schmale, D.G., Prussin, A.J., and Baudoin, A.B. 2014. Fitness of *Erysiphe necator* with G143A-based resistance to quinone outside inhibitors. *Plant Dis.* 98:1494–1502.
- Rantsiou, K., Giacosa, S., Pugliese, M., Englezos, V., Ferrocino, I., Río Segade, S., Monchiero, M., Gribaudo, I., Gambino, G., Gullino, M.L., and Rolle, L. 2020. Impact of chemical and alternative fungicides applied to grapevine cv Nebbiolo on microbial ecology and chemical-physical grape characteristics at harvest. *Front. Plant Sci.* 11:700.
- Raposo, R., Gomez, V., Urrutia, T., and Melgarejo, P. 2000. Fitness of *Botrytis cinerea* associated with dicarboximide resistance. *Phytopathology* 90:1246–1249.
- Riffle, V.L., Arredondo, J.A., Lomonaco, I., Appel, C., Catania, A.A., Peterson, J.C.D., et al. 2022. Vine age affects vine performance, grape and wine chemical and sensory composition of cv. Zinfandel from California. *Am. J. Enol. Vitic.* 73:276–292.
- Rupp, S., Weber, R.W.S., Rieger, D., Detzel, P., and Hahn, M. 2017. Spread of *Botrytis cinerea* strains with multiple fungicide resistance in German horticulture. *Front. Microbiol.* 7:2075.
- Saito, S., Michailides, T.J., and Xiao, C.L. 2016. Fungicide resistance profiling in *Botrytis cinerea* populations from blueberry in California and Washington and their impact on control of gray mold. *Plant Dis.* 100:2087-2093.
- Saito, S., Michailides, T.J., and Xiao, C.L. 2019. Fungicide-resistant phenotypes in *Botrytis cinerea* populations and their impact on control of gray mold on stored table grapes in California. *Eur. J. Plant Pathol.* 154:203-213.
- Saito, S., and Xiao, C.L. 2018. Fungicide resistance in *Botrytis cinerea* populations in California and its influence on control of gray mold on stored mandarin fruit. *Plant Dis.* 102:2545-2549.
- Sagar, N., Jamadar, M.M., Reddy, C.N.L., Sayiprathap, B.R., Bharath, M., Shalini, N.H., Jagginavar, S.B., Pattar, P.S., and Basha, C.J. 2023. First report of quinone outside

- inhibitor stigmatellin binding type (QoSI) resistance in *Plasmopara viticola* in India. New Dis. Rep. 48. e12223.
- Sang, C., Ren, W., Wang, J., Xu, H., Zhang, Z., Zhou, M., Chen, C.J., and Wang, K. 2018. Detection and fitness comparison of target-based highly fludioxonil-resistant isolates of *Botrytis cinerea* from strawberry and cucumber in China. Pestic. Biochem. Phys. 147:110-118.
- Sano, S., Kasahara, I., and Yamanaka, H. 2007. Development of a novel fungicide, cyflufenamid. J. Pestic. Sci. 32:137–138.
- Santos, R.F., Fraaije, B.A., Garrido, L.da R., Monteiro-Vitorello, C.B., and Amorim, L. 2020. Multiple resistance of *Plasmopara viticola* to QoI and CAA fungicides in Brazil. Plant Pathol. 69:1708–1720.
- Sawant, S.D., Ghule, M.R., and Sawant, I.S. 2016. First report of QoI resistance in *Plasmopara viticola* from vineyards of Maharashtra, India. Plant Dis. 100:229.
- Schmitt, M.R., Carzaniga, R., Cotter, H.V.T., O’Connell, R., and Hollomon, D. 2006. Microscopy reveals disease control through novel effects on fungal development: A case study with an early-generation benzophenone fungicide. Pest Manag. Sci. 62:383–392.
- Shao, W., Sun, J., Zhang, X., and Chen, C. 2020. Amino acid polymorphism in succinate dehydrogenase subunit C involved in biological fitness of *Botrytis cinerea*. Mol. Plant Microbe Interact. 33:580-589.
- Sharma, N., Nasrollahiazar, E., Miles, L., and Miles, T.D. 2023. Michigan grape facts: Managing grapevine downy mildew. MSU Extension.
- Sharma, N., Heger, L., Neill, T., Mahaffee, W., Gold, K.M., Combs, D., Brannen, P.M., Oliver, C., Moyer, M.M., Holland, L.A., and McFadden-Smith, W. 2022. Investigating QoI and CAA resistance in grape powdery mildew and downy mildew populations in vineyards of the eastern United States and Canada. Phytopathology. 112:97-98.
- Sierotzki, H., Parisi, S., Steinfeld, U., Tenzer, I., Poirey, S., and Gisi, U. 2000. Mode of resistance to respiration inhibitors at the cytochrome bc1 enzyme complex of *Mycosphaerella fijiensis* field isolates. Pest Manag. Sci. 56:833-841.
- Sierotzki, H., Blum, M., Olaya, G., Waldner-Zulauf, M., Buitrago, C., Wullschleger, J., Cohen, Y., and Gisi, U. 2011. Sensitivity to CAA fungicides and frequency of mutations in cellulose synthase (CesA3) gene of oomycete pathogen populations. Pest Manag. Sci. 67:103-110.
- Sierotzki, H., Kraus, N., Assemet, P., Stanger, C., Cleere, S., and Windass, J. 2005. Evolution of resistance to QoI fungicides in *Plasmopara viticola* populations in Europe. Pages 73-80

- in: Modern Fungicides and Antifungal Compounds IV. Dehne, H.W., Gisi, U., Kuck, K.H., Russell, P.E., Lyr, H., eds. BCPC, Alton, UK.
- Sun, H., Wang, H., Stammeler, G., Ma, J., Liu, J., and Zhou, M. 2010. Sensitivity of Chinese isolates of *Plasmopara viticola* to metalaxyl and dimethomorph. J. Phytopathol. 158:450-452.
- Stummer, B.E., Francis, I.L., Markides, A.J., and Scott, E.S. 2003. The effect of powdery mildew infection of grape berries on juice and wine composition and on sensory properties of Chardonnay wines. Aust. J. Grape Wine Res. 9:28–39.
- Thomas, C.S., Boulton, R.B., Silacci, M.W., and Gubler, W.D. 1993. The effect of elemental sulfur, yeast strain, and fermentation medium on hydrogen sulfide production during fermentation. Am. J. Enol. Vitic. 44:211-216.
- Teng, F., Guo, L., Cui, T., Wang, X.-G., Xu, K., Gao, Q., Zhou, Q., and Li, W. 2019. CDetection: CRISPR-Cas12b-based DNA detection with sub-attomolar sensitivity and single-base specificity. Genome Biol. 20:132.
- Toffolatti, S.L., Serrati, L., Sierotzki, H., Gisi, U., and Vercesi, A. 2007. Assessment of QoI resistance in *Plasmopara viticola* oospores. Pest Manage. Sci. 63:194-201.
- Veloukas, T., Kalogeropoulou, P., Markoglou, A.N., and Karaoglanidis, G.S. 2014. Fitness and competitive ability of *Botrytis cinerea* field isolates with dual resistance to SDHI and QoI fungicides, associated with several *sdhB* and *cytB G143A* mutations. Phytopathology. 104:347–356.
- Vignutelli, A., Hilber-Bodmer, M., and Hilber, U. W. 2002. Genetic analysis of resistance to the phenylpyrrole fludioxonil and the dicarboximide vinclozolin in *Botryotinia fuckeliana* (*Botrytis cinerea*). Mycol. Res. 106:329-335.
- Viret, O., Keller, M., Jaudzems, V. G., and Cole, F. M. 2004. *Botrytis cinerea* infection of grape flowers: Light and electron microscopical studies of infection sites. Phytopathology. 94:850-857.
- Volpi, I., Guidotti, D., Mammini, M., and Marchi, S. 2021. Predicting symptoms of downy mildew, powdery mildew, and gray mold diseases of grapevine through machine learning. Ital. J. Agrometeorol. 2:57-69.
- Walton, V. M., Dreves, A. J., Gent, D. H., James, D. G., Martin, R. R., Chambers, U., and Skinkis, P. A. 2007. Relationship between rust mites *Calepitrimerus vitis* (Nalepa), bud mites *Colomerus vitis* (Pagenstecher) (Acari: Eriophyidae) and short shoot syndrome in Oregon vineyards. Int. J. Acarol. 33:307-318.

- Walker, A.-S., Micoud, A., Rémuson, F., Grosman, J., Gredt, M., and Leroux, P. 2013. French vineyards provide information that opens ways for effective resistance management of *Botrytis cinerea* (grey mould). *Pest Manag. Sci.* 69:667-678.
- Warneke, B. W., Nackley, L. L., and Pscheidt, J. W. 2022. Management of grape powdery mildew with an intelligent sprayer and sulfur. *Plant Dis.* 106:1837-1844.
- Weber, R. W. S., and Hahn, M. 2011. A rapid and simple method for determining fungicide resistance in *Botrytis*. *J. Plant Dis. Prot.* 118:17-25.
- Wicks, T. J., Hall, B. H., and Somers, A. 2005. First report of metalaxyl resistance of grapevine downy mildew in Australia: Proceedings of the 15th Biennial Australasian Plant Pathology Society Conference. Australas. Plant Pathol. Soc., Geelong, Australia.
- Wicks, T. J., Wilson, D., Stammler, G., Paton, S., and Hall, B. H. 2013. Development of grape powdery mildew strains resistant to QoI fungicides in Australia. In: Dehne, H. W., Deising, H. B., Fraaije, B., Gisi, U., Hermann, D., Mehl, A., Oerke, E. C., Russell, P. E., Stammler, G., Kuck, K. H., editors. *Modern Fungicides and Antifungal Compounds*, Vol. VII. Deutsche Phytomedizinische Gesellschaft; Braunschweig, Germany: 253-256.
- Wilcox, W. F., Burr, J. A., Riegel, D. G., and Wong, F. P. 2003. Practical resistance to QoI fungicides in New York populations of *Uncinula necator* associated with quantitative shifts in pathogen sensitivities. (Abstr.) *Phytopathology*. 93:S90.
- Wilcox, W. F., and Riegel, D. G. 2012a. Evaluation of fungicide programs for control of grapevine powdery mildew, 2011. Online publication. *Plant Dis. Manage. Rep.* 6. <http://www.plantmanagementnetwork.org/pub/trial/pdmr/volume6/abstracts/smf044.asp>.
- Wilcox, W. F., and Riegel, D. G. 2012b. Evaluation of fungicide programs for control of grapevine powdery mildew, 2010. Online publication. *Plant Dis. Manage. Rep.* 6. <http://www.plantmanagementnetwork.org/pub/trial/pdmr/volume6/abstracts/smf048.asp>.
- Wilcox, W. F., and Riegel, D. G. 2012c. Evaluation of fungicide programs for control of powdery mildew on Chardonnay grapes, 2010. Online publication. *Plant Dis. Manage. Rep.* 6. <http://www.plantmanagementnetwork.org/pub/trial/pdmr/volume6/abstracts/smf049.asp>.
- Wright, L. P. 2001. Use of trellising and pruning systems to manage grapevine fungal diseases. Masters thesis, University of Guelph.
- Yarden, O., and Katan, T. 1993. Mutations leading to substitutions at amino acids 198 and 200 of beta-tubulin that correlate with benomyl resistance phenotypes of field strains of *Botrytis cinerea*. *Phytopathology*. 83:1478-1483.

- Yin, Y. N., Kim, Y. K., and Xiao, C. L. 2012. Molecular characterization of pyraclostrobin resistance and structural diversity of the cytochrome b gene in *Botrytis cinerea* from apple. *Phytopathology*. 102:315-322.
- Yin, Y., Miao, J., Shao, W., Liu, X., Zhao, Y., and Ma, Z. 2023. Fungicide resistance: Progress in understanding mechanism, monitoring, and management. *Phytopathology* 113:707-718.
- Zia-Khan, S., Kleb, M., Merkt, N., Schock, S., and Müller, J. 2022. Application of infrared imaging for early detection of downy mildew (*Plasmopara viticola*) in grapevine. *Agriculture* 12:617.
- Ziogas, B. N., and Malandrakis, A. A. 2015. Sterol biosynthesis inhibitors: C14 demethylation (DMIs). *Fungicide Resistance in Plant Pathogens: Principles and a Guide to Practical Management*. 199-216.
- Zhang, H., Kong, F., Wang, X., Liang, L., Schoen, C. D., Feng, J., and Wang, Z. 2017. Tetra-primer ARMS PCR for rapid detection and characterisation of *Plasmopara viticola* phenotypes resistant to carboxylic acid amide fungicides. *Pest Manag. Sci.* 73:1655-1660.

CHAPTER 2: DEVELOPMENT OF A PNA-LNA-LAMP ASSAY TO DETECT A SNP ASSOCIATED WITH QOI RESISTANCE IN *ERYSIPHE NECATOR*

Abstract

The repetitive use of quinone outside inhibitor fungicides (QoIs, strobilurins; Fungicide Resistance Action Committee (FRAC) 11) to manage grape powdery mildew has led to development of resistance in *Erysiphe necator*. While several point mutations in the mitochondrial cytochrome *b* gene are associated with resistance to QoI fungicides, the substitution of glycine to alanine at codon 143 (G143A) has been the only mutation observed in QoI-resistant field populations. Allele-specific detection methods such as digital droplet PCR and TaqMan probe-based assays can be used to detect the G143A mutation. In this study, a peptide nucleic acid-locked nucleic acid mediated loop-mediated isothermal amplification (PNA-LNA-LAMP) assay consisting of an A-143 reaction and a G-143 reaction, was designed for rapidly detecting QoI resistance in *E. necator*. The A-143 reaction amplifies the mutant A-143 allele faster than the wild-type G-143 allele, while the G-143 reaction amplifies the G-143 allele faster than the A-143 allele. Identification of resistant or sensitive *E. necator* samples was determined by which reaction had the shorter time to amplification. Sixteen single-spore QoI-resistant and sensitive *E. necator* isolates were tested using both assays. Assay specificity in distinguishing the single nucleotide polymorphism (SNP) approached 100% when tested using purified DNA of QoI-sensitive and -resistant *E. necator* isolates. This diagnostic tool was sensitive to one-conidium equivalent of extracted DNA with an R^2 value of 0.82 and 0.87, for G-143 and A-143 reactions, respectively. This diagnostic approach was also evaluated against a TaqMan probe-based assay using 92 *E. necator* samples collected from vineyards. The PNA-LNA-LAMP assay detected QoI resistance in ≤ 30 minutes and showed 100% agreement with

the TaqMan probe-based assay (≤ 1.5 hours) for the QoI-sensitive and -resistant isolates. There was 73.3% agreement with the TaqMan probe-based assay when samples had mixed populations with both G-143 and A-143 alleles present. Validation of the PNA-LNA-LAMP assay was conducted in three different laboratories with different equipment. The results showed 94.4% accuracy in one laboratory and 100% accuracy in two other laboratories. The PNA-LNA-LAMP diagnostic tool was faster and required less expensive equipment relative to the previously developed TaqMan probe-based assay, making it accessible to a broader range of diagnostic laboratories for detection of QoI resistance in *E. necator*. This research demonstrates the utility of the PNA-LANA-LAMP for discriminating SNPs from field samples and its utility for point-of-care monitoring of plant pathogen genotypes.

Introduction

Erysiphe necator Schwein (syn. *Uncinula necator*), an obligate ectobiotrophic fungal pathogen, causes grape (*Vitis* sp.) powdery mildew (GPM) worldwide and leads to deterioration of yield and fruit quality (Gadoury et al. 2012). Management of grape powdery mildew typically requires 4 to 17 preventive fungicidal applications annually, accounting for more than 30% of production costs (Baudoin et al. 2008; Dufour et al. 2011; Fuller et al. 2014; Sambucci et al. 2019). Effective management of this disease has been widely dependent on the combination of both contact fungicides and systemic fungicides. Among the systemic fungicides used for GPM management worldwide, the quinone outside inhibitors (QoIs, strobilurins; FRAC 11) are frequently applied throughout the growing season (Miles et al. 2012). There are more than 12 commercial products formulated using five FRAC 11 active ingredients (azoxystrobin, kresoxim-methyl, mandestrobin, pyraclostrobin, and trifloxystrobin) labeled for use on grapes (Wise et al. 2020). QoI fungicides are popular due to high efficacy of their active ingredients,

effectiveness against multiple grape diseases (*Botrytis* bunch rot, GPM, and grape downy mildew), and relative affordability (Bartlett et al. 2002; Baudoin et al. 2008; Miles et al. 2012; Miles et al. 2021).

QoI fungicides have site-specific activity and are effective against major groups of plant pathogens, namely, ascomycetes, basidiomycetes, and oomycetes (Bartlett et al. 2002). QoI fungicides inhibit mitochondrial respiration by binding to the Q₀ site (ubiquinol oxidation center) of the cytochrome *b* gene (*Cytb*). This binding results in blockage of electron transfer from cytochrome *b* to cytochrome *c*₁ and eventually stops the energy cycle by preventing synthesis of adenosine-5'-triphosphate (ATP) (Bartlett et al. 2002; Kunova et al. 2021). However, due to repetitive use and the single gene site mode of action, resistance to QoI fungicides in several grape pathogens has been reported in many growing regions of the United States and other countries (Baudoin et al. 2008; Dufour et al. 2011; Miles et al. 2012). The FRAC has also compiled a list reporting QoI resistance in 36 plant pathogens in other field crops (FRAC 2012). In the *Cytb* gene, more than 11 single nucleotide polymorphisms (SNPs) have been identified that confer different levels of QoI resistance in a variety of organisms. However, three mutations, namely G143A, F129L, and G137R, are most commonly detected in plant pathogenic fungi resistant to QoI fungicides (Ishii 2009; Ma and Michailides 2005). Among these mutations, G143A (substitution of glycine by alanine at codon 143) is the only one observed in QoI-resistant field isolates of *E. necator* (Baudoin et al. 2008; Miles et al. 2012; Miles et al. 2021; Rallos et al. 2014).

To minimize the impact of fungicide resistant populations in the vineyard, it would be beneficial to monitor resistance in field populations to prevent management failures. Several traditional methods have been used to monitor QoI resistance in *E. necator*, such as spore

germination assays on media altered with different fungicide concentrations and quantitative real-time PCR (qPCR)-based assays using SYBR Green-based mechanisms to detect the mutant-type allele (A-143) (Baudoin et al. 2008; Dufour et al. 2011; Miles et al. 2012). However, these methods are laborious, time-consuming, often inaccurate, expensive, and require additional verification (Miles et al. 2012; Miles et al. 2021). More recently, digital droplet PCR- and qPCR-based allelic discrimination assays using TaqMan probes have been developed that can effectively differentiate wild-type (G-143) and mutant-type (A-143) alleles in *E. necator* simultaneously in the same reaction (Miles et al. 2021). These TaqMan probe-based assays utilize specific primers for the target region and discriminating probes that are optimized for amplifying specific alleles that increase accuracy (Miles et al. 2021). However, these assays require expensive equipment and a trained operator, making them unsuitable for point-of-care use by growers.

Unlike the aforementioned detection methods, isothermal amplification techniques do not require expensive and complicated equipment or intense labor inputs. These techniques can deliver point-of-care capability, as they can amplify crude DNA at a constant temperature and do not always require an expensive thermocycler apparatus or time-consuming DNA extractions (Notomi et al. 2000). Several isothermal techniques such as recombinase polymerase amplification (RPA) (TwistDx Ltd., Cambridge, UK) and helicase-dependent amplification (HDA) (Biohelix Corp., Beverly, MA, USA) are available, but are proprietary (Miles et al. 2015), which can limit licensing and thus adoption. One main advantage of the RPA technique is the availability of commercial kits in several formats that can be used with user-designed primers and probes. This technique, similar to TaqMan qPCR, can also be multiplexed using fluorescent-

labelled probes for real-time DNA detection (Li et al. 2019; Lobato and O'Sullivan 2018; Miles et al. 2015).

Loop-mediated isothermal amplification (LAMP) is another isothermal method (Fan et al. 2018; Notomi et al. 2000) that can be highly specific, efficient, and rapid, with less than 30 min amplification time (Notomi et al. 2000). Amplified products can be visualized by using metal-ion indicators including calcein, CuSO_4 , and hydroxynaphthol blue in the reaction (Goto et al. 2009; Zhang et al. 2013). Various DNA-intercalating dyes including SYBR Green I, Quant-iT PicoGreen, and ethidium bromide, can also be used for unaided visual detection (Pan et al. 2015). Since LAMP reactions can be visually assessed in relatively inexpensive devices (e.g. block heater water bath), or fluorometrically (Kubota et al. 2011) using portable devices (e.g. Genie II (OptiGene Ltd, Horsham, UK), T16-ISO Axxin (Axxin, El Segundo, CA), it is a promising candidate for point-of-care diagnostics (Notomi et al. 2000).

Heavily modified oligos using peptide nucleic acids (PNA) and locked nucleic acids (LNA) have recently been used in real-time DNA detection technologies to increase sequence specificity (Itonaga et al. 2016). A PNA clamping qPCR method has been employed for detecting hereditary hemochromatosis gene mutations (Kyger et al. 1998). PNAs are synthetic DNA analogs with a 2-aminoethylglycine chain that replaces the normal phosphodiester backbone. LNAs are synthetic DNA/RNA analogs in which the ribonucleotide structure is modified by joining the 2'-oxygen and 4'-carbon atoms with a methylene bridge. These PNA probes are more sensitive to mismatches than DNA probes since a completely matched PNA-DNA duplex has a higher melting temperature (T_m) compared to a completely matched DNA-DNA duplex (Kyger et al. 1998). In addition, PNA can be designed as a probe to block the amplification of a perfectly matched DNA template. The flexibility and accuracy have enabled

the PNA-LNA-LAMP technology to detect mutations such as the Kirsten rat sarcoma viral oncogene homologue (KRAS) mutation in breast cancer cells (Itonaga et al. 2016).

These developments in isothermal amplification technologies seem promising for monitoring point mutations associated with fungicide resistance in *E. necator*. In this study, we focused on: (i) developing isothermal technologies such as RPA and PNA-LNA mediate LAMP assays for G143A detection in QoI-sensitive and -resistant isolates in mixed *E. necator* samples; (ii) optimizing newly developed isothermal tools and validating those optimized tools on field samples collected from various vineyards in the Great Lakes region; and (iii) validating these technologies in separate laboratories and developing a protocol for technology transfer. To our understanding, this is the first study that uses the PNA-LNA-LAMP technique to distinguish SNP in plant pathogens.

Materials and methods

Erysiphe necator sample collection

In 2019, a total of 92 *E. necator* samples were collected from 17 commercial vineyards across MI, WI, IN, OH, and NY and from three research station vineyards operated by Michigan State University (MSU). *E. necator* was collected throughout the growing season from infected grape leaves and berries. Four infected leaves/clusters per variety per vineyard site were collected, and in the case when a site had multiple varieties, multiple collections were made.

After field collection, infected grape leaves and berries were placed into sealable plastic bags and transported in a cooler back to the lab at MSU (East Lansing, MI, USA). In the lab, single powdery mildew colonies were collected from leaves and berries using Tough-Spots (Diversified Biotech, Inc., Dedham, MA, USA) (Thiessen et al 2019). As positive and negative control, purified DNA of QoI-resistant (A-143 allele) and -sensitive (G-143 allele) *E. necator* isolates from a

previous study were used (Miles et al. 2012). In addition, DNA from 12 air samples collected by Thiessen et al. (2016, 2018) from Oregon vineyards were also tested using both G-143 and A-143 reactions of the PNA-LNA-LAMP assays.

Crude DNA isolation from field samples

Crude DNA extractions of field samples were conducted following a modified version of the tape DNA extraction method described by Brewer and Milgroom (2010) and Thiessen et al. (2019). The 2-ml microcentrifuge tubes containing Tough-Spots samples were centrifuged for 1 min at 16,000 x g to move the Tough-Spots to the bottom of the tube. To each sample tube, 200 µl of 5% (w/v) Chelex (Sigma-Aldrich, Saint Louis, MO, USA) in molecular-grade water was added. Tubes were vortexed horizontally for 5 min at 3,200 rpm and centrifuged for 20 s at 16,000 x g to collect the content at the bottom of the tube. Tubes were incubated at 95°C for 10 min on a heat block. After incubation, each sample tube was vortexed for 5 s, centrifuged for an additional 20 s at 16,000 x g, followed by another 10 min incubation at 95°C. Each tube was then kept at 22°C for 20 min to cool. After cooling to room temperature, each tube was centrifuged for 2 min at 16,000 x g and the supernatant was transferred to a sterile 1.5-ml microcentrifuge tube. Crude DNA samples were stored at -20°C until detection analysis.

*Development of an RPA assay to detect QoI resistance of *E. necator**

An RPA assay was designed using RPA TwistAmp Exo kits (TwistDx Inc., Cambridge, UK; Product code: TAEXO02KIT), and the primers and probes outlined in Miles et al. (2021) for the *Cytb* region. All reactions followed manufacturer's protocols, and reaction volumes were 50 µl. Using the manufacturer's guidance, the fluorophore was conjugated to the nucleotides at the unique SNP location in the *Cytb* gene responsible for the G143A amino acid shift. In addition, lengthened primers and a modified probe (Table 2.1) from Miles et al. (2021) were developed. A

collection of eight *E. necator* phenol chloroform-extracted DNA samples were used from Miles et al. (2012) to screen for specificity (i.e., four samples containing the G-143 allele and four samples containing the A-143 allele). Sensitivity was tested by conducting a serial dilution from 1 ng/μl to 1 fg/μl of purified DNA using two *E. necator* DNA samples from Miles et al. (2012) (TC-BD-V08 containing G-143 allele and AV-C-28 containing the A-143 allele). Balanced and unbalanced primer concentrations (Table 2.5) were tested to achieve allelic discrimination as in Miles et al., (2015). All reactions were conducted in three times using Bio-Rad CFX96 machine (Bio-Rad Laboratories, Hercules, CA, USA) to monitor the FAM and HEX fluorescence at 39 to 42°C every 20 s for a period of 60 min. Onset of amplification threshold (OT) was determined by methods outlined in Miles et al. (2015).

Development of a LAMP assay to detect QoI resistance of E. necator

Mitochondrial DNA sequences of *E. necator* (accession numbers/scaffold information/isolate name: JNUS01000009.1/scaffold_10/branching, JNVN01000008.1/scaffold_14/c c strain, JOKO01000016.1/scaffold_16/e1-101, JNUU01000038.1/scaffold_43/lodi and JNUT01000020.1/scaffold_23/ranch-9) and four closely related Erysiphales species (Jones et al. 2014; Miles et al. 2021) were obtained from the National Center for Biotechnology Information (NCBI) database and aligned using Geneious R9 (Biomatters Ltd., New Zealand). Several sets of four primary LAMP primers (F3, FIP, B3, BIP) were generated based on the *Cytb* gene of *E. necator* using Primer Explorer V5 (Eiken Chemical, Japan) and manually modified using Geneious R9. To selectively amplify the G143A mutation, different strategies were used: a mismatch placed before the SNP, a mismatch introduced two bases away from the SNP, an extra base after the SNP at the 3' end, and reduced distance in the primers. However, none of these primer sets could consistently detect the G143A mutation when

samples were analyzed using qPCR (Table 2.6). Hence, a PNA-LNA-LAMP assay was developed instead of a conventional LAMP assay.

Development of PNA-LNA- LAMP assay to detect QoI resistance of E. necator

A PNA-LNA-LAMP assay consisting of two competitive reactions was developed, with modifications, to detect QoI resistance in *E. necator* based on the principle of PNA-LNA LAMP as described by Itonaga et al. (2016) (Fig. 2.1). This assay consisted of an independent A-143 reaction designed for rapid amplification of the mutant A-143 allele, and a G-143 reaction designed for amplification of the wild-type G-143 allele. Each experimental sample was tested with both reactions simultaneously and results of “sensitive” (wild-type) or “resistant” (mutant) were based on which reaction amplified first.

A set of four LAMP primers and a specific LNA primers and PNA probes were designed for each of G-143 and A-143 reactions of the PNA-LNA-LAMP assay (Table 2.1). In the G-143 reaction, a LNA primer complementary to a sequence containing the wild-type nucleotide, and a clamping PNA probe complementary to a sequence containing mutated nucleotide were designed using Geneious R9 (Biomatters Ltd., New Zealand). Similarly, a LNA primer complementary to a sequence containing the mutated nucleotide, and a clamping PNA probe complementary to a sequence containing wild-type nucleotide, were designed for A-143 reaction. LNA primers and PNA probes were obtained from PNA BIO INC (California, USA) and QIAGEN (Hilden, Germany).

Optimization of G-143 and A-143 reactions of PNA-LNA-LAMP assay

Six different concentrations of the FIP and BIP (0.96, 1.2, 1.28, 1.6, 2, and 2.4 μM), five concentrations of the F3 and B3 (0.12, 0.16, 0.2, 0.24, and 0.4 μM), five concentrations of the LNA primer (0.2, 0.4, 0.8, 1.2, and 1.6 μM), and five concentrations of the PNA probe (0.25, 1.0,

1.25, 1.5, and 2.0 μM) were tested. The primer optimization reactions were run at 50 to 68°C with 3°C increments to determine the optimal temperature based on specificity. Each reaction had three technical replicates, and experiment was conducted three times using a Bio-Rad CFX96 qPCR machine.

The optimized reaction had an initial volume of 12.5 μl , containing 7.5 μl of GspSSD Isothermal Mastermix (Optigene), 0.96 μM each FIP and BIP, 0.12 μM each F3 and B3, 0.8 μM LNA, 1.25 μM PNA, 1.32 μl of ddH₂O and 1 μl of DNA template. LNA-WT and PNA-WT, and LNA-MT and PNA-MT were used for the G-143 reaction and A-143 reaction of PNA-LNA-LAMP assay, respectively. The reaction was carried out at 62°C for 60 cycles (the cutoff from for a positive sample) and fluorescence read every 30 s. The optimized PCR reagents used in this study are listed in Table 2.1. Although LAMP reactions are not typically recorded terms of Ct values, for the Bio-Rad CFX96 qPCR machine a cycle threshold (Ct) value is also mentioned as an indication of the onset of amplification because fluorescence is read at discrete intervals and not continuously.

Sensitivity of the PNA-LNA-LAMP assay

The limit of detection of the G-143 and A-143 reactions of the PNA-LNA-LAMP assay were determined by analyzing known concentrations of both *E. necator* purified DNA and conidia. First, purified DNA of a QoI-resistant and a QoI-sensitive *E. necator* isolate were serially diluted ranging from 1 ng/ μl to 100 ag/ μl and loaded separately for both reactions. The PNA-LNA-LAMP assay was conducted at 62°C for 30 s with a repeat for 70 cycles (translates to 52.5 min) on the Bio-Rad CFX96 qPCR machine. The reaction time threshold cutoff was set higher here than in the rest of the experiments optimized assay (60 cycles) to observe if lower DNA concentrations required greater time to amplify. Template DNA from three separate extractions were used to

construct the standard curve plots of the \log_{10} DNA concentration and onset of amplification threshold (OT) in minutes for both reactions of the PNA-LNA mediated LAMP assay. Second, conidial suspensions of a QoI-sensitive isolate EnFRAME01 and a QoI-resistant isolate BPPQ1B.5 were prepared by suspending conidia from detached *V. vinifera* ‘Chardonnay’ leaves (Miles et al. 2021) in 200 μ l of 5% (w/v) Chelex suspension (prepared as above) in 1.5-ml Eppendorf tubes. The conidial concentration of the suspension was evaluated using a hemocytometer, and adjusted to 1000, 10,000, and 10,000 conidia per ml. This translates into 100, 1000, and 10,000 conidia per 100 μ l which is approximate volume of total suspension after DNA extractions. Similarly, one-conidium and 10-conidia per 100 μ l concentrations were prepared by manually transferring conidia using an eyelash brush to 1.5-ml Eppendorf tubes containing 200 μ l of 5% (w/v) Chelex suspension. The DNA extractions performed as described above. Four replicate extractions of each conidial concentration were tested using G-143 and A-143 reactions of the PNA-LNA-LAMP assay and the TaqMan probe-based G143A qPCR assay (Miles et al. 2021) to construct standard curve plots.

Specificity of the PNA-LNA-LAMP assay

The specificity of the PNA-LNA-LAMP assay to discriminate between mutant and wild-type alleles of *E. necator* as well as its ability to discriminate other Erysiphales was conducted in two approaches. First, purified DNA of eight QoI-resistant and eight QoI-sensitive isolates were tested using the PNA-LNA-LAMP assay. These isolates were also tested with the G143A TaqMan assay (Miles et al. 2021) and the results from both assays were compared using ROC analyses (Turechek and Wilcox 2005) where the TaqMan probe-based assay was assumed to be accurate and treated as the gold-standard. Next, the PNA-LNA-LAMP assay was run using DNA isolated from other powdery mildew species within the Erysiphales that infect blueberry (*E. vaccinii*), oak

(*E. alphitoides*), rose (*P. pannosa*), pea (*E. pisi*), and squash (*Podosphaera xanthii*) collected from Monterey County, California (Miles et al. 2021). A total of 12 samples (two samples for each species) were tested. In both approaches, all LAMP and qPCR reactions had three technical replicates, and experiment was conducted using the Bio-Rad CFX96 qPCR machine.

To understand potential cross reactivity across powdery mildew species a partial alignment was performed using Geneious R9 (Biomatters Ltd., New Zealand). A small region of the *Cytb* gene containing the G143A SNP of several powdery mildew species including *E. necator*, *E. pisi*, *E. alphitoides*, *Blumeria graminis* and *Podosphaera leucotricha* were partially aligned to evaluate the likelihood of cross-reaction of these diagnostic tools. Mitochondrial DNA sequences of different isolates of *E. necator* (Jones et al. 2014; Zaccaron et al. 2021) and other powdery mildew species were obtained from the NCBI database and aligned using Geneious R9.

Evaluation of PNA-LNA-LAMP assay on in vitro mixed genotype samples

An *in vitro* experiment was conducted to determine differences in onset of amplification between the G-143 and A-143 reactions of PNA-LNA-LAMP assay when mixed genotype samples were used. Purified DNA from QoI-sensitive and -resistant isolates with equal DNA concentrations (starting concentration of each isolate = 1 ng/μl) were mixed at different ratios, each totaling 1 ng of DNA (1 ng/μl = 100%). Seven mixed samples were prepared with the following mutant-type to wild-type ratios 100:0, 90:10, 75:25, 50:50, 25:75, 10:90, 0:100. All reactions had three technical replicates, and experiment was conducted two times using Bio-Rad CFX96 qPCR machine.

Validation of PNA-LNA-LAMP assay on field samples

The efficiency of the PNA-LNA-LAMP assay to detect wild-type and mutant-type alleles was tested on field samples collected from vineyards in Michigan, Ohio, Wisconsin, New York,

and Indiana. Crude DNA (see *DNA isolation*) isolated from 92 field samples of *E. necator* from diseased grape leaf and fruit clusters and 12 air samples were evaluated for the G143A mutation. All samples were also tested utilizing the TaqMan probe-based assay to verify the accuracy of the results obtained from the PNA-LNA-LAMP assay. In both assays, all reactions had three technical replicates, and experiment was conducted two times using Bio-Rad CFX96 qPCR machine.

Evaluation of robustness of the PNA-LNA-LAMP assay using different machines

The accuracy of the PNA-LNA-LAMP assay was tested on three different PCR machines. Purified DNA of one QoI-resistant and one QoI-sensitive isolate, crude DNA of two field samples and water used as a negative control were tested for the G143A mutation using the PNA-LNA-LAMP assay on three machine platforms including Genie II, T16-ISO Axxin, and Bio-Rad CFX96 qPCR detection system. The PNA-LNA-LAMP assay was conducted at 62°C for 30 min on the Genie II and T16-ISO Axxin machines; and the reaction conditions for Bio-Rad CFX96 qPCR were 62°C for 60 cycles. All reactions had three technical replicates. The low-profile tubes (Bio-Rad Laboratories, Hercules, CA) were used to conduct the assay in all machines.

Evaluation of reproducibility of the PNA-LNA-LAMP assay

To test reproducibility of the assay, an experiment using the PNA-LNA-LAMP assay was conducted by different personnel at three separate laboratories located in Corvallis, OR using an Applied Biosystems QuantStudio 5 Real-Time PCR System: Parlier, CA, and Prosser, WA using a Bio-Rad CFX96 machine. A technology transfer protocol was developed and provided to the laboratories. This experiment was done in three progressive steps, including: 1) Test seven purified *E. necator* DNA samples with G-143 status known to users; 2) Test seven crude DNA from field samples of *E. necator* with G-143 status unknown to users; and 3) Test user-supplied *E. necator* samples, these samples were specific to each location. These samples were tested two times at

each location and had three technical replicates to ensure the specificity and consistency of results. All samples were also tested at the MSU laboratory using the PNA-LNA-LAMP assay and TaqMan-probe based assay to confirm the results from the other laboratories.

Comparison of the newly developed SNP distinguishing PNA-LNA-LAMP assay with previously developed E. necator LAMP detection tool

Crude DNA of sixteen field samples of *E. necator* including 15 QoI-resistant samples were tested using the PNA-LNA-LAMP assay and *E. necator* LAMP detection tool developed by Thiessen et al. (2016). All tested samples were QoI-resistant, therefore only the A-143 reaction of the PNA-LNA-LAMP assay was conducted. The reactions had two technical replicates, and water was used as negative control. Both assays were conducted on Bio-Rad CFX96 qPCR machine. The PNA-LNA-LAMP assay was conducted at 62°C for 30 s with a repeat for 60 cycles. *Erysiphe necator* LAMP detection assay was conducted at 65°C for 30 s with a repeat for 60 cycles. Regression analysis was done using Ct values from both assays as data points to understand the correlation between these two assays while detecting *E. necator*.

Statistical analysis

For the PNA-LNA-LAMP assay, the experiment setup and data generation were done using CFX Manager 3.1 software (Bio-Rad Laboratories), T16 Desktop software (Axxin), and Genie Explorer (OptiGene Ltd), while only the CFX Manager 3.1 software was used for TaqMan probe-based assay. Microsoft Excel (Redmond, WA, USA) and SigmaPlot 11 (Systat Software, Inc., San Jose, CA, USA) were used for all other data analyses. In this study, accuracy was defined as the ability of the assay to distinguish between true positive and true negative correctly using the formula $((\text{True Positive} + \text{True Negative}) / (\text{Total no. of samples}))$ (Baratloo et al. 2015).

Simple regression analysis was conducted using SigmaPlot 11 (Systat Software, Inc., San Jose, CA, USA).

Results

Efficacy of RPA reactions to discriminate the G143A alleles in E. necator

A variety of attempts were made utilizing the RPA in order to discriminate the G- or A-143 alleles of *E. necator* (Table 2.5). However, optimizing the RPA reaction conditions by modifying either temperature or primer concentration was not effective, and end point relative fluorescent values and onset of amplification values were similar, regardless of the allele being tested. Given these challenges, we pursued the PNA-LNA-LAMP assays as the primary isothermal method in this study.

Sensitivity of the PNA-LNA-LAMP assay

Even at very low DNA concentrations, the PNA-LNA-LAMP assay was sensitive and successfully identified the G-143 allele (wild-type) and the A-143 allele (mutant-type), respectively (Fig. 2.2). For the sensitivity assay using genomic DNA, the limit of detection of G-143 and A-143 reactions of the PNA-LNA-LAMP assay when tested on seven-fold dilutions of purified DNA was 100 fg/μl for their specific target (Fig. 2.2A; B). For sensitivity assay using conidial concentrations, the detection limit was one-conidium for both G-143 and A-143 reactions of the PNA-LNA-LAMP assay (Fig. 2.3A; B). However, reactions with one-conidium and 10-conidial concentrations amplified in ≤ 30 minutes. Even at the higher cutoff of reaction time threshold value (52.5 min), the water control did not amplify. The TaqMan probe-based assay consistently detected down to 100 conidia but did not consistently amplify all reactions at 1 and 10-conidial concentrations using the Chelex extraction method (Fig. 2.3C; D).

Specificity of the PNA-LNA-LAMP assay

Step one: Results showed that the time to amplification was useful for discrimination of the G-143 and A-143 alleles in purified DNA for all tested QoI-sensitive and -resistant isolates. Both G-143 and A-143 reactions of the PNA-LNA-LAMP assay amplified their respective target in less than 22 mins, while their off-target typically amplified 7 or more minutes later (Table 2.2). The PNA-LNA-LAMP assay showed 100% accuracy when confirmed with the TaqMan probe-based assay.

Step two: Analysis of genomic DNA of several other powdery mildews species in the Erysiphales with the *E. necator* PNA-LNA-LAMP assay yielded mixed results. No real-time amplification was detected for *P. pannosa* in both the G-143 and A-143 reaction of the PNA-LNA-LAMP. Both reactions amplified *E. alphitoides*, *E. vaccinii* and *E. pisi* and only the G-143 reaction of PNA-LNA-LAMP assay amplified *P. xanthii*. Actual fungicide resistance status of these mildew species was unknown.

The partial alignment of the *Cytb* region of *E. necator* and other powdery mildew species showed that *E. necator* and *E. pisi*, are highly similar in the target region that are amplified by the PNA-LNA-LAMP assay and the TaqMan probe-based assay (Miles et al. 2021). However, *E. alphitoides*, *B. graminis* and *Podosphaera leucotricha* showed far less resemblance with our target region of the *Cytb* gene of *E. necator* (Fig. 2.4).

Evaluation of PNA-LNA-LAMP assay on in vitro mixed genotype samples

An *in vitro* experiment was conducted on samples containing DNA from QoI-sensitive and -resistant isolates mixed in varying ratios. Results showed that the samples containing 100% G-143 allele (wild-type) amplified approximately 17 mins earlier in the G-143 reaction than in the A-143 reaction of the PNA-LNA-LAMP assay (Fig. 2.5). Similarly, for samples containing 100%

A-143 allele (mutant), the A-143 reaction amplified 8 mins faster than the G-143 reaction (Fig. 2.5). However, the difference in amplification time between the two reactions of the PNA-LNA-LAMP assay was less than 4.5 mins with samples containing both alleles, regardless of relative allele concentration (Fig. 2.5). Based on this *in vitro* mixed sample experiment, a sample was considered a ‘mixed sample’ if the amplification time difference between both assays was ≤ 4.5 mins.

Validation of the PNA-LNA-LAMP assay using field samples

For the field samples tested, the PNA-LNA-LAMP assay was in 100% agreement with the TaqMan probe-based assay when samples were either QoI-sensitive or QoI-resistant, but not when the sample was mixed (Table 2.3). In the case of the mixed samples, the PNA-LNA-LAMP assay was able to accurately detect 73.3% (22/30) mixed samples; it otherwise misclassified 10% (3/30) mixed samples as QoI-sensitive and 16.7% (5/30) mixed samples as QoI-resistant. For air samples tested, the PNA-LNA-LAMP assay accurately detected 75% (9/12) samples but failed to detect 16.7% (2/12) and incorrectly detected 8.3% (1/12) mixed samples (Table 2.7).

Evaluation of robustness of the PNA-LNA-LAMP assay using different machines

The PNA-LNA-LAMP assay worked well on all three machines tested (T16-ISO Axxin, Genie II, and Bio-Rad CFX96 qPCR) in this study with consistent results and low background noise (Fig. 2.6). All machines showed 100% accuracy in detection of G-143 or A-143 allele of the tested samples and no amplifications were observed for the negative water control. The time of the onset of amplification for a purified DNA sample was shorter with T16-ISO Axxin (Fig. 2.6A), while approximately similar time frames of amplification were observed with the other two machines (Fig. 2.6B; C).

Evaluation of reproducibility of the PNA-LNA-LAMP assay

An experiment consisting of three parts was conducted to ensure easy transfer of the PNA-LNA-LAMP technology to other research or diagnostic laboratories. The results performed well for a variety of samples in the other laboratories (Table 2.4). The PNA-LNA-LAMP assay was 100% (14/14) accurate in detecting QoI-resistance for two locations (Table 2.4). For test conducted in Corvallis, OR, the PNA-LNA-LAMP assay showed 94.4% accuracy (17/18) in the user-supplied samples, when the assay incorrectly detected one mixed sample as QoI-sensitive.

*Comparison of the newly developed SNP distinguishing PNA-LNA-LAMP assay with previously developed *E. necator* LAMP detection tool*

The results from regression analysis of detecting *E. necator* samples using PNA-LNA-LAMP assay and the *E. necator* LAMP detection assay (Thiessen et al. 2016) were significant ($P < 0.001$) and $R^2 = 0.57$. The *E. necator* LAMP detection tool developed by Thiessen et al. (2016) detected all samples earlier than the PNA-LNA-LAMP assay with ≈ 14 Ct value (approximately ≈ 10.5 min) difference (Fig. 2.7). The samples that had lower DNA concentrations amplified later in both assays. These samples amplified at ≈ 14 Ct value (approximately ≈ 10.5 min) for *E. necator* LAMP detection tool (Thiessen et al. 2016) and ≈ 32 Ct value (approximately ≈ 24 min) for PNA-LNA-LAMP assay. The negative control did not amplify in both assays.

Discussion

This PNA-LNA-LAMP assay is a novel isothermal technology that utilizes six independent regions in the first stage (formation of stem-loop DNA) followed by four independent regions in the final stage (amplification of stem-loop DNA) to recognize a target SNP (Notomi et al. 2000). Since *E. necator* is an obligate pathogen, detecting QoI-resistance using conventional conidial germination assays is inefficient, laborious, and does not produce

results in a timeframe that can be used for actionable decision making by interested parties (e.g., growers and field managers). Several molecular-based detection methods such as conventional PCR, ARMS-SYBR Green qPCR assays (Miles et al. 2012), TaqMan-probe based qPCR assays, and digital-droplet PCR assays have been developed for G143A detection (Baudoin et al. 2008; Miles et al. 2021). However, this PNA-LNA-LAMP assay has advantages: 1) It can be performed under isothermal conditions at 62C; and 2) Unlike other detection methods, this assay can be performed with inexpensive equipment. It also has a short detection time (less than 30 min), while the TaqMan probe-based qPCR assay and other assays have longer reaction times (more than 1.5 hrs). The consistent limit of detection of the TaqMan probe-based qPCR assay presented here is 100 conidia; while some detections occurred at 1 and 10 conidia, all replicates did not consistently amplify. However, based on the sensitivity results presented here, the PNA-LNA-LAMP assay consistently detected down to 1 conidium when the limit of reaction time threshold cutoff was set higher (70 cycles ~52.4 min). Therefore, the PNA-LNA-LAMP assay is more consistent and sensitive than TaqMan probe-based qPCR assay. While the conventional PCR and ARMS-SYBR Green qPCR require higher concentration of high-quality DNA, the PNA-LNA LAMP assay could detect the G143A mutation at very low concentrations of rapidly extracted, crude DNA of *E. necator*. Our results showed that although the TaqMan probe-based qPCR assay is more accurate in detecting mixed samples, however, the PNA-LNA-LAMP assay was able to accurately detect the G-143 allele (wild-type) and the A-143 allele (mutant-type) from field samples when only one of the alleles was present.

Several sample types, such as high-quality DNA, crude extracted DNA from colonies on infected leaves and berries, and crude-extracted DNA from air samples, were tested using this new approach. The PNA-LNA-LAMP assay was not effective on crude DNA extracted from air

samples, likely due to very low quantities of template DNA (Table 2.7) and/or the presence of PCR inhibitors such as humic acids from soil particles in air, spider webs, pollen, etc., that cannot be removed in crude Chelex extractions (Wilson 1997; Thiessen et al. 2018) (Table 2.7). Similarly, a quantitative LAMP (qLAMP) that was developed for in-field detection of *E. necator* also showed inconsistencies in detection of *E. necator* spores from air samples (Thiessen et al. 2018). Even though LAMP is considered tolerant to the presence of inhibitors, this is not always the case (Nixon et al. 2014). Thiessen et al. (2018) also found that use of the PowerSoil DNA extraction resulted improved detection in the air samples compared to Chelex extraction. However, PowerSoil DNA extraction is expensive, time-consuming, and not fit for on-farm detection protocols.

Isothermal technologies such as LAMP, RPA and HDA have been used for identifying fungi, bacteria, viruses, and transgenic plants. Many species-specific RPA assays are commercially available for detection of plant pathogens, e.g., *Banana bunchy top virus* (BBTV), *Clavibacter michiganensis* subsp. *michiganensis*, *C. michiganensis* subsp. *sepedonicus*, and *Xylella fastidiosa* (Agdia Inc. Elkhart, IN USA). Recombinase polymerase amplification (RPA) combined with surface-enhanced Raman scattering (SERS) labelled nanotags has also been deployed for multiplex detection of *Botrytis cinerea*, *Fusarium oxysporum* and *Pseudomonas syringae* in a single tube (Lau et al. 2016). This technology is highly efficient and sensitive due to its tolerance of PCR inhibitors, background DNA, temperature fluctuation, and mismatches. RPA is very tolerant to mismatches within primer sequences (nine nucleotides) across the primer and probe binding sites (Daher et al. 2015). Although the mismatch tolerance could be advantageous for designing primers for highly polymorphic targets, it can be a drawback for detecting closely related species and SNPs that are associated with fungicide resistance. In this

study, the RPA assay also failed to differentiate between the G-143 allele (wild-type) and the A-143 allele (mutant-type) as onset of amplification values were similar, irrespective of allele type. Further research into primer and/or probe design with regards to SNP placement is required for the RPA technology to be successful.

In contrast, LAMP assays are promising for detection of point mutations. For example, a LAMP method was applied for detection of: (1) the I1781L mutation in American slough grass that confers resistance to fenoxaprop-p-ethyl (Pan et al. 2015); (2) the F167Y mutation in carbendazim-resistant *Fusarium graminearum* (Duan et al. 2014); and (3) the H272R mutation in succinate dehydrogenase inhibitors (SDHI)-resistant isolates of *Botrytis cinerea* (Fan et al. 2018). Similarly, the PNA-LNA-LAMP assay developed here efficiently detected the G143A mutation in *E. necator*. These results indicate that LAMP technology could be broadly useful for rapid in-field detection of known fungicide resistance alleles (Alzohairy et al. 2021).

Transferability of any diagnostic tool is needed if it is to be adopted on a large scale. The PNA-LNA-LAMP assay performed well when tested using different machine platforms and in different laboratories by different personnel. Although there were slight differences in amplification while using different machines, results showed that samples were correctly identified when a single genotype was present. The key to transferability is providing reference samples (positive and negative controls) with the protocol. This appears to be true of the assay developed in this study, but is also true of TaqMan assays, as it aids in interpreting and understanding the methodology and results (Miles et al. 2021). The drawbacks of the PNA-LNA-LAMP assay are that it still requires some laboratory skills and equipment, like pipettes, centrifuges, vortexes, microcentrifuge tubes and heat blocks. While relatively inexpensive compared to the purchase of PCR machines, they still might be cost-prohibitive to growers who

might only be processing a few samples. If growers perform this assay using a heat block and visualize the results by adding SYBR Green following amplification, this could potentially lead to cross-contamination of future samples and potential false positives since LAMP amplicons are very stable. Inexperienced practitioners could also face consistency challenges while pipetting the reagents, which could affect the results.

This PNA-LNA LAMP assay had difficulty in detecting both wild-type and mutant-type alleles in mixed samples, but it worked well when a single allele was present. This should be taken into consideration while interpreting results, especially if amplification time difference between G-143 and A-143 reactions is ≤ 4.5 mins (~ 6 cycles). Diagnostic laboratories can potentially use this point-of-care detection assay for surveillance of QoI-resistance in *E. necator*. Unfortunately, results from the specificity tests also showed some Erysiphales closely related to *E. necator* were also amplified by the PNA-LNA- LAMP assay. This could be explained by the low heterogeneity in the *Cytb* gene of *E. necator* from other closely related powdery mildews that would allow for potential cross-reactions.

Our results showed that the *E. necator* LAMP detection tool developed, by Thiessen et al. (2016) is faster at detecting *E. necator* than this PNA-LNA-LAMP assay. Low R^2 value ($=0.57$) while correlating these two detection tools was observed, however, this could be due to crude DNA extractions from field samples which may affect the efficiency due to poor quality and quantity of DNA. Therefore, use of this already available LAMP tool for detecting *E. necator* could be used in conjunction with this PNA-LNA-LAMP assay to initially screen samples for the presence of *E. necator*. The PNA-LNA-LAMP assay could then be used for the purpose of detecting QoI-resistance in samples containing *E. necator*.

Although these isothermal assays have emerged as an alternative to conventional PCR technologies, sensitivity and specificity of these methods still needs to be refined for in-field use. Recently, various CRISPR-Cas-based detection systems such as integrated lateral flow assays (CORDS, CRISPR/Cas12a-LFD); naked-eye detection (CRISPR/Cas-based colorimetric platform, fluorescence-based POC system); and specific high-sensitivity enzymatic reporter unlocking (SHERLOCK) platforms have been explored for human and animal pathogen detection due to their high specificity, sensitivity, and accuracy (Bai et al. 2019; Wang et al. 2020; Yuan et al. 2020). A CRISPR-Cas12b-based DNA detection system combined with RPA was also shown to discriminate a 3232A>G mutation in human *BRCA1* gene responsible for breast cancer (Teng et al. 2019). The specificity and sensitivity of our PNA-LNA-LAMP assay may be enhanced by combining it with CRISPR-Cas detection systems (Pang et al. 2020; Li et al. 2018). The SNP detection process could be simplified for grower use by coupling these LAMP assays with a lateral flow dipstick since it would be easy to perform and read results with the naked eye (Yongkiettrakul et al. 2020).

Overall, our results suggest that this PNA-LNA-LAMP assay has the potential to robustly and effectively detect the G143A mutation associated with QoI-resistance in *E. necator*. This tool could be used for detection of this mutation in public and private diagnostic laboratories, and thus, generate results that growers can use to adjust their grape powdery mildew resistance management strategies. We also believe that this technique will be beneficial in the point-of-care (i.e., farm / field) detection of point mutations in other pathosystems.

Acknowledgements

Many thanks to L. Miles from MSU for generously providing initial DNA samples of *E. necator* used for optimizing PNA-LNA-LAMP assay and comparing results with the TaqMan

probe-based assay; our grape growers from Michigan, Indiana, Ohio and New York who permitted us to get *E. necator* samples from their vineyards; and funding from a USDA-SCRI Award No. 2018-03375 and United States Department of Agriculture (USDA) CRIS 5358-22000-041-00D. The use of trade, firm, or corporation names in this publication is for information and convenience of the reader. Such use does not constitute an official endorsement or approval by the or the Agricultural Research Service of any product or service to the exclusion of others that may be suitable.

Figures

Figure 2.1. Graphical representation of the principle of the peptide nucleic acid-locked nucleic acid mediated loop-mediated isothermal amplification (PNA-LNA-LAMP) tool (modified from Itonaga et al. 2016). When the target allele is present, the LNA primer binds to it, and the extension process starts. However, if the off-target allele is present, then the clamping PNA probe will bind to the off-target allele, interfere with the LNA primer's annealing and extension, and ultimately delay the amplification process. B, The DNA sequence of a region of the *Cytb* gene and position of primers and probes that are used in this study. (Bottom) Bold blue face (G for the G-143 allele; C for the A-143 allele) represents wild and mutated nucleotides, respectively, in the *Cytb* gene. Sequences used as PNA are shown in the blue box, and LNA sequences are indicated by bold type and underlined.

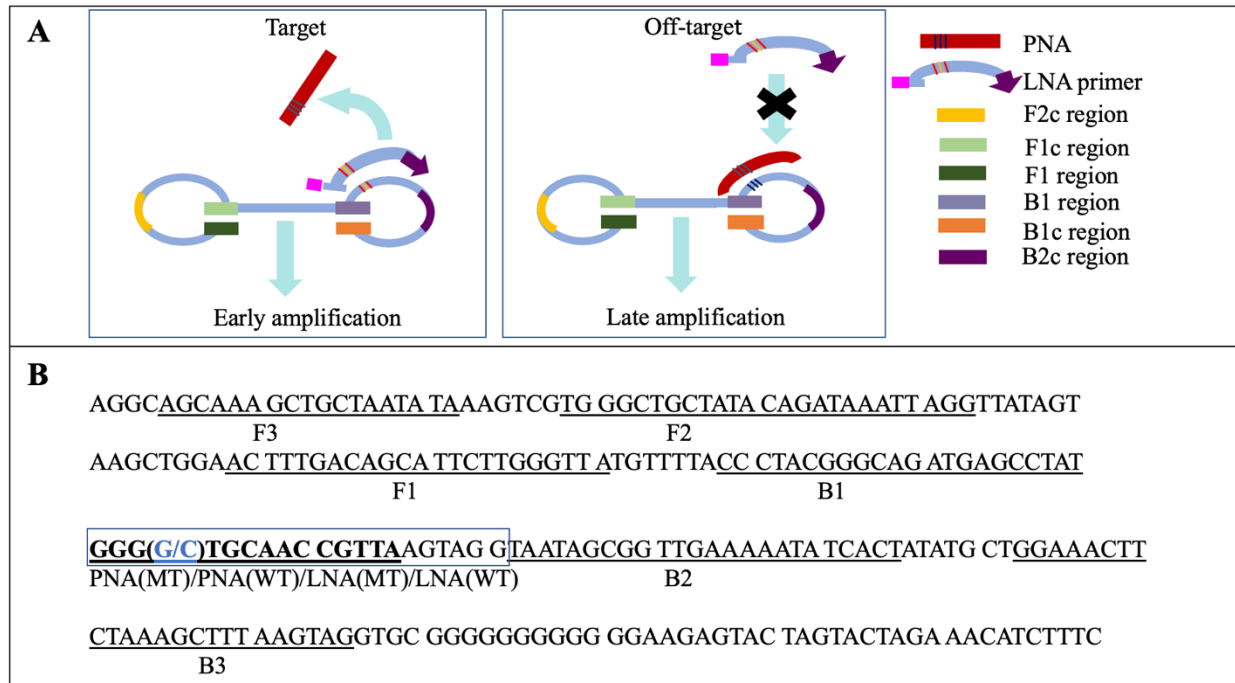


Figure 2.2. Sensitivity of peptide nucleic acid-locked nucleic acid mediated loop-mediated isothermal amplification (PNA-LNA-LAMP) assay with varying purified DNA concentrations. **A**, Various DNA concentrations (ng) of the wild-type (WT) isolate were compared with reaction time threshold values (mins) of the G-143 reaction of PNA-LNA-LAMP assay. **B**, Various DNA concentrations (ng) of the mutant-type (MT) isolate were compared with reaction time threshold values (mins) of the A-143 reaction of PNA-LNA-LAMP assay. The MT isolate (AV-C-28) containing the A-143 allele and the WT isolate (TC-BD-V08) containing G-143 allele were compared at various concentrations from 1 ng/ μ l to 100 ag/ μ l and tested to determine the limit of detection of the assay. All reactions had three technical replicates.

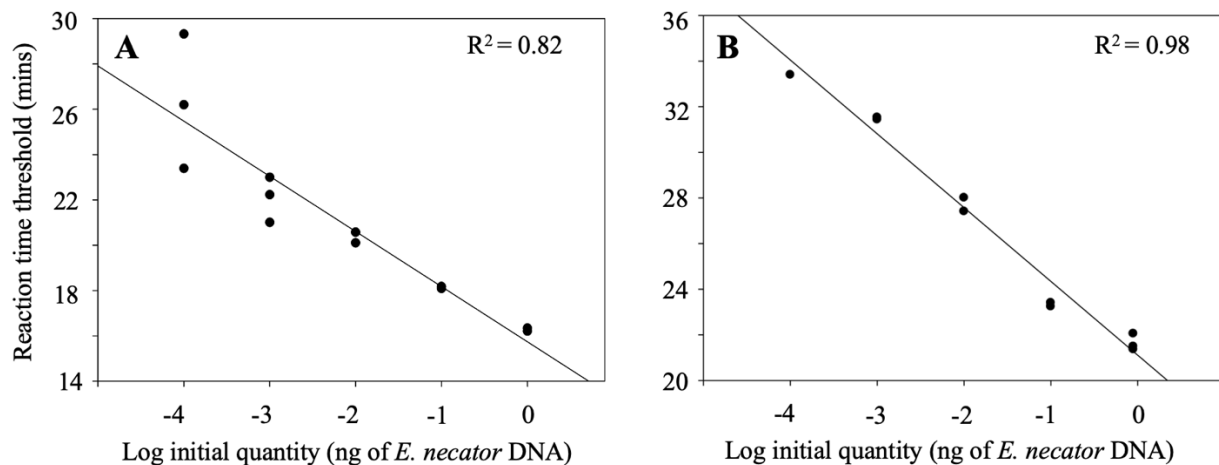


Figure 2.3. Comparison of peptide nucleic acid-locked nucleic acid mediated loop-mediated isothermal amplification (PNA-LNA-LAMP) and TaqMan qPCR-based assay (Miles et al. 2021) sensitivity to varying *Erysiphe necator* conidial concentrations. A, varying conidial concentrations of a wild-type (WT) isolate compared with reaction time threshold values (mins) of the G-143 reaction of PNA-LNA-LAMP assay. B, varying conidial concentrations of a mutant-type (MT) isolate compared with reaction time threshold values (mins) of the A-143 reaction of PNA-LNA-LAMP assay. C, Varying conidial concentrations of a WT isolate compared with cycle threshold (Ct) values of the TaqMan qPCR-based assay. D, varying conidial concentrations of an MT isolate compared with Ct values of the TaqMan qPCR-based assay. A WT isolate (En-FRAME01) containing G-14 allele and an MT isolate (BPPQ1B.5) containing the A-143 allele were serially diluted from 10,000 conidia to 100 conidia, while 1 and 10 conidia of these isolates were manually transferred and tested to determine the limit of detection of the assays. Four biological replicates for each conidial concentration were tested.

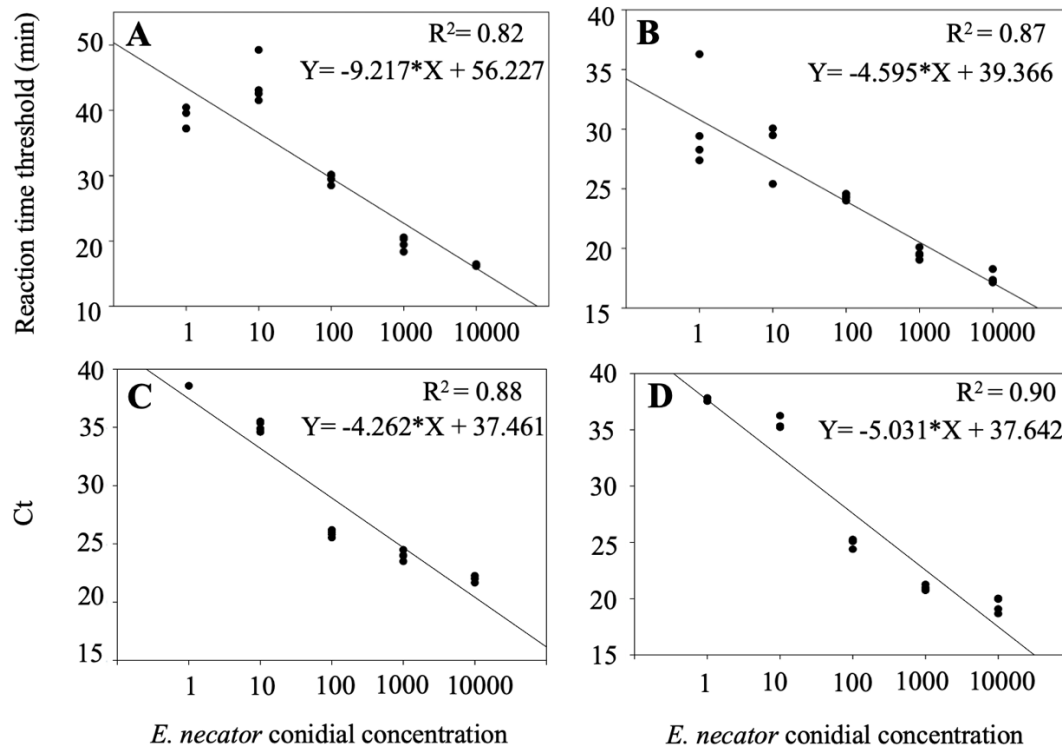


Figure 2.4. Partial alignment of the Cytb gene from *E. necator* and other powdery mildew species (i.e. *E. pisi*, *E. alphitoides*, *Blumeria graminis* and *Podosphaera leucotricha*). '*' denotes Cytb sequences of strains of *E. necator* from Jones et al., 2014, and '**' denotes a mitochondrial genome from Zaccaron et al., 2021. Genbank accession numbers are listed on the figure for related powdery mildews. Shaded area is approximately 450 bp long and is the locus where the TaqMan marker and PNA-LNA-LAMP assay (this manuscript target). In Miles et al 2021 the TaqMan marker targets the G143A mutation (gray arrows denote forward and reverse primers) and the green triangles denote the location of the allelic species probe for G-143 allele and A-143 allele. Dark lines in the sequence denote single nucleotide polymorphisms which differ from the consensus sequence (primarily *E. necator* derived).

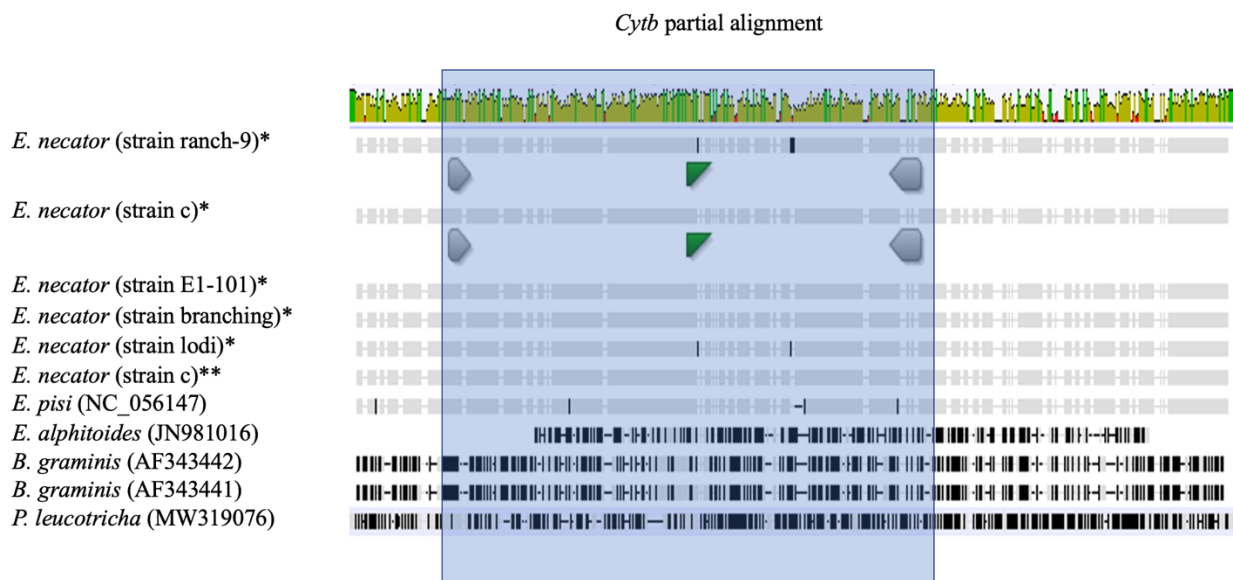


Figure 2.5. Amplification time of peptide nucleic acid-locked nucleic acid mediated loop-mediated isothermal amplification (PNA-LNA-LAMP) assay in identifying G-143 allele (wild-type; WT) or A-143 allele (mutant-type; MT) in in vitro mixed DNA samples. Open circles with dotted lines represented the G-143 reaction of PNA-LNA-LAMP assay, and closed circles with solid lines represented the A-143 reaction of the PNA-LNA-LAMP assay. Samples were prepared using TC-BD-V08 (WT isolate) and AV-C-28 (MT isolate) with initial equal concentration ($1 \text{ ng}/\mu\text{l} = 100\%$) mixed at seven fixed MT:WT ratios.

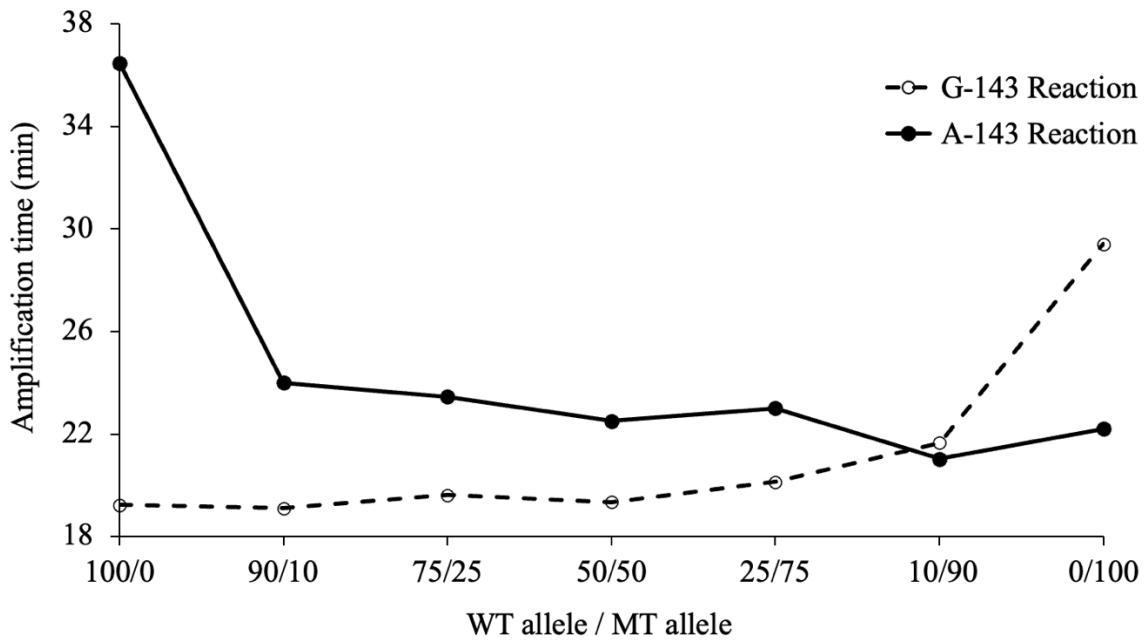


Figure 2.6. Data visualization of PNA-LNA-LAMP assay on three different detection devices including: (A) a T16-ISO Axxin unit; (B) a Genie II unit; and (C) Bio-RadCFX96 PCR machine using a purified DNA (AV-C-28) of a mutant-type *E. necator* isolate. Amplification of mutant-type isolate for A-143 reaction and G-143 reaction of PNA-LNA- LAMP assay with *E. necator* DNA are denoted by open circles and closed circles, respectively. Amplifications for A-143 reaction and G-143 reaction of PNA-LNA-LAMP assay with water (negative control) are shown by open and closed triangles, respectively.

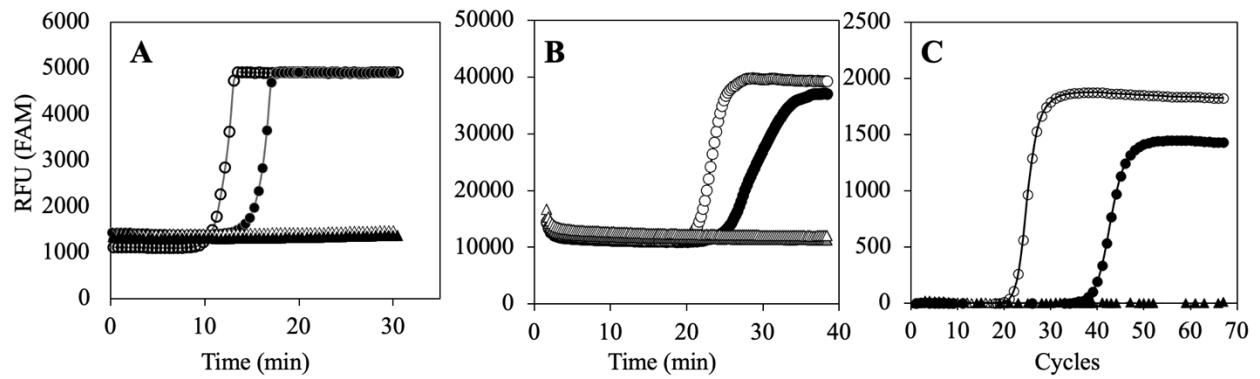
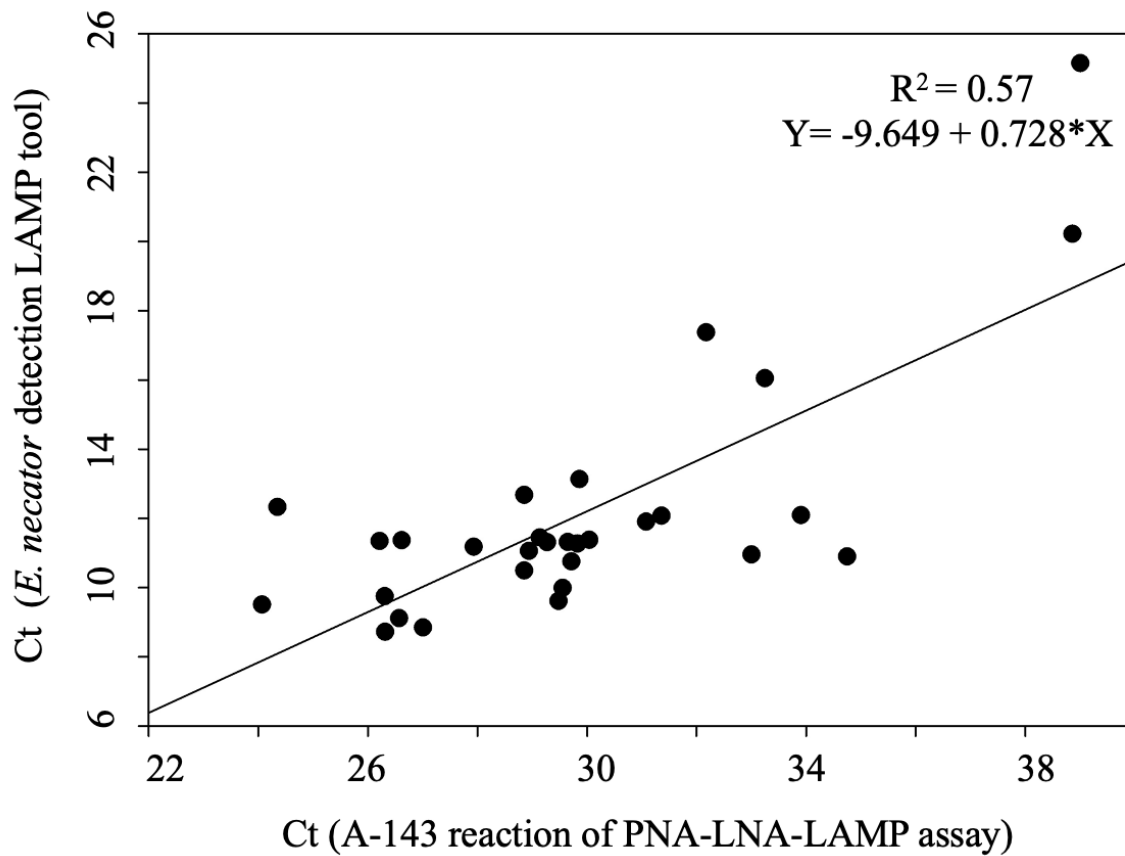


Figure 2.7. Regression plot of peptide nucleic acid-locked nucleic acid mediated loop-mediated isothermal amplification (PNA-LNA-LAMP) assay with the *Erysiphe necator* detection tool (Theissen et al. 2016). Cycle threshold (Ct) values of the *E. necator* detection tool were compared with Ct values of the A-143 reaction of PNA-LNA-LAMP assay. Fifteen mutant-type *E. necator* samples were tested, and reactions were duplicated.



Tables

Table 2.1. Primers and probes used to amplify the *Cytb* region and detect the G143A mutation in *E. necator*.

Assay	Primer/ Probe	Sequence (5'-3')	Aim
LAMP	F3	AGCAAAGCTGCTAATATA	Amplification of <i>Cytb</i>
	FIP	TAACCCAAGAATGCTGTCAAAGTTGGGCTGCTATA CAGATAAATTAGG	Amplification of <i>Cytb</i>
	B3	CTACTTAAAGCTTTAGAAGTTTCC	Amplification of <i>Cytb</i>
	BIP	CCCTACGGGCAGATGAGCCTATAGTGATATTTTTC AACCGCTATTA	Amplification of <i>Cytb</i>
	LNA-MT ^{ab}	GCACTCTGGG GCT GCAACCGTTAAGTAGG	Amplification of A-143
	LNA-WT ^{ab}	GCACTCTGGG GGT GCAACCGTTAAGTAGG	Amplification of G-143
	PNA-WT ^{ac} probe	GGGCTGCAACCGTTA	Delay amplification of A-143
	PNA-MT ^{ac} probe	GGG G TGCAACCGTTA	Delay amplification of G-143
TaqMan	83F ^c	CGCTACAGACTGGGTCACTG	Amplification of <i>Cytb</i>
	517R ^c	AGTCTCTTAGGGCCCCCATT	Amplification of <i>Cytb</i>
	WT probe ^{cd}	[FAM] AGCCTATGGGGTGCAACCGT [BHQ1]	G-143 detection
	MT probe ^{cd}	[HEX] AGCCTATGGGCTGCAACCGT [BHQ1]	A-143 detection
RPA	RPAexo_F2	TTATATGATCGCTACAGACTGGGTCACTGC	Amplification of <i>Cytb</i>
	RPAexo_R2	AGTCTCTTAGGGCCCCCATTCTAAAGGT	Amplification of <i>Cytb</i>
	WT probe ^c	TTTTACCCTACGGGCAGATGAGCCTATGGG[G(FAM)][T[THF]C[A(BHQ-1)]ACCGTTAAGTAG [C3 Spacer]	G-143 detection
	MT probe ^c	TTTTACCCTACGGGCAGATGAGCCTATGGG[C(HEX)][T[THF]C[A(BHQ-1)]ACCGTTAAGTAG [C3 Spacer]	A-143 detection

Table 2.1. (cont'd)

^a LNA-MT and PNA-MT indicate LNA primer and PNA probe, respectively, specific to A-143 reaction of PNA-LNA-LAMP assay; similarly, LNA-WT and PNA-WT indicate LNA primer and PNA probe, respectively, specific to G-143 reaction of PNA-LNA-LAMP assay.

^b Italics show extra bases at 5'end of LNA primers; Bold and Italics indicate LNA modification site.

^c Bold indicates SNP in PNA probes in PNA-LNA-LAMP assay, and wild-type and mutant-type probes used in RPA and TaqMan probe-based assay; brackets indicate fluorophores and quenchers.

^d Developed in Miles et al. (2021).

Table 2.2. Detection of quinone outside inhibitor (QoI)-resistant *E. necator* in purified DNA using the PNA-LNA-LAMP assay and G143A allele-specific TaqMan probe-based assay.

	Sample ^a size (n)	PNA-LNA-LAMP ^b		<i>Cytb</i> allele		TaqMan ^c	
		A-143 reaction (mins)	G-143 reaction (mins)	G-143	A-143	A-143 Ct ^d	(G-143 Ct ^d)
QoI- resistant	8	22.0 ± 1.5	29.3 ± 0.7	-	8	24.5 ± 0.5	-
QoI- sensitive	8	34.4 ± 1.9	19.1 ± 0.3	8	-	-	21.5 ± 0.5

^a Purified DNA was obtained from *E. necator* single-spore isolates that were collected in Michigan in 2009 by Miles et al. (2012).

^b PNA-LNA-LAMP reactions were carried out at 62°C using Bio-Rad CFX96 machine. A-143 reaction = Reaction capable of detecting mutant-type allele; G-143 reaction = Reaction capable of detecting wild-type allele.

^c Fluorophores used in TaqMan probe-based assay are fluorescein (FAM) and hexachlorofluorescein (HEX) dyes.

^d Ct= cycle threshold. TaqMan reactions were carried out as described in Miles et al. (2021) using Bio-Rad CFX96 machine.

Table 2.3. Validation of PNA-LNA-LAMP assay using crude DNA samples collected from the Great Lakes region (United States) by comparing outcome with TaqMan probe-based assay.

Sample QoI sensitivity status ^a (TaqMan assay)	Number of samples with QoI sensitivity status	PNA-LNA-LAMP assay results			Accuracy of PNA-LNA-LAMP assay relative to TaqMan assay ^b
		Sensitive	Resistant	Mixed	
Sensitive	10	10	-	-	100%
Resistant	52	-	52	-	100%
Mixed	30	3	5	22	73.33%

^a *E. necator* samples on leaves and berries were collected from Michigan, Ohio, Wisconsin, New York, Indiana in 2019 using Tough-Spots method.

^b Accuracy of the assay was calculated using formula: ((True Positive + True Negative)/(Total no. of cases)).

PNA-LNA-LAMP reactions were carried out at 62°C using Bio-Rad CFX96 machine. TaqMan reactions were carried out as described in Miles et al. (2021) using Bio-Rad CFX96 machine.

Table 2.4. Validation of PNA-LNA-LAMP assay to detect QoI-resistance in *E. necator* at three independent laboratories. Protocol included conducting PNA-LNA-LAMP amplifications in three step series with: Step one: known purified DNA. Step two: blind crude DNA of field samples. Step three: Crude DNA of samples of their choice.

Location ^a	Sample size (n)	Step number ^b	Positive detections by TaqMan / Positive detection by PNA-LNA-LAMP			Accuracy ^c
			QoI sensitive	QoI resistant	Mixed	
Corvallis, OR	7	Purified DNA	4/4	3/3	-	94.44%
	7	Blind samples	3/3	4/4	-	
	4	User-supplied samples	1/1	1/1	2/1 ^d	
	18*		8/8	8/8	2/1	
Parlier, CA	7	Purified DNA	4/4	3/3	-	100%
	7	Blind samples	3/3	4/4	-	
	6	User-supplied samples	3/3	1/1	2/2	
	20*		10/10	8/8	2/2	
Prosser, WA	7	Purified DNA	4/4	3/3	-	100%
	7	Blind samples	3/3	4/4	-	
	5	User-supplied samples	-	5/5	-	
	19*		7/7	12/12	-	

^a Institution: United States Department of Agriculture – Agricultural Research Service, Horticultural Crops Disease and Pest Management Research Unit, Corvallis, OR, USA; United States Department of Agriculture – Agricultural Research Service, Crop Diseases, Pests and Genetics Unit, San Joaquin Valley Agricultural Sciences Center, Parlier, CA, USA; Washington State University Irrigated Agriculture Research and Extension Center, Prosser, WA, USA.

^b Purified DNA (resistance status known to users): In 2009, *E. necator* single-spored isolates were collected by Miles et al. (2012) throughout Michigan; Blind samples (resistance status unknown to users): Chelex extraction was performed on samples collected throughout Michigan in 2019 using Tough-Spots to gather *E. necator* colonies on leaves and TaqMan assay was performed at MSU, East Lansing, MI, USA to confirm the QoI-resistance status of these samples; User-supplied samples: *E. necator* samples that were collected from their own locations using Chelex DNA extraction method.

^c Accuracy of the assay was calculated using formula: ((True Positive + True Negative)/(Total no. of cases)). Accuracy for each location was calculated using the total number of samples tested in that location.

Table 2.4. (cont'd)

^d One mixed samples from User-supplied samples at Corvallis, OR was incorrectly detected as QoI-sensitive.

‘*’ denotes total number of samples tested at the respective location.

Table 2.5. Recombinase polymerase amplification (RPA) reactions tested at varying forward and reverse primer concentrations to detect different *Cytb* alleles of *E. necator* (i.e., G-143 and A-143) in a sensitive and resistant isolate. Values reported are relative fluorescence units (RFU) after 20 min and the onset of amplification threshold (OT) in minutes.

Treatment Purpose	Isolate	Allele present	10 μ M F2, (μL)	10 μ M R2, (μL)	RPA maximum (RFU) after 20 min		OT value (min)	
					FAM	HEX	FAM (WT)	HEX (MT)
Manufacturer recommendation	WT	G-143	2.1	2.1	3023.0	4616.7	3.52	3.06
		G-143			3061.2	2869.5	5.35	3.06
	MT	A-143	2.1	2.1	3169.7	4074.0	3.55	3.55
		A-143			3319.4	3872.3	4.95	1.65
No Forward Primer (F2) High Reverse Primer (R2)	WT	G-143	0.0	4.2	1435.8	2499.8	5.55	3.60
	MT	G-143	0.0	4.2	2204.3	3224.7	5.58	3.68
Low Forward Primer (F2), Excess Reverse Primer (R2)	WT	A-143	0.6	3.6	2104.1	3402.6	3.56	3.56
	MT	A-143	0.6	3.6	2486.9	4008.6	3.58	3.15
Excess Forward (F2), Low Reverse Primer (R2)	WT	G-143	3.6	0.6	2214.0	3046.0	5.5	3.16
		G-143			2544.7	2645.4	5.4	3.53
	MT	A-143	3.6	0.6	1726.3	3020.6	6.95	3.60
		A-143			2205.4	2692.8	5.41	3.56
Excess Forward (F2), Lower Reverse Primer (R2)	WT	G-143	4.0	0.2	1663.6	1574.5	5.45	5.45
	MT	A-143	4.0	0.2	1518.3	1816.3	6.91	5.03
Excess Forward (F2), No Reverse Primer (R2)	WT	G-143	4.2	0.0	1260.3	1360.5	6.95	5.50
	MT	A-143	4.2	0.0	1298.9	1280.8	6.96	5.53

Table 2.6. List of failed primers and probes that were tested for developing a LAMP assay for detection of G143A mutation conferring QoI resistance in *E. necator*.

Primer/Probe	Purpose ^a	Sequence	Result ^b
En_G143A_1_F3	F3	TCTTGGGTATGTTTACCC	Inconsistent detection of G143A mutation
En_G143A_3_F3	F3	CTTTGACAGCATTCTTGGGT	Delayed amplification of G-143 mutation
En_G143A_4_F3	F3	GTTTCCAGCATATAGTGATA	No amplification
En_G143A_5_F3	F3	CATATAGTGATATTTTCAA	Inconsistent detection of G143A mutation
En_G143A_6_F3	F3	ACAGCATTCTTGGGTATGT	No amplification
En_G143A_7_F3	F3	GGAACCTTGACAGCATTCTT	Inconsistent detection of G143A mutation
En_G143A_9_F3	F3	CAGCATATAGTGATATTTT	Delayed amplification of G143A mutation
B3-1	B3	GTTTCCTGCTGATTGTTTCA	Inconsistent detection of G143A mutation
En_G143A_3_B3	B3	AAAGGTTTCCTGCTGATTGT	Delayed amplification of G-143 mutation
En_G143A_4_B3	B3	GGTTAGACAAGGCTTTAAAG	No amplification
En_G143A_5_B3	B3	GTTCTAGAGGCAGCAAAGCT	Inconsistent detection of G143A mutation
En_G143A_6_B3	B3	TCCTGCTGATTGTTTATTAT	No amplification
En_G143A_7_B3	B3	AGGTTTCCTGCTGATTGTTT	Inconsistent detection of G143A mutation

Table 2.6. (cont'd)

En_G143A_9_B3	B3	TAGAGGCAGCAAAGCTGCTA	Delayed amplification of G143A mutation
En_G143A_1_FIP	FIP	ATAGTGATATTTTCAACCGCTAT CGGGCAGATGAGCCTATGGGG	Inconsistent detection of G143A mutation
En_G143A_2_FIP	FIP	ATAGTGATATTTTCAACCGCTA TCGGGCAGATGAGCCTATGGGC	No amplification
En_G143A_3_FIP	FIP	TTCCAGCATATAGTGATATTTTTCAGGGCAGA TGAGCCTATGGGC	Delayed amplification of G-143 mutation
En_G143A_4_FIP	FIP	TTGACAGCATTCTTGGGTATGTTTTACCTACT TAACGGTTGCAC	No amplification
En_G143A_3V1B_FIP	FIP	TTCCAGCATATAGTGATATTTTTCAGGGCAGA TGAGCCTATGGGG	Inconsistent detection of G143A mutation
En_G143A_3V2B_FIP	FIP	TTCCAGCATATAGTGATATTTTTCAGGGCAGA TGAGCCTATGGGGT	No amplification
En_G143A_3V3B_FIP	FIP	TTCCAGCATATAGTGATATTTTTCAGGGCAGA TGAGCCTATGCGG	Poor sensitivity
En_G143A_3V2A_FIP	FIP	TTCCAGCATATAGTGATATTTTTCAGGGCAGA TGAGCCTATGGGCT	No amplification
En_G143A_3V3A_FIP	FIP	TTCCAGCATATAGTGATATTTTTCAGGGCAGA TGAGCCTATGCGC	Poor sensitivity
En_G143A_5_FIP	FIP	TGGGTTATGTTTTACCCTACGGGCATACCTAC TTAACGGTTGCAC	Inconsistent detection of G143A mutation
En_G143A_5V2A_FIP	FIP	TGGGTTATGTTTTACCCTACGGGCATACCTAC TTAACGGTTGCAGC	Amplification of negative control
En_G143A_5V3A_FIP	FIP	TGGGTTATGTTTTACCCTACGGGCATACCTAC TTAACGGTTGGAG	Amplification of negative control
En_G143A_5V2B_FIP	FIP	TGGGTTATGTTTTACCCTACGGGCATACCTAC TTAACGGTTGCACC	No amplification

Table 2.6. (cont'd)

En_G143A_5V3B_FIP	FIP	TGGGTTATGTTTTACCCTACGGGCATACCTAC TTAACGGTTGGAC	Inconsistent detection of G143A mutation
En_G143A_7_FIP	FIP	AGCATATAGTGATATTTTTCAACCGCTACGGG CAGATGAGCCTAT	Inconsistent detection of G143A mutation
En_G143A_9_FIP	FIP	TTATGTTTTACCCTACGGGCAGATGT- ATTACCTACTTAACGGTT	Delayed amplification of G143A mutation
En_G143A_1_BIP	BIP	ACTTCTAAAGCTTTAAGTAGGTGCGTGTCCT GTAGAAAGATGTTC	Inconsistent detection of G143A mutation
En_G143A_3_BIP	BIP	GCTTTAAGTAGGTGCGGGGGGGGAGGTTGTC ACTGTAGAAAGATG	Delayed amplification of G143A mutation
En_G143A_4_BIP	BIP	TTACTATAACCTAATTTATCTGTTTTGTTCTAG AGGCAGCAAAGC	No amplification
En_G143A_5_BIP	BIP	GCTGTCAAAGTTCCAGCTTACTATAAAGTCGT GGGCTGCTATACA	Inconsistent detection of G143A mutation
En_G143A_6_BIP	BIP	AAAGCTTTAAGTAGGTGCGGGGGTTGTCCT GTAGAAAGATGTTT	No amplification
En_G143A_7_BIP	BIP	TAAAGCTTTAAGTAGGTGCGGGGGTTGTCCT GTAGAAAGATGTT	Negative control amplified
En_G143A_9_BIP	BIP	GAATGCTGTCAAAGTTCCAGCTTGTCGTGGGC TGCTATACAGATA	Delayed amplification of G143A mutation
En_G143A_7_LNA	LNA	GCACTCTCTATTACCTACTTAACGGTTGCAGC CC	Inconsistent detection of G143A mutation
En_G143A_1_PNA	PNA	GGGTGCAACCGT	Inconsistent detection of G-143 allele

^a Purpose of the primers and probes in the LAMP reaction.

^b LAMP reactions were carried out using purified DNA from single-spored isolates of *E. necator* collected from Michigan in 2009 by Miles et al. (2012).

PNA-LNA-LAMP reactions were carried out at 62°C for using Bio-Rad CFX96 machine.

Table 2.7. Comparison of PNA-LNA-LAMP assay and TaqMan assay in detecting the G143A mutation in air samples of *E. necator*.

Sample Name ^a	Estimated Conidia Number	PNA-LNA-LAMP ^b		TaqMan ^c	
		G-143 reaction (mins)	A-143 reaction (mins)	G-143 Ct ^d	A-143 Ct ^d
DDO-5/28/15	11	30.96	28.04	35.37	40.54
DD-8/8/13	95	25.72	nd ^e	30.91	nd
AR 6/11/15	12	25.41	37.37	33.35	nd
DD-7/29/13	97	29.65	nd	32.52	nd
AS-7/29/13	103	25.89	nd	31.35	nd
LR 5/28/15	4	nd	nd	36.12	38.92
JHVC(AZ) 6-7-13	6	24.35	31.23	36.41	nd
TH 5/28/15	65	29.77	nd	32.40	nd
AA 4/6/15	36	nd	nd	36.71	nd
LS 7-24-14	9	39.10	nd	38.31	nd
DDO 5/7/15	29	27.43	nd	35.11	39.44
AD 8/7/14	5	30.57	nd	35.54	nd

^a DNA from air samples that were collected from Oregon by Thiessen et al. (2016) using custom impaction spore samplers.

^b PNA-LNA-LAMP reactions were carried out at 62°C using Bio-Rad CFX96 machine.

^c Fluorophores used in TaqMan probe-based assay are fluorescein (FAM) dye for G-143 allele and hexachlorofluorescein (HEX) dye for A-143 allele. TaqMan reactions were carried out as described in Miles et al. (2021) using Bio-Rad CFX96 machine,

^d Ct= cycle threshold

^e “nd” represents no detection

LITERATURE CITED

- Abdelghafour, F., Keresztes, B., Germain, C., and Da Costa, J.P. 2020. In field detection of downy mildew symptoms with proximal colour imaging. *Sensors* 20:4380.
- Adnan, M., Hamada, M.S., Li, G.Q., and Luo, C.X. 2018. Detection and molecular characterization of resistance to the dicarboximide and benzamide fungicides in *Botrytis cinerea* from tomato in Hubei Province, China. *Plant Dis.* 102:1299-1306.
- Alzohairy, S. A., Gillett, J., Saito, S., Naegele, R. N., Xiao, C. L., and Miles, T. D. 2021. Fungicide resistance profiles of *Botrytis cinerea* isolates from Michigan vineyards and development of a TaqMan assay for detection of Fenhexamid resistance. *Plant Dis.* 105:285-294.
- Bai, J., Lin, H., Li, H., Zhou, Y., Liu, J., Zhong, G., Wu, L., Jiang, W., Du, H., Yang, J., and Xie, Q. 2019. Cas12a-based on-site and rapid nucleic acid detection of African swine fever. *Front. Microbiol.* 10:2830.
- Baratloo, A., Hosseini, M., Negida, A., El Ashal, G. 2015. Part 1: Simple definition and calculation of accuracy, sensitivity and specificity. *Emerg (Tehran)* 3:48-49.
- Bartlett, D. W., Clough, J. M., Godwin, J. R., Hall, A. A., Hamer, M., and Parr-Dobrzanski, B. 2002. Review The strobilurin fungicides. *Pest Manag. Sci.* 58: 649-662.
- Baudoin, A., Olaya, G., Delmotte, F., Colcol, J. F., and Sierotzki, H. 2008. QoI resistance of *Plasmopara viticola* and *Erysiphe necator* in the Mid-Atlantic United States . *Plant Heal. Prog.* 9:25.
- Brewer, M. T., and Milgroom, M. G. 2010. Phylogeography and population structure of the grape powdery mildew fungus, *Erysiphe necator*, from diverse *Vitis* species. *BMC Evol. Biol.* 10:268.
- Daher, R. K., Stewart, G., Boissinot, M., Boudreau, D. K., and Bergeron, M. G. 2015. Influence of sequence mismatches on the specificity of recombinase polymerase amplification technology. *Mol. Cell. Probes.* 29:116–121.
- Duan, Y., Zhang, X., Ge, C., Wang, Y., Cao, J., Jia, X., Wang, J., and Zhou, M. 2014. Development and application of loop-mediated isothermal amplification for detection of the F167Y mutation of carbendazim-resistant isolates in *Fusarium graminearum*. *Sci. Rep.* 4:1–8.
- Dufour, M.-C., Fontaine, S., Montarry, J., and Corio-Costet, M.-F. 2011. Assessment of fungicide resistance and pathogen diversity in *Erysiphe necator* using quantitative real-time PCR assays. *Pest Manag. Sci.* 67:60–69.
- Fan, F., Yin, W. X., and Li, G. Q. 2018. Development of a LAMP method for detecting SDHI fungicide resistance in *Botrytis cinerea*. *Plant Dis.* 102: 1612-1618.

- FRAC. 2012. Species with QoI-resistance. Available at: www.frac.info [Accessed May 21, 2020].
- Fuller, K. B., Alston, J. M., and Sambucci, O. S. 2014. The value of powdery mildew resistance in grapes: Evidence from California. *Wine Econ. Policy.* 3:90–107.
- Gadoury, D. M., Cadle-Davidson, L., Wilcox, W. F., Dry, I. B., Seem, R. C., and Milgroom, M. G. 2012. Grapevine powdery mildew (*Erysiphe necator*): A fascinating system for the study of the biology, ecology and epidemiology of an obligate biotroph. *Mol. Plant Pathol.* 13:1–16.
- Goto, M., Honda, E., Ogura, A., Nomoto, A., and Hanaki, K. I. 2009. Colorimetric detection of loop-mediated isothermal amplification reaction by using hydroxy naphthol blue. *Biotechniques.* 46:167–172.
- Ishii, H. 2009. QoI fungicide resistance: current status and the problems associated with DNA-based monitoring. Pages 37-45 in: *Recent Developments in Management of Plant Diseases*. U. Gisi, I. Chet, and M. L. Gullino, eds. Springer, Dordrecht, The Netherlands.
- Itonaga, M., Matsuzaki, I., Warigaya, K., Tamura, T., Shimizu, Y., Fujimoto, M., Kojima F., Ichinose, M., and Murata, S. 2016. Novel methodology for rapid detection of KRAS mutation using PNA-LNA mediated loop-mediated isothermal amplification. *PLoS One.* 11: e0151654.
- Jones, L., Riaz, S., Morales-Cruz, A., Amrine, K. C. H., McGuire, B., Gubler, W. D., Walker, A. M., and Cantu, D. 2014. Adaptive genomic structural variation in the grape powdery mildew pathogen, *Erysiphe necator*. *BMC Genomics* 15:1081.
- Kubota, R., Alvarez, A., Su, W., and Jenkins, D. 2011. FRET-based assimilating probe for sequence-specific real-time monitoring of loop-mediated isothermal amplification (LAMP). *Biol. Eng. Trans.* 4:81–100.
- Kunova A., Pizzatti C., Saracchi M., Pasquali M., and Cortesi P. 2021. Grapevine powdery mildew: fungicides for its management and advances in molecular detection of markers associated with resistance. *Microorganisms.* 9:1541.
- Kyger, E. M., Krevolin, M. D., and Powell, M. J. 1998. Detection of the hereditary hemochromatosis gene mutation by real-time fluorescence polymerase chain reaction and peptide nucleic acid clamping. *Anal. Biochem.* 260:142–148.
- Lau, H. Y., Wang, Y., Wee, E. J. H., Botella, J. R., and Trau, M. 2016. Field demonstration of a multiplexed point-of-care diagnostic platform for plant pathogens. *Anal. Chem.* 88:8074–8081.
- Li, L., Li, S., and Wang, J. 2018. CRISPR-Cas12b-assisted nucleic acid detection platform. *bioRxiv.* :362889.

- Lobato I., and O'Sullivan C. 2018. Recombinase polymerase amplification: Basics, applications and recent advances. *Trends Analyt Chem.* 98:19-35.
- Ma, Z., and Michailides, T. J. 2005. Advances in understanding molecular mechanisms of fungicide resistance and molecular detection of resistant genotypes in phytopathogenic fungi. *Crop Prot.* 24:853–863.
- Miles, L. A., Miles, T. D., Kirk, W. W., and Schilder, A. M. C. 2012. Strobilurin (QoI) resistance in populations of *Erysiphe necator* on grapes in Michigan. *Plant Dis.* 96:1621–1628.
- Miles, T. D., Neill, T. M., Colle, M., Warneke, B., Robinson, G., Stergiopoulos, I., and Mahaffee, W. 2021. Allele-specific detection methods for QoI fungicide-resistant *Erysiphe necator* in vineyards. *Plant Dis.* 105:175-182.
- Miles, T.D., Martin, F. and Coffey, M. 2015. Development of rapid isothermal amplification assays for detection of *Phytophthora* species in plant tissue. *Phytopathology* 105:265-278.
- Nixon, G., Garson, J. A., Grant, P., Nastouli, E., Foy, C. A., and Huggett, J. F. 2014. Comparative study of sensitivity, linearity, and resistance to inhibition of digital and nondigital polymerase chain reaction and loop mediated isothermal amplification assays for quantification of human cytomegalovirus. *Anal. Chem.* 86:4387–4394.
- Notomi, T., Okayama, H., Masubuchi, H., Yonekawa, T., Watanabe, K., Amino, N., and Hase, T. 2000. Loop-mediated isothermal amplification of DNA. *Nucleic Acids Res.* 28: e63.
- Pan, L., Li, J., Zhang, W., and Dong, L. 2015. Detection of the I1781L mutation in fenoxaprop-*p*-ethyl-resistant American sloughgrass (*Beckmannia syzigachne* Steud.), based on the loop-mediated isothermal amplification method. *Pest Manag. Sci.* 71:123–130.
- Pang, B., Xu, J., Liu, Y., Peng, H., Feng, W., Cao, Y., Wu, J., Xiao, H., Pabbaraju, K., Tipples, G., Joyce, M., Saffran, H., Tyrell, D., Zhang, H., Le, X. 2020. Isothermal amplification and ambient visualization in a single tube for the detection of SARS-CoV-2 using loop-mediated amplification and CRISPR technology. *Anal Chem.* 92: 16204-16212.
- Rallos L., Johnson N., Schmale D., Prussin A., Baudoin A.. 2014. Fitness of *Erysiphe necator* with G143A-based resistance to quinone outside inhibitors. *Plant Dis.* 98:1494-1502.
- Sambucci, O., Alston, J. M., Fuller, K. B., and Lusk, J. 2019. The pecuniary and nonpecuniary costs of powdery mildew and the potential value of resistant grape varieties in California. *Am. J. Enol. Vitic.* 70:177–187.
- Teng, F., Guo, L., Cui, T., Wang, X. G., Xu, K., Gao, Q., Zhou, Q., and Li, W. 2019. CDetection: CRISPR-Cas12b-based DNA detection with sub-attomolar sensitivity and single-base specificity. *Genome Biol.* 20:132.

- Thiessen, L.D., Keune, J.A., Neill, T.M., Turechek, W.W., Grove, G.G., and Mahaffee, W.F. 2016. Development of a grower-conducted inoculum detection assay for management of grape powdery mildew. *Plant Path.* 65:238-249.
- Thiessen, L. D., Neill, T. M., and Mahaffee, W. F. 2018. Development of a quantitative loop-mediated isothermal amplification assay for the field detection of *Erysiphe necator*. *PeerJ*. 2018:e4639.
- Thiessen, L. D., Neill, T. M., and Mahaffee, W. F. 2019. Formation of *Erysiphe necator* chasmothecia in the Pacific Northwest United States. *Plant Dis.* 103: 890-896.
- Turechek, W.W., and Wilcox, W.F. 2005. Evaluating predictors of apple scab with receiver operating characteristic curve analysis. *Phytopathology* 95:679-691.
- Wang, D., He, S., Wang, X. Yan, Y., Liu, J., Wu, S., Liu S., Lei, Y., Chen, M., Li, L., Zhang, J., Zhang L., Hu X., Zheng, X., Bai, J., Zhang, Y., Zhang Y., Song, M, and Tang, Y. 2020. Rapid lateral flow immunoassay for the fluorescence detection of SARS-CoV-2 RNA. *Nat. Biomed. Eng.* 4:1150–1158.
- Wilson IG. 1997. Inhibition and facilitation of nucleic acid amplification. *Appl. Environ. Microbiol.* 63:3741–3751.
- Wise, J., Gut, L., Isaacs, R., Miles, T., Sundin, G., Zandstra, B., Beaudry, R., and Lang. G. 2020. Michigan Fruit Management Guide 2019. Extension Bulletin E-154. Michigan State University, East Lansing.
- Yongkiettrakul, S., Kolié, F. R., Kongkasuriyachai, D., Sattabongkot, J., Nguitragool, W., Nawattanapaibool, N., Suansomjit, C., Warit, S., Kangwanrangsang, N., and Buates, S. 2020. Validation of PfSNP-LAMP-lateral flow dipstick for detection of single nucleotide polymorphism associated with pyrimethamine resistance in *Plasmodium falciparum*. *Diagnostics.* 10:948.
- Yuan, X., Yang, C., He, Q., Chen, J., Yu, D., Li, J., Zhai, S., Qin, Z., Du, K., Chu, Z., and Qin, P. 2020. Current and perspective diagnostic techniques for COVID-19. *ACS Infect Dis.* 6:1998-2016.
- Zaccaron, A., De Souza, J., and Stergiopoulos, I. 2021. The mitochondrial genome of the grape powdery mildew pathogen *Erysiphe necator* is intron rich and exhibits a distinct gene organization. *Sci Rep* 11, 13924
- Zhang, J., Zhu, J., Ren, H., Zhu, S., Zhao, P., Zhang, F., Lv, H., Hu, D., Hao, L., Geng, M., Gong, X., Pan, X., Wang, C., and Qi, Z. 2013. Rapid visual detection of highly pathogenic *Streptococcus suis* serotype 2 isolates by use of loop-mediated isothermal amplification. *J. Clin. Microbiol.* 51:3250–3256.

CHAPTER 3: SUB-LETHAL DOSE EXPOSURE OF CYFLUFENAMID, FLUTIANIL, QUINOXYFEN AND METRAFENONE: EFFECTS ON SPORE GERMINATION AND GENE EXPRESSION IN THE GRAPE POWDERY MILDEW PATHOGEN

Abstract

Erysiphe necator is a destructive obligate plant pathogen that infects grapevines worldwide. Recently, specialized fungicides like cyflufenamid, flutianil, metrafenone, and quinoxifen have been widely employed to control grape powdery mildew. However, their modes of action remain unclear. In this study, a spore germination assay was conducted on *E. necator* conidia to determine the EC₅₀ concentrations of cyflufenamid (FRAC U06), flutianil (FRAC U13), quinoxifen (FRAC 13), and metrafenone (FRAC 50). The results showed that cyflufenamid and metrafenone did not consistently inhibit spore germination, even at concentrations as high as 100 ppm. In contrast, flutianil and quinoxifen effectively suppressed conidial germination. Transcriptomic analyses of *E. necator* conidia treated with flutianil, quinoxifen, and trifloxystrobin revealed limited overlap in differentially expressed genes compared to the control group. These fungicides upregulated genes involved in respiration, including the electron transport chain, glycolysis, and Krebs cycle pathways. Specific genes such as Cytochrome P450 monooxygenase, Maltose permease MAL31, and NADP-dependent oxidoreductase RED1 were upregulated. However, Thioredoxin-1 gene was downregulated at both quinoxifen and trifloxystrobin treatments that could act in the cellular defense against oxidative stress. Quinoxifen exposure led to reduced expression of protein kinase genes, suggesting a disruption in signal transduction, while flutianil treatment showed increased expression of sugar transporters and chitinase, possibly reflecting enhanced energy demand and cell wall remodeling. Additionally, in samples treated with quinoxifen and flutianil, there was an

overexpression of MFS and ABC multidrug transporters, indicating a potential risk for developing fungicide resistance. The findings of this study suggest that while quinoxifen, flutianil, and trifloxystrobin inhibit spore germination, they operate through distinct mechanisms. This knowledge may be valuable for developing improved fungicide resistance management strategies for managing *E. necator*.

Introduction

Grapevine powdery mildew (GPM) caused by an obligate biotrophic fungus *Erysiphe necator* Schwein (syn. *Uncinula necator*), is one of the most destructive of viticulture worldwide. This disease causes major reductions in both grape production and fruit quality (Gadoury et al., 2012). Effective control of grape powdery mildew requires multiple repetitive fungicide treatments, contributing to more than 30% of the overall production expenses (Baudoin et al., 2008; Dufour et al., 2011; Fuller et al., 2014; Sambucci et al., 2019; Sharma et al. 2023). The most commonly used fungicides include contact fungicides like sulfur, as well as systemic fungicides such as demethylation inhibitors (DMIs; FRAC 3), quinone outside inhibitors (QoIs or strobilurins; FRAC 11), and succinate dehydrogenase inhibitors (SDHIs; FRAC 7), all of which are applied consistently throughout the growing season (Sharma et al. 2023). These fungicides are also known for their broad-spectrum activity against multiple diseases of grapes (Bartlett et al. 2002; Baudoin et al. 2008; Miles et al. 2012; Sharma et al. 2023).

In recent years, new fungicide classes, including phenyl-acetamides (FRAC U06), cyanomethylenethiazolidines (FRAC U13), aza-naphthalenes (FRAC 13), and aryl-phenyl ketones (FRAC 50), have been introduced as innovative solutions targeting powdery mildew in cereals and specialty crops. Specifically, the active ingredients cyflufenamid (FRAC U06; available since 2012), flutianil (FRAC U13; available since 2017), quinoxifen (FRAC 13; available since

2003), and metrafenone (FRAC 50; available since 2010) have been registered for their effectiveness against *E. necator*. Cyflufenamid and metrafenone are known for possessing both as a protectant and curative properties against *E. necator*. Moreover, Flutianil is highly valued for its residual, translaminar, and curative effects against powdery mildew pathogens. Additionally, quinoxyfen provides protective properties with systemic movement and translocation within the plant with redistribution through vapors. These specialty fungicides are seen as a valuable resource while considering resistance risk management strategies for grape powdery mildew.

Repetitive use of fungicides with single-site mode of action has potential for risk of fungicide resistance development due to selection pressure. Fungicide resistance of QoI fungicides has been already reported in several grape pathogens including *E. necator*, *Botrytis cinerea* and *Plasmopara viticola* in the United States (Baudoin et al. 2008; Dufour et al. 2011; Miles et al. 2012; Sharma et al. 2023). Although, the point mutations G143A, F129L and G137R are the most frequently observed in QoI resistant fungal populations, the G143A mutation is specifically associated with QoI-resistant *E. necator* field populations (Ishii 2009; Ma and Michailides 2005; Baudoin et al. 2008; Miles et al. 2012, 2021; Rallos et al. 2014; Sharma et al. 2023). Unfortunately, quinoxyfen resistant *E. necator* isolates have been also detected with EC₅₀ values exceeding 100 mg/L in Europe (Genet and Jaworska 2009). Reduced quinoxyfen efficacy against *E. necator* was observed in field trials in New York in 2010 and 2011. Additionally, in a single vineyard of West Virginia, field isolates of *E. necator* have shown high levels of resistance to quinoxyfen in leaf disc assays (Feng et al. 2018). Similarly, resistance to metrafenone in *E. necator* also started appearing a few years after the introduction of the fungicide (Kunova et al. 2016). *Erysiphe necator* isolates with moderate and high resistance have

been detected in various European countries (Graf 2017). Interestingly, highly resistant strains were able to thrive and sporulate at concentrations as high as 1250 mg/L (Kunova et al. 2016). Fortunately, resistance to cyflufenamid and flutianil in *E. necator* has not yet been reported.

Mechanism of QoI fungicides is well studied in plant pathogens. These fungicides interfere with mitochondrial function by attaching to the Q_o site (ubiquinol oxidation center) on the cytochrome b (Cytb) gene. This attachment disrupts the electron flow from Cytb to cytochrome c₁, effectively shutting down the energy production cycle by inhibiting adenosine triphosphate (ATP) synthesis (Bartlett et al. 2002; Kunova et al. 2021). Although the exact mode of action of quinoxifen is not known, initial studies showed that quinoxifen hampers the detection of host signals that are essential for proper germling development, and potentially affects serine esterase function, causing subsequent disruptions in cellular signaling pathways (Lee et al. 2008; Wheeler et al. 2003). Unfortunately, the mechanisms of cyflufenamid, flutianil, and metrafenone are still unknown. However, to understand the underlying risk of resistance in *E. necator*, it is important to know the mechanism of action of these specialty fungicides

Understanding the biochemical target of the fungicide is crucial because it supports studies on the relationship between structure and activity, which can improve a fungicide's binding strength and specificity (Cools and Kosack 2012). Moreover, it allows to uncover the resistance mechanism and will aid development of rapid molecular tools for detection of fungicide resistance. Recently, a complete chromosome-scale genome of *E. necator* has been constructed (Zaccaron et al. 2023). This high-quality assembly along with in-vitro phenotyping such as spore germination assays can help in understanding the metabolic and physiological consequences of the fungicide on the pathogen (Cools and Kosack 2012). Therefore, the goal of this study was to (i) conduct spore germination assay on conidia of *E. necator* to determine EC₅₀

concentrations of trifloxystrobin (QoI, FRAC 11), cyflufenamid (FRAC U06), flutianil (FRAC U13), quinoxyfen (FRAC 13) and metrafenone (FRAC 50) (ii) conduct transcriptomic analysis comparing trifloxystrobin, quinoxyfen and flutianil to identify common candidate genes and genomic pathways among these fungicides that could be associated with the mechanism of flutianil.

Materials and Methods

Culturing and maintenance of Erysiphe necator isolate

The *E. necator* isolate EnFRAME01 was collected from grapevines cultivated in a greenhouse located in Corvallis, Oregon, US in 2018. Fresh, disease-free grapevine leaves used for culturing *E. necator* were sourced from the third-fourth node of healthy grapevines (Chardonnay, *Vitis vinifera*) grown in hydroponics. Before use, the leaves were treated in a 0.6% sodium hypochlorite solution, agitated for 1 minute manually, and rinsed multiple times with sterile water. The EnFRAME01 isolate was grown by carefully transferring individual conidial chains onto sterilized leaves with an ethanol-sterilized eyelash. These leaves were placed in a double-Petri dish isolation setup and incubated at 21°C under a 16-hour light and 8-hour darkness cycle. Every 2 weeks, EnFRAME01 isolate was moved onto newly disinfected, healthy leaves following same procedure using clean paintbrushes. Non-inoculated sterilized leaves were used as control.

Fungicide preparation

Five fungicides, each from a different chemical class, were utilized in this study, all of which were commercially available products. These included Torino (10% cyflufenamid, Gowan, Yuma, AZ), Quintec (22.58% quinoxyfen, Dow AgroSciences, Indianapolis, IN), Vivando (25.20% metrafenone, BASF Corporation, Research Triangle Park, NC), Flint Extra

(42.6% trifloxystrobin, Bayer, St. Louis, MO), and Gatten (4.7% flutianil, Nichino America, Wilmington, DE). Stock solutions at 1,000 ppm were prepared by dissolving each commercial fungicide in sterile distilled water, followed by the preparation of a 100-ppm working solution for each. All stock solutions were kept in the dark at 4°C.

Determination of EC₅₀ for each fungicide

The EnFrame isolate was evaluated to determine the EC₅₀ values for the five fungicides mentioned earlier: cyflufenamid, flutianil, metrafenone, trifloxystrobin, and quinoxyfen. Cyflufenamid, flutianil, metrafenone, and quinoxyfen were tested using half-strength water agar, while trifloxystrobin was assessed on half-strength water agar with the addition of salicylhydroxamic acid, an inhibitor of alternative oxidase, at a concentration of 100 µg/ml (Mondal et al. 2005; Wise et al. 2008). Following autoclaving, the media were cooled to 50°C in a water bath before the fungicide was incorporated. All fungicides were tested at 0.0001, 0.001, 0.01, 0.1, 1, 10, 50, and 100 ppm concentrations. Three milliliters of each fungicide-containing medium was dispensed into wells of a 24-well cell plate. Similarly, fungicide-free medium was also added to use as a control to verify the fungicidal effect during the experiment. All wells containing fungicide treatments were randomized using randomized complete block design. These 24-well plates were prepared and used on the same day for phenotyping.

Before use, the 24-well plates were left to air-dry in a biosafety cabinet. Conidia from 10-12 day-old cultures were dispersed onto these plates using an ethanol-sterilized settling tower. The fungicide-treated plate was positioned at the bottom, while a suspension dish containing the powdery mildew-covered leaf was placed above. To dislodge the conidia, a quick burst of air from an airbrush set to 25 psi was directed at the leaf for one second. The conidia were left undisturbed for five minutes to allow them to settle, and the evenness of distribution was

confirmed using a compound microscope. Afterward, the plates were incubated in dark at room temperature for 16 hours. Upon completion of incubation, 25 conidia per well per treatment were examined under a compound microscope ($\times 10$ magnification) to assess germination and the length of the germ tube. Each treatment was carried out in four replicated wells, with all experiments repeated three times.

A conidium was considered germinated if the length of its germ tube exceeded its own diameter. The effective concentration of the fungicide that caused a 50% reduction in conidial germination (EC_{50}) was calculated using linear regression analysis, based on the logarithmic scale of the active ingredient concentration and the corresponding germination percentages of *E. necator* conidia (Miles et al. 2012). Fungicides that demonstrated spore inhibition were used for transcriptomics analysis experiments.

RNA Extraction and Sequencing

The EC_{50} concentrations for Flutianil, quinoxifen, and trifloxystrobin, as determined previously, were used for transcriptomics experiment. Fungicide-amended half-strength water agar was prepared in petri dishes for flutianil and quinoxifen, while trifloxystrobin media also included 100 $\mu\text{g/ml}$ of salicylhydroxamic acid. Autoclaved piece of cellophane was placed on top of the fungicide-amended media, and the plates were left to air-dry in a biosafety cabinet for one hour. Once dried, conidia collected from three powdery mildew-infected leaves were dusted onto each petri-dish containing fungicide amended media using sterilized paintbrushes. The petri-dishes were then incubated in the dark at 24°C . Conidia were re-harvested at 3, and 6 hours using sterilized paintbrushes and transferred to 1.5 ml Eppendorf tubes containing DNA-RNA shield (Zymo Research, Irvine, CA). A control experiment was performed on fungicide-free

media, with conidia collected at 0, 3, and 6-hour intervals. Each treatment had three biological replicates. These samples were kept at -80C until further processing.

For processing, samples were thawed at room temperature. Two large size beads were added to the Eppendorf tubes containing samples and conidia were disrupted in the TissueLyser II (Qiagen, Hilden, Germany) Hz for 1.5 min. Subsequently, lysis buffer was immediately added to each tube and tubes were kept at 75C for 5 min. RNA extraction was then carried out manually according to the manufacturer's instructions for the *Quick*-RNA Microprep Kit (Zymo Research, Irvine, CA). The RNA concentration was measured using the Qubit High Sensitivity (HS) Assay Kit (Invitrogen, Carlsbad, CA). The RNA quality was verified with HS RNA ScreenTape assay using Agilent 4200 TapeStation (Agilent, Santa Clara, CA).

The RNA samples were sent to the RTSF Genomics Core at Michigan State University for library preparation and sequencing. Libraries were prepared using the Roche KAPA mRNA HyperPrep Kit with KAPA Unique Dual-Index primers following manufacturer's recommendations. Completed libraries were quality checked and quantified using a combination of Biotium AccuGreen High Sensitivity dsDNA and Agilent 4200 TapeStation HS DNA1000 assays. The libraries were normalized and pooled in equimolar proportions and the pool quantified using the Invitrogen Colibri Quantification qPCR kit.

After pooling, the libraries were loaded using the Xp loading kit and workflow onto an Illumina NovaSeq 6000 S4 flow cell, and sequencing was conducted in a 2×150 bp paired-end format using a NovaSeq v1.5 300-cycle reagent cartridge (Illumina). Base calling was done by Illumina Real Time Analysis (RTA) v3.4.4 and output of RTA was demultiplexed and converted to FastQ format with Illumina Bcl2fastq v2.20.0.

Bioinformatics analysis

The 150bp Illumina raw reads were filtered for low quality reads, adapters were trimmed using Fastp v 0.23.2 (Chen et al. 2018), with parameters for filtering, along with `--trim-poly-g` to remove polyG tail trimming. Duplicated reads were removed with additional flag `--dedup` along with `--dup-calc-accuracy` set to 6 for highest accuracy. Reads were aligned to the *E. nectar* reference genome (GCA_024703715.1) obtained from NCBI. HiSAT2 v2.1.0 (Kim et al. 2019) was utilized for aligning raw reads to the reference genome using default parameters. These analyses used the resources provided by Michigan State University's high performance computing center. SAMtools v1.16.1 (Li et al. 2009) was used for converting SAMs to BAMs followed by sorting and indexing of bam files. FeatureCounts v2.0.6 (Liao et al. 2014) was used for extracting raw counts assigned to genes. FastQC v0.11.7 (<https://www.bioinformatics.babraham.ac.uk/projects/fastqc/>) was used to analyze quality parameters of the raw and filtered reads, along with MultiQC v1.14 (Ewels et al. 2016) for summarizing all quality scores.

The raw counts were corrected for batch effects using Combat-Seq tool (Zhang et al. 2020). ComBat_Seq is based on using negative binomial regression specifically catered for RNA-seq count Data. The Adjusted counts matrix produced after batch effect correction was utilized for downstream analysis. The analysis involved contrasting each treatment and time point, treating them as distinct groups. Comparisons were made between the control at 3 hours and the corresponding treatments at the same time point, as well as between the control at 6 hours and the treatments at that time point. The differentially expressed genes (DEGs) for the responsive and constitutive gene expression were done using EdgeR v4.2.1 (Robinson et al. 2010). The criteria for up- or down regulated genes included log-fold change of 1, and adjusted

p-value of less than 0.05. The control at 3hr and 6hr were used as baseline for comparison among treatment.

Results

In vitro determination of EC₅₀ concentrations for all fungicides

The EC₅₀ concentrations for EnFrame isolate of *E. necator* for five fungicides including trifloxystrobin, quinoxyfen, metrafenone, cyflufenamid and flutianil were tested using conidial germination experiment on the fungicide amended media. An average EC₅₀ concentrations of trifloxystrobin, quinoxyfen, and flutianil were determined as approximately 0.002 ppm, 0.0001 ppm, and 5 ppm, respectively (Fig. 3.1A;B;C). Interestingly, varying fungicidal concentrations of metrafenone and cyflufenamid did not have consistent inhibitory effect on conidial germination. While some inhibition of conidial germination was observed at higher concentrations (10 and 100 ppm), the results were inconsistent across replicates, and most conidia exhibited at least some degree of germ tube formation (Fig. 3.1D;E). Therefore, EC₅₀ concentrations for metrafenone and cyflufenamid were not determined. Hence, the fungicides trifloxystrobin, quinoxyfen, and flutianil were selected for further transcriptomics experiments, using their respective approximate EC₅₀ concentrations.

Gene expression analysis

RNA quality control, filtering, and metrics

The percentage of adapters trimmed were on averaged 11%. An average of 85.8 million reads were obtained from each sampled isolate after filtering by quality. The duplication rate was an average of 37% across the samples isolates. Approximately 99% of reads passed the quality filter. On average, 94.67% of the reads were successfully mapped to the genome, with 88.97% mapping uniquely and 5.70% aligning to multiple locations. A total of 7011 genes of the 7146

genes present in the reference genome passed the initial filter. Counts ranged from 17 million to 23 million per sample. The two biological replicates from quinoxifen treated samples that were collect at 6hours have the lowest read counts.

Principle component analysis

The PCA analysis summarizes the variance in the transcriptomic data after applying batch correction with the combat method. This reflects that the variation in the data is more likely to reflect real biological differences rather than technical artifacts. The PC1 and PC2 explained 41.23% and 27.57% of the variance of data. The control samples at 0 time appear to be grouped near the origin or at one extreme along the PC1 axis. All fungicide-treated and control samples collected at 3 hours and 6 hours are clustered at the opposite end of the PCA plot, showing clear separation in gene expression profiles from the control samples taken at 0 hours. Trifloxystrobin-treated samples at 3 hours exhibit grouping within treatment and a clear separation from the control samples at the same time point. Moderate separation was observed by 6 hours. In contrast, quinoxifen-treated samples showed grouping within treatment, while exhibiting divergence from the control samples at 3 hours, with this separation becoming even greater at 6 hours. Flutianil-treated samples form a distinct cluster and are moderately separated from the control samples at both 3 and 6 that time. Interestingly, flutianil-treated samples cluster relatively close to the quinoxifen-treated samples at 3 hours.

Gene expression differences among control and each fungicide

Differential gene expression in quinoxifen-treated samples

Gene expressions in samples treated with quinoxifen were compared to control samples at both 3 and 6 hrs. This comparison aimed to identify specific expression patterns that could be related to the effects on the germination of *E. necator* conidia due to exposure to EC₅₀ dose of

quinoxifen. A total of 32 genes were upregulated and 70 genes were downregulated in quinoxifen-treated samples at 3 hours compared to the control (Table 3.1). At 6 hour, the number of upregulated genes increased to 169, while downregulated genes increased to 148 (Table 3.1). Specifically, at 3 hour, 24 upregulated and 58 downregulated genes were associated uniquely with quinoxifen treatment and were not observed in samples treated with flutianil or trifloxystrobin (Fig. 3.3; Table 3.2). Similarly, at 6 hour, 136 upregulated and 145 downregulated genes were specifically linked to quinoxifen treatment (Fig. 3.4; Table 3.3). Upregulated genes only specific to quinoxifen at 3 hour included velvet complex subunit 2 (HI914_04859), oleate hydroxylase FAH12 (HI914_01636), spore development regulator RYP2 protein (HI914_06764), diphosphoinositol polyphosphate phosphohydrolase APS1 (HI914_01388), putative inorganic phosphate transporter 1-6 (HI914_05073), putative sucrose utilization protein (HI914_03138), secreted RxLR effector protein (HI914_00981), and putative yippee family protein (HI914_03392), along with 16 other genes that were identified as hypothetical proteins (Table 3.2).

In the quinoxifen-treated samples, there were 126 additional genes exclusively upregulated at 6 hours compared to those at 3 hour, using baseline controls at 6 and 3 hours, respectively. At both 3 and 6 hours, velvet complex subunit 2 (HI914_04859), diphosphoinositol polyphosphate phosphohydrolase aps1 (HI914_01388), Oleate hydroxylase FAH12 (HI914_01636), and several hypothetical proteins were consistently upregulated. At 6 hours, notable upregulated genes included heat shock proteins (e.g., HI914_04743, HI914_03968), secondary metabolism regulators LAE1 (HI914_04568, HI914_00771), and metabolic enzymes like NADP-dependent malic enzyme (HI914_04980) and malate synthase (HI914_02641). Important transport proteins, such as ABC multidrug transporter (HI914_05697), and regulatory

proteins, including clock-controlled protein (HI914_03415) and serine/threonine-protein kinase KIN28 (HI914_03302), were also upregulated. Downregulation at 3 and 6 hours affected glutathione transporter (HI914_04140), nicotinate transcription factor (HI914_05032), acetyltransferase (HI914_00994), and various transporter proteins like putative peptide transporter ptr2 (HI914_02488) at 6 hours, suggesting broad effects on cellular transport and regulatory pathways (Table 3.3).

Of the 58 genes downregulated in quinoxifen-treated samples at 3 hours, 35 were also downregulated in the samples treated for 6 hours. Of these genes, 18 were classified as hypothetical, and 17 were among listed above. Additionally, among the 110 genes exclusively downregulated at the 6-hour duration, 97 were identified as hypothetical proteins.

Downregulation of various genes encoding transport proteins, including glutathione transporter (HI914_04140) and plasma membrane ATPase (HI914_04132). Metabolic enzymes, including hexokinase-1 (HI914_02059) and O-acetyltransferase PaAT-1 (HI914_00921), also showed downregulation. Genes that could be involved in regulatory and cellular signaling such as the transcription factor sge1 (HI914_00897) and serine/threonine-protein kinase mph1 (HI914_02426, HI914_00845, HI914_02608, HI914_05102) also had reduced expression.

Downregulation of ras guanine nucleotide exchange factor A (Ras-GEF A) protein was also found. Structural genes, including G2/mitotic-specific cyclin-4 (HI914_05967) and cell wall mannoprotein CIS3 (HI914_00681), indicated impacts on cell division and structural integrity.

At 6 hours, transporter genes like the low affinity vacuolar monovalent cation/H⁺ antiporter (HI914_02252) and Na⁽⁺⁾/H⁽⁺⁾ antiporter (HI914_06615) were further downregulated, along with regulatory genes, such as the transcriptional activator hac1 (HI914_00580) and secondary metabolism regulators LAE1 (HI914_04568, HI914_00771). Downregulation of enzymes like

cytochrome P450 monooxygenases (HI914_05519, HI914_07477), was also observed (Table 3.3).

Differential gene expression in flutianil-treated samples

Gene expression in samples exposed to flutianil was analyzed at both 3 and 6 hours, to discern any specific changes related to the impact of an EC₅₀ dose of flutianil on the germination of *E. necator* conidia. In this analysis, flutianil-treated samples exhibited significant gene expression changes over time. At the 3-hour, there was an upregulation of 16 genes and a downregulation of 2 genes compared to the controls (Table 3.1; Fig 3.3). By the 6-hour, the number of upregulated genes had increased to 23, while 3 genes were downregulated (Table 3.1; Fig 3.4). Specifically, at 3 hours, 4 upregulated and 1 downregulated gene were unique to the flutianil treatment and not observed with any other fungicide; however, these genes were all classified as hypothetical proteins. At 6 hours, the upregulated genes, including chitinase HI914_05902 and another hypothetical protein, along with two downregulated hypothetical proteins, were specifically expressed in the flutianil-treated samples only (Table 3.4).

Differential gene expression in trifloxystrobin-treated samples

Gene expression was analyzed in samples exposed to an EC₅₀ dose of trifloxystrobin, comparing with controls at both 3 and 6 hours. At the 3-hour mark, there was a significant change with 17 genes upregulated and 19 genes downregulated compared to the control (Table 3.1; Fig. 3.3). The upregulated genes included NADP-dependent oxidoreductase RED1 (HI914_00115), trichothecene C-4 hydroxylase (HI914_07478), cytochrome P450 monooxygenase acIL (HI914_07477), and five unidentified hypothetical proteins, all uniquely expressed in the trifloxystrobin-treated samples. Downregulated genes at this time point included O-methyltransferase VdtC (HI914_00987), vacuolar membrane amino acid uptake transporter

fnx2 (HI914_05456), potassium transport protein 1 (HI914_05987), alongside five other hypothetical proteins, with these changes not observed with any other fungicides (Table 3.4). By the 6-hour interval, the count of upregulated genes rose to 26, while downregulated genes decreased to seven (Table 3.1; Fig. 3.4). Specific to the 6-hour timeframe, 7 upregulated and 5 downregulated genes were all classified as hypothetical proteins, exclusively altered in the trifloxystrobin-treated samples.

Comparison of gene expression differences among quinoxyfen, trifloxystrobin and flutianil using control as baseline, at 3- and 6-hours durations

Results indicated that three genes were consistently upregulated at the 3-hour point and seven at the 6-hour point across all samples treated with quinoxyfen, trifloxystrobin, and flutianil (Table 3.1; Figs. 3.3; 3.4). However, no genes were commonly downregulated at these time points. At 3 hours, the cytochrome P450 monooxygenase HI914_05519 and two unidentified hypothetical proteins were commonly upregulated in all fungicide treatments (Table 3.5). At 6 hours, the maltose permease MAL31 HI914_00719 and the sphingolipid long chain base-responsive protein LSP1 HI914_05871, together with five other hypothetical proteins, were consistently upregulated (Table 3.5).

An analysis comparing gene expression differences between quinoxyfen and trifloxystrobin, with control samples as a baseline, revealed that only one gene was consistently upregulated at the 3-hour duration, while eleven genes were downregulated (Fig 3.3). The upregulated gene was identified as encoding a putative PPE family protein (HI914_01187). The downregulated genes included thioredoxin-1 (HI914_03920), demethyl-4-deoxygadusol synthase (HI914_01057), chitinase (HI914_05904), along with eight additional genes classified as hypothetical proteins. At the 6-hour interval, the number of upregulated genes increased to

twelve, including NADP-dependent oxidoreductase RED1 (HI914_00115) and eleven hypothetical proteins, whereas downregulated genes decreased to two hypothetical proteins (Table 3.5).

A comparison between samples treated with trifloxystrobin and flutianil revealed that only five genes, including maltose permease MAL31 (HI914_00719) and four genes that code for hypothetical proteins, were commonly upregulated in both treatments at the 3-hour mark (Fig. 3.3). By the 6-hour point, there were no genes that were commonly upregulated across the two treatments (Fig. 3.4). Additionally, there were no genes commonly downregulated at either the 3-hour or 6-hour intervals in both fungicide treatments.

Additionally, the expression of four genes, including a putative F-box domain-containing protein (HI914_04666) and three unidentified hypothetical proteins, was found to be commonly increased in both quinoxifen and flutianil-treated samples at the three-hour. By the six-hour interval, the count of genes commonly upregulated in these treatments increased to fourteen genes. This group of genes also included MFS transporters (HI914_04831), rifampicin monooxygenase (HI914_02452), and enoyl-CoA delta isomerase 3 (HI914_02682) (Table 3.5). At the 3-hour interval, one gene that was commonly downregulated between both fungicides was identified as a hypothetical protein. Similarly, at the 6-hour interval, another commonly downregulated gene was also classified as a hypothetical protein.

Discussion

Quinoxifen, metrafenone, cyflufenamid, and flutianil are among the recently developed key specialty fungicides recently developed to combat grape powdery mildew. These fungicides play a crucial role in resistance management strategies for *E. necator*, especially given the widespread resistance to QoI and DMI fungicides (Miles et al. 2021; Sharma et al. 2023). An in

vitro spore germination test was performed in this study to establish the EC₅₀ concentrations using a sensitive *E. necator* isolate for the fungicides quinoxyfen, metrafenone, cyflufenamid, flutianil and trifloxystrobin. The conidial germination of *E. necator* isolate was successfully inhibited in 50% of the conidia at determined EC₅₀ concentrations of quinoxyfen, trifloxystrobin and flutianil fungicides. While flutianil was effective at inhibiting conidial germination, most conidia still exhibited germ tubes that were mostly shorter than half the length of the conidia at 16-hour duration. On the other hand, cyflufenamid and metrafenone were not effective in consistently inhibiting conidial germination, suggesting that these fungicides might target different biological processes in *E. necator* than affecting conidial germination directly. Research on *Blumeria graminis* f. sp. *hordei* and *B. graminis* f. sp. *tritici* has shown that metrafenone affects the formation of appressoria, the development of hyphae, and directed hyphal growth, while also inhibiting sporulation due to the development of abnormal conidiophores (Opalski et al. 2006). Similarly, cyflufenamid has also shown inhibitory pattern on haustoria formation in *B. graminis* but no effect on conidial germination (Haramoto et al. 2006). Thus, flutianil appears to resemble quinoxyfen and trifloxystrobin in its ability to inhibit spore germination in *E. necator*. Since the mechanism of action for trifloxystrobin (a QoI fungicide) is well understood, it was included in the transcriptomics study to offer insights that might be compared with the effects of flutianil and quinoxyfen.

The transcriptomic study presented here provides an initial understanding of how these fungicides affect the early phase of spore germination in *E. necator*, using EC₅₀ as a snapshot concentration. This approach serves as a valuable starting point for identifying genes that are differentially expressed at sublethal doses. It offers insights into the early molecular responses and adaptations *E. necator* may undergo when exposed to such stress. However, to capture a

broader range of differentially expressed genes that may be linked to fungicide resistance, a more comprehensive approach could be taken. This would involve repeatedly transferring *E. necator* through a wider range of fungicide concentrations, followed by transcriptomic analysis on conidia collected after multiple transfers. Such an approach would help reveal dose-dependent responses and provide a deeper understanding of how specific genes or pathways contribute to resistance at varying exposure levels. That said, *E. necator* is an obligate biotrophic pathogen, which means conducting multiple successive transfers would require grape leaves treated with different fungicide concentrations. These logistical challenges make the experiment more difficult to execute, requiring careful planning and preparation in advance.

Our study revealed a limited overlap in the differentially expressed genes triggered by the fungicides flutianil, quinoxyfen, and trifloxystrobin, at both 3-hour and 6-hour intervals. This indicates that each fungicide induces a distinct gene expression pattern compared to the control, as a large number of the genes were unique to each fungicide treatment. For example, at the 6-hour mark, quinoxyfen upregulated 136 genes, with only 14 genes shared among all treatments. A similar trend was observed for downregulated genes, with few overlaps and many being specific to each fungicide treatment. These results suggest that flutianil, quinoxyfen, and trifloxystrobin may have substantial different mechanisms, leading to unique transcriptional responses in *E. necator*. This points to the possibility that each fungicide targets distinct cellular or molecular pathways, potentially disrupting different biological processes within the *E. necator*.

Although the number of differentially expressed genes is limited, several key genes are shared among these fungicides indicating that the *E. necator* prioritize respiration cycle at various stages including electron transport chain, glycolysis, and kreb cycle. At the 3-hour

interval, one of the most prominent upregulated genes common to all fungicide treatments is cytochrome P450 monooxygenase (HI914_05519). This gene plays a pivotal role in the electron transport chain, where it is essential for oxidative phosphorylation, the primary mechanism through which ATP is produced in the mitochondria (Munro et al. 2018). This reflects an early cellular response to oxidative stress caused by fungicidal exposure. By enhancing the function of this enzyme, the fungus is likely increasing their capacity to detoxify reactive oxygen species (ROS) generated during fungicide action, while maintaining the electron flow necessary for efficient ATP production. This suggests that the electron transport chain is an immediate target for adaptation in the presence of fungicides, ensuring that energy production is sustained despite external stress. At the 6-hour interval, the upregulated genes show a broader metabolic shift. Maltose permease MAL31 (HI914_00719), was also commonly upregulated across all treatments aiding in upregulating glycolytic pathways to provide substrates for energy production. It is an important gene in glycolysis as it encodes as a transporter that facilitates the maltose uptake, which is then hydrolyzed into glucose. Glucose enters the glycolytic pathway, providing pyruvate that can subsequently fuel the krebs cycle and the electron transport chain for energy production (Medintz et al. 1996). The upregulation of maltose permease was observed in trifloxystrobin and flutianil at 3 hours, and in all three fungicide treatments at 6 hours suggesting that as the fungi continue to face fungicidal stress, they increase sugar metabolism to supply more substrates for cellular respiration. This enhanced glycolytic activity supports the production of ATP, ensuring that energy demands are met. Moreover, NADP-dependent oxidoreductase RED1 (HI914_00115) was upregulated at 6 hours in both quinoxifen and trifloxystrobin treatments. The increased expression of NADP-dependent oxidoreductase indicates that redox homeostasis by regulating the NADP/NADPH balance. This ensures a steady supply of reducing

power necessary for electron transport chain function, thereby protecting the cell from oxidative stress and supporting ATP synthesis. Also, the upregulation of enoyl-CoA delta isomerase 3 was found in flutianil and quinoxifen at 6 hours, indicating increased fatty acid metabolism through β -oxidation in mitochondria, providing the necessary acetyl-CoA for the Krebs cycle to generate NADH and FADH₂ (Xin et al. 2022). These electron carriers subsequently provide reducing equivalents to the electron transport chain for ATP production via oxidative phosphorylation. This metabolic shift suggests that the organism is prioritizing lipid breakdown to meet its energy requirements, likely in response to high energy demand (Xin et al. 2022).

Another important commonly upregulated gene at 6 hours in all fungicide treatments is the sphingolipid long chain base-responsive protein LSP1 (HI914_05871). Sphingolipids are crucial components of the cell membrane and are involved in signaling pathways that mediate cellular responses as well as repolarization of the actin cytoskeleton due to stress, particularly membrane damage (Yang et al. 2015). Increased expression of LSP1 suggests that fungicidal treatment causes changes to the fungal cell membrane, and this protein helps mitigate those effects. The upregulation of this gene supports the integrity of cellular structures that are critical for maintaining respiration and other metabolic processes.

In contrast, thioredoxin-1 (HI914_03920) gene was downregulated at 3 hours in both quinoxifen and trifloxystrobin treatments. thioredoxin-1 is crucial for activating Hog1, a protein that helps cells respond to oxidative and osmotic stress. Hog1 is part of the MAPK pathway, which protects cells under stress. When thioredoxin-1 levels are low, Hog1 activation may decrease, making it harder for the cell to cope with oxidative stress. Its downregulation could imply that the fungi are relying on alternative redox-balancing mechanisms (da Silva Dantas et al. 2010). Also, other genes associated with protein kinase family was also downregulated,

indicating interruption in signal transduction pathways (Turrà et al. 2014). Other studies have also found that quinoxifen acts on signal transduction pathways of the powdery mildew fungi (Lee et al. 2008).

Additionally, in quinoxifen and flutianil treatments at the 6-hour interval, MFS transporters (HI914_04831) and Rifampicin monooxygenase (HI914_02452) were commonly upregulated, indicating a broader metabolic response. The upregulation of MFS transporters suggests increased nutrient and metabolite transport involved in drug efflux systems, secretion of endogenously produced toxins, which could be necessary for sustaining cellular metabolism and detoxification processes as fungicidal exposure continues (Del Sorbo et al. 2000). This gene has been also associated with multidrug resistance in fungicides. Hence, its upregulation could have a strong connection with development of fungicide resistance to flutianil in future. Furthermore, Rifampicin monooxygenase might also play a role in detoxifying harmful compounds, further highlighting the importance of metabolic adaptation to fungicidal stress.

Based on prior research and our findings, flutianil appears to affect multiple stages of powdery mildew fungal development, from spore germination to haustoria formation (Kimura et al. 2020; Kimura et al. 2021). This study, combined with previous research on gene expression changes in *B. graminis* treated with flutianil during haustoria formation (Kimura et al. 2021), reveals a broader pattern in fungal responses to fungicide treatment. Kimura et al. (2021) reported overexpression of sugar transporter genes, MFS transporter genes, and endochitinase genes in flutianil-treated samples, suggesting that these pathways play crucial roles in fungal defense mechanisms and adaptation under fungicidal stress. Similarly, our analysis detected upregulation of genes encoding sugar transporters (such as Maltose permease), MFS transporters, and chitinase in flutianil-treated samples during spore germination, an early

developmental stage in the fungal life cycle. These findings suggest a consistent strategy in which fungi activate nutrient uptake to support energy production via glycolysis, increase membrane transport to enhance multidrug resistance and metabolite transport (potentially allowing fungi to expel toxic compounds and optimize nutrient intake), and remodel their cell walls to adapt their composition as a protective measure in response to fungicide exposure, regardless of developmental stage. In a broader context, these responses demonstrate a common adaptive mechanism in fungi, where metabolic pathways related to nutrient acquisition, cell wall modification, and efflux systems are mobilized to overcome fungicidal stress.

The transcriptional changes specifically triggered by quinoxifen treatment suggest that it disrupts a wide array of cellular processes in the fungus, impacting metabolism, stress response, transport, signal transduction, and growth regulation. A critical component of the fungal response appears to be the regulation of signal transduction pathways, particularly those involving the MAPK (Mitogen-Activated Protein Kinase) pathway. In this study, the downregulation of serine/threonine-protein kinase *mph1* was found, which is part of the MAPK pathway, suggests that quinoxifen interferes with cellular signaling networks that are essential for regulating cellular defense mechanisms, coordinating responses to environmental changes, including oxidative stress, osmotic stress, and nutrient availability. Similarly, regulation of proteins involved in MAPK pathway has been also reported in another study conducted on quinoxifen treated *E. necator* isolates. They also found downregulation of GTPase- mediated signal transduction. Another study has also reported genes related to GTP-binding or GTPase activity were over expressed in quinoxifen treated *Blumeria graminis* f. sp. *hordei* compared to untreated samples (Wheeler et al. 2000; Wheeler et al. 2003). We also found downregulation of Ras guanine nucleotide exchange factor A (Ras-GEF A) protein. These Ras proteins are a class

of GTP-binding, that interact with GAPs (GTPase-activating protein) and act as molecular switches by cycling between a GDP-bound inactive state and a GTP-bound active state and can disrupt the degradation of the GAP signal and termination of signal transmission (Cox et al. 2014; Wittinghofer et al. 1997). In addition, the downregulation of key transcriptional regulators, such as global transcription regulator *sgel* and transcription factor *vib-1*, suggests that quinoxifen impacts the ability of the fungus to reprogram its gene expression in response to stress. This repression could have a cascading effect on downstream genes regulated by these factors, further impairing the organism's ability to adapt to the fungicide.

Moreover, the impairment of transport proteins, including glutathione transporter, Na(+)/H(+) antiporter, and aquaporins, suggests that quinoxifen interferes with the fungus's capacity to maintain ion balance and detoxify harmful substances as these transporters are critical for redox homeostasis (Bachhawat et al. 2013). The reduction in glutathione transport likely compromises the cellular redox balance, increasing vulnerability to reactive oxygen species (ROS), while the loss of ion transporters affects cellular homeostasis, potentially leading to osmotic stress and energy depletion. This is further compounded by the reduced expression of genes involved in oxidative stress management, such as catalase-peroxidase and gamma-glutamylputrescine oxidoreductase, which suggests that the fungus's ability to detoxify ROS is impaired, increasing the likelihood of cellular damage. In contrast, the upregulation of genes involved in metabolic processes, such as the NADP-dependent malic enzyme and malate synthase, points to an attempt by *E. necator* to maintain energy production under stress. The upregulation of heat shock proteins, MFS and ABC multidrug transporters further underscores the activation of stress response and fungicide resistance pathways by drug efflux, indicating that

quinoxifen creates an environment that challenges protein stability and cellular integrity (Del Sorbo et al. 2000).

The abundance of hypothetical proteins in our transcriptomic analysis suggests that we may have overlooked some critical genes with significant roles in fungicide response. This raises questions about their biological significance, reliability, and the quality of the gene model. Hypothetical proteins are predicted proteins encoded by genes that have not yet been experimentally characterized. They are derived through computational predictions based on genomic data, often due to the lack of homologous sequences with known functions in public databases. These proteins could be real, however, currently their functions remain unknown, making it challenging to fully understand their roles in cellular processes. Another possibility is that the current gene model could be limited or not of great quality, particularly if functional annotations are based solely on sequence homology. This limitation could obscure potentially novel or unique proteins in fungi that are crucial for survival and adaptation. Moving forward, it is essential to prioritize re-annotating the gene model and conducting experimental validation of these hypothetical genes. Techniques such as gene knockout/knockdown studies can help confirm the presence and function of these proteins. Addressing these hypothetical genes can expand our understanding of the molecular mechanisms of these fungicide against *E. necator* and other powdery mildews.

To build on our current findings, several next steps could provide a more comprehensive understanding of gene expression changes and functional mechanisms in response to these fungicide treatments. Expanding the transcriptomic analysis to include additional time points would help capture dynamic gene expression patterns over time, offering insights into later stages including appressorium formation, haustoria formation and hyphal elongation etc.

responses to fungicide exposure. This could be specifically beneficial for fungicides including flutianil, cyflufenamid, metrafenone and quinoxyfen as all of these fungicides has been reported to affect processes related to appressoria or haustoria formation and secondary hyphal elongation based on morphological studies (Kimura et al. 2020). This broader temporal resolution could identify transiently expressed genes and regulatory cascades that are not visible at only a few time points. In addition, conducting qPCR validation for key genes identified in our transcriptomic analysis would provide quantitative confirmation of expression changes. Moreover, functional studies such as gene knockouts, knockdowns, or overexpression studies can help us to further characterize the biological roles of these key genes. These functional studies, particularly for hypothetical proteins, would help bridge the gap between sequence-based predictions and actual cellular roles, potentially uncovering new mechanisms of action for these fungicides. Examining genetic diversity across a population of *E. necator* isolates can be used as another approach to find mutations or changes in gene expression that may correlate with fungicide resistance. By comparing susceptible and resistant isolates, we can identify genetic markers or mutations associated with resistance phenotypes, providing insights into potential targets for managing resistance. This could be beneficial for quinoxyfen, as resistance in *E. necator* has been already reported in Virginia (Feng et al. 2018). Assessment of quinoxyfen resistant *E. necator* populations in relation to fitness penalties can help us to know whether resistant population might face survival or reproduction disadvantages. If resistant strains have fitness penalties, they may reproduce or spread more slowly, giving non-resistant strains a benefit when the fungicide is removed. However, if resistant strains have minimal or no fitness penalties, this will increase the likelihood of greater resistance issues in future. Also,

understanding any potential fitness penalties in resistant strains could also shape the timing and frequency of quinoxyfen use.

Our study provides important insights into the similarities and differences in the mechanisms of key fungicides used to control powdery mildew. Among the fungicides tested—quinoxyfen, flutianil, and trifloxystrobin—only a few differentially expressed genes were shared, indicating that quinoxyfen and flutianil function through distinct mechanisms from each other and from trifloxystrobin. Upregulation of MFS transporters and ABC multidrug transporters reflect greater chances of resistance development in quinoxyfen and flutianil. These findings can guide the development of more effective strategies for fungicide resistance managing strategies. This can help in extending the effectiveness of these fungicides for longer durations in controlling grape powdery mildew.

Acknowledgments

Michigan State University is situated on the ancestral, traditional, and contemporary lands of the Anishinaabe, including the Three Fires Confederacy of the Ojibwe, Odawa, and Potawatomi peoples. These lands were ceded in the 1819 Treaty of Saginaw. We recognize the ongoing presence of Indigenous peoples and their enduring connection to this land.

Figures

Figure 3.1. Percentage of conidial germination of *Erysiphe necator* relative to the control after treatment with fungicides at different concentrations. Conidial germination assay was conducted using a sensitive isolate of *E. necator*. Each concentration had three replicates and experiment was repeated twice.

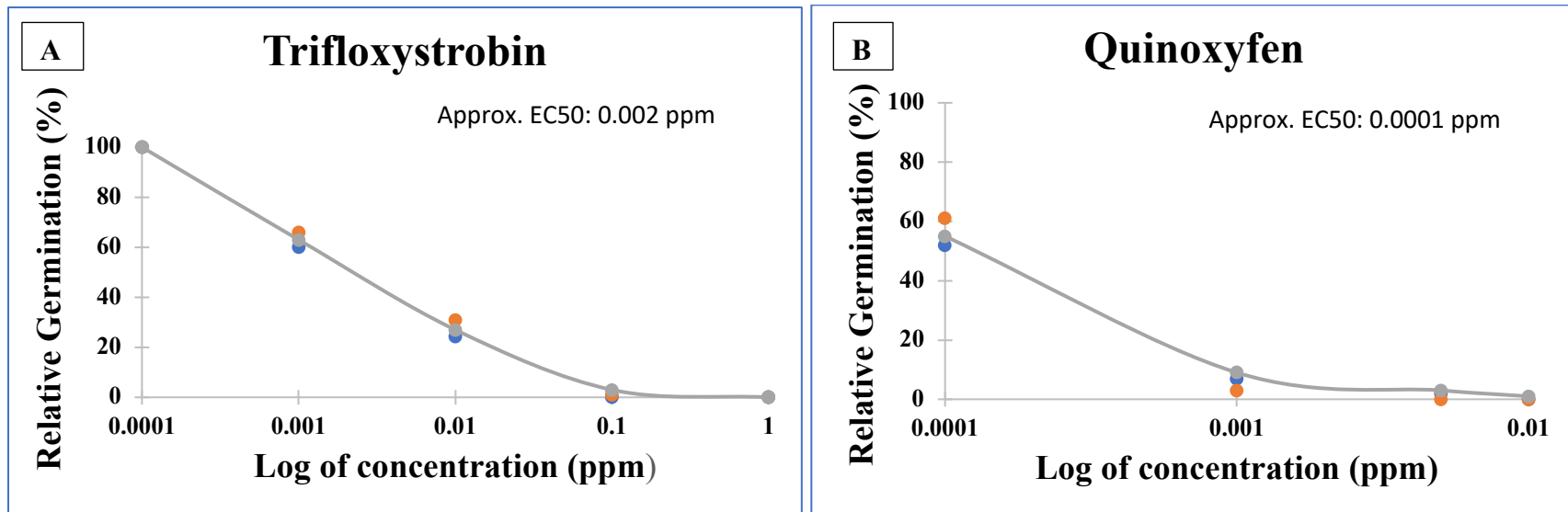


Figure 3.1. (cont'd)

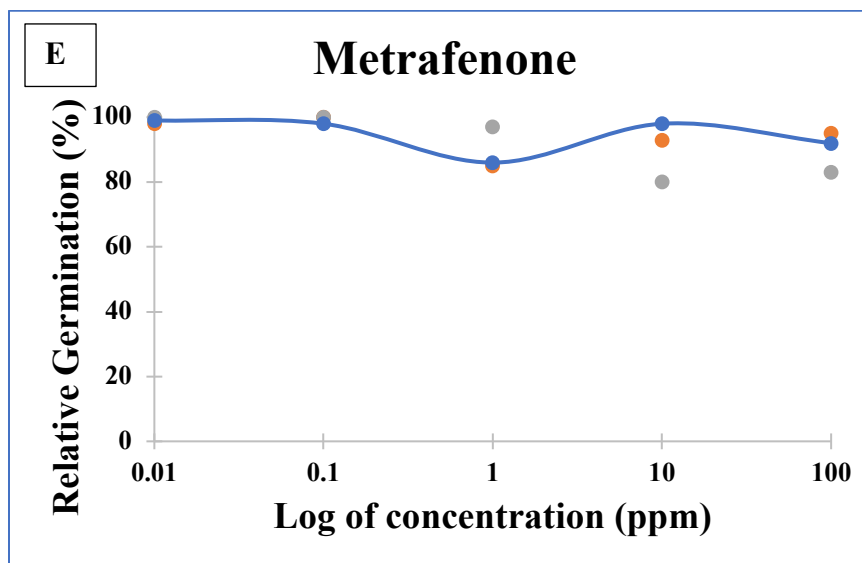
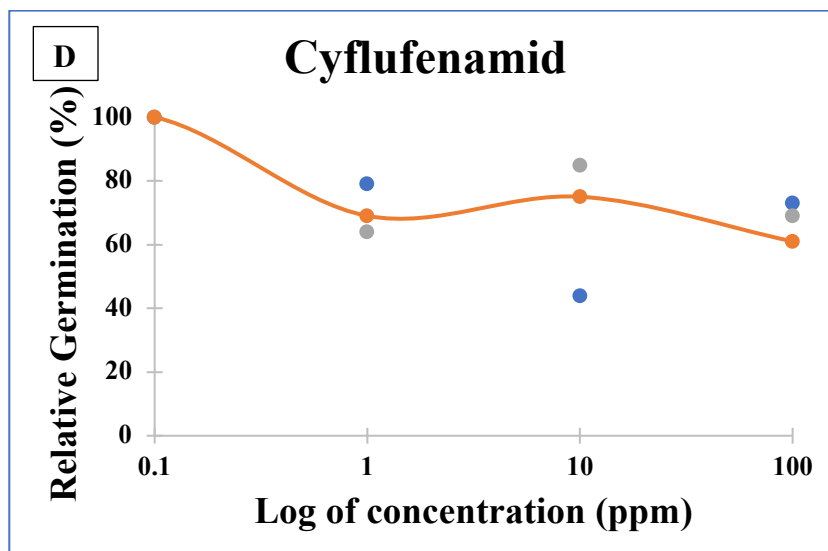
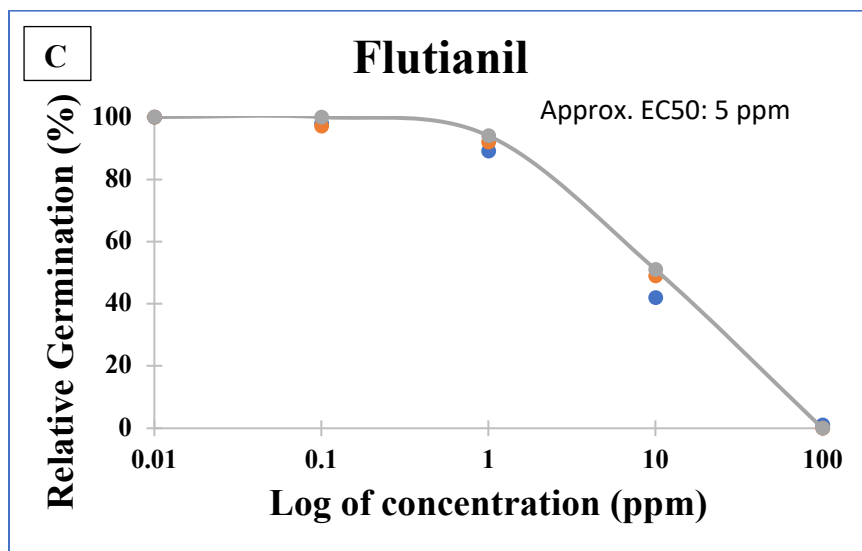


Figure 3.2. Principal component analysis of read counts. The shape and color represent the fungicide treatment (quinoxyfen, flutianil, and trifloxystrobin)/control, and exposure time duration, respectively. PC1 explains 41.23% of the variance and PC2 explains 27.57% of the variance.

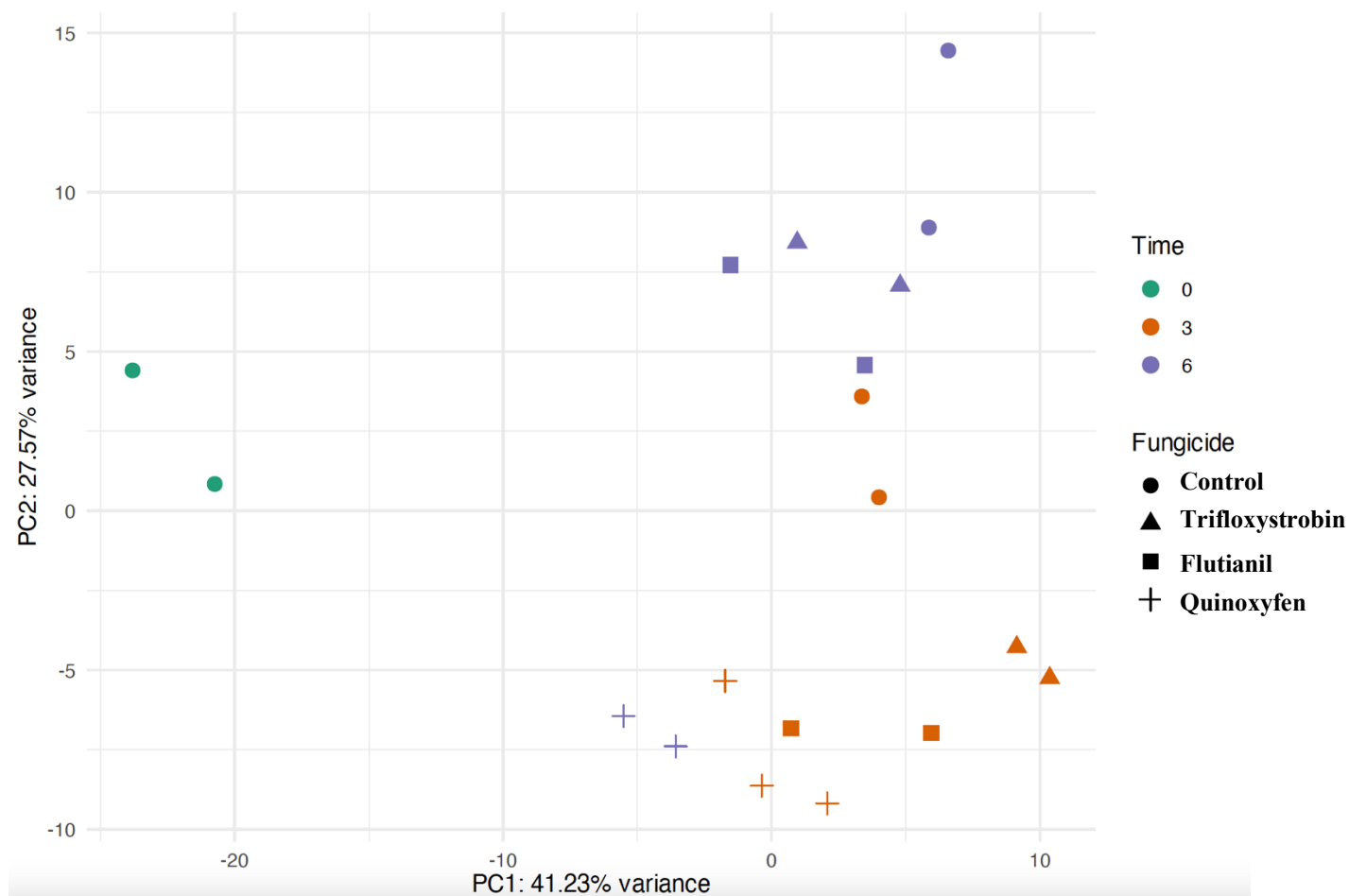


Figure 3.3. Venn diagrams show similarities and dis-similarities between the number of differentially expressed genes across treatments. Number of genes upregulated and downregulated in fungicide (trifloxystrobin, flutianil, and quinoxyfen) treated *Erysiphe necator* conidia were compared to control at 3-hour treatment exposure. Genes were classified as up- and down- regulated using an adjusted P value of 0.05 with a log-fold change of 1.

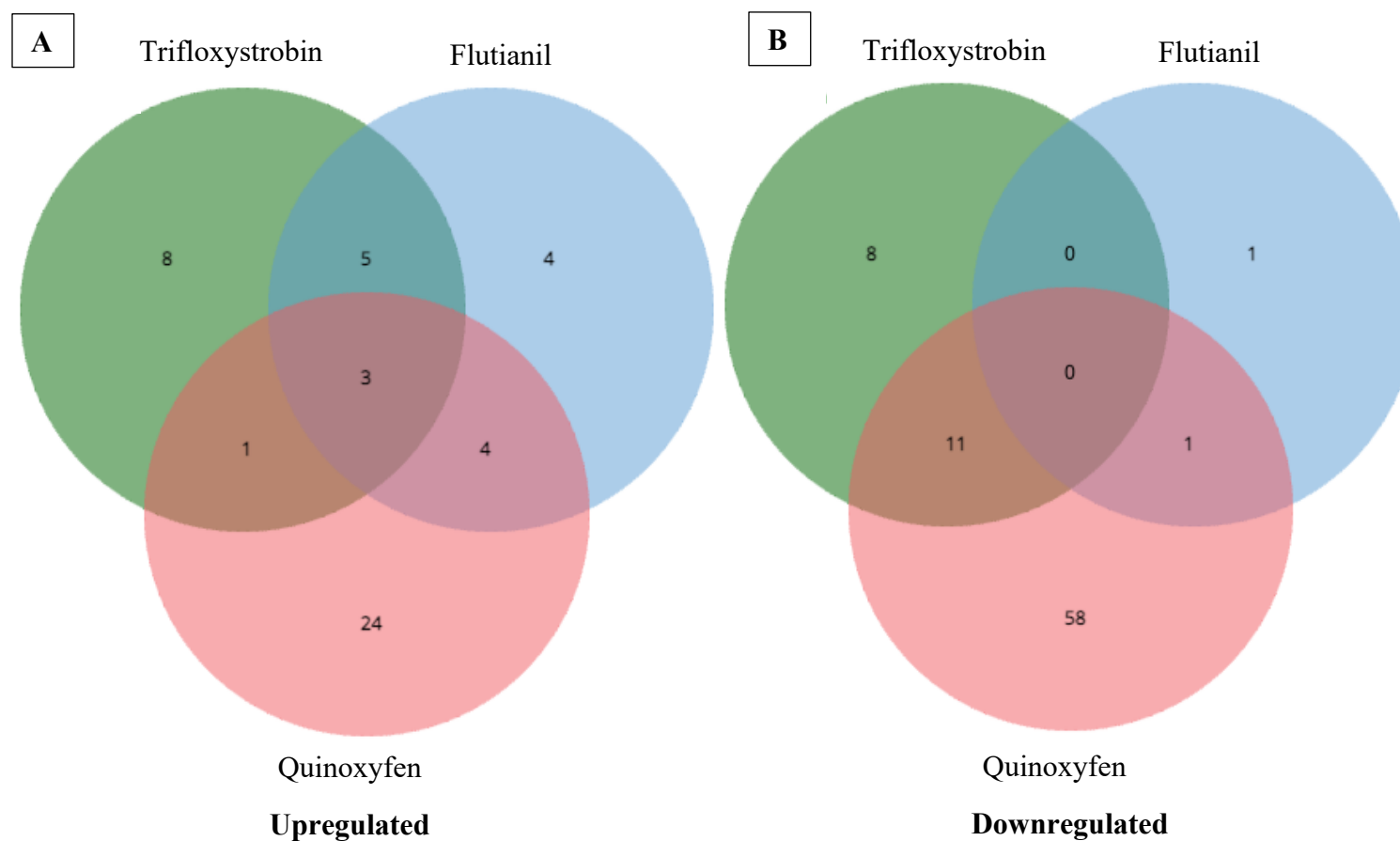
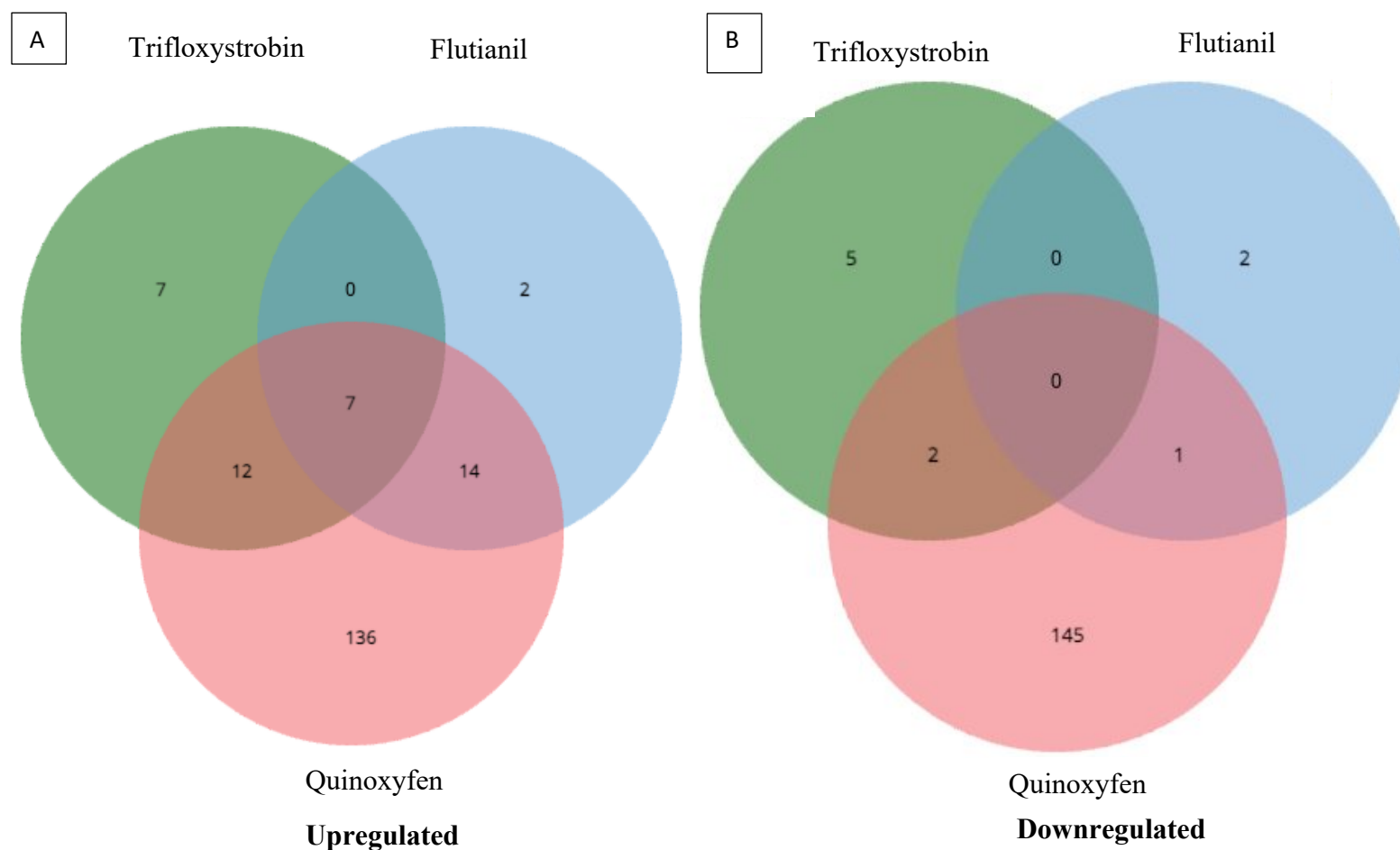


Figure 3.4. Venn diagrams show similarities and dis-similarities between the number of differentially expressed genes across treatments. Number of genes upregulated and downregulated in fungicide (trifloxystrobin, flutianil, and quinoxyfen) treated *Erysiphe necator* conidia were compared to control at 6-hour treatment exposure. Genes were classified as up- and down- regulated using an adjusted P value of 0.05 with a log-fold change of 1.



Tables

Table 3.1. Number of upregulated and downregulated genes in *Erysiphe necator* following 3-hour and 6-hour fungicide exposure during conidial germination. Control at 3-hour and 6-hour were used as baseline for identifying differentially expressed genes. Genes were classified as up- and down- regulated using an adjusted P value of 0.05 with a log-fold change of 1.

Time Duration (hour)	Fungicide	No. of genes upregulated	No. of genes downregulated
3	Flutianil	16	2
	Quinoxifen	32	70
	Trifloxystrobin	17	19
6	Flutianil	23	3
	Quinoxifen	169	148
	Trifloxystrobin	26	7

Table 3.2. Log-fold changes in uniquely upregulated and downregulated genes in *Erysiphe necator* conidia treated with quinoxifen compared to control at 3-hour exposure. Genes were classified as up- and down- regulated using an adjusted P value of 0.05 with a log-fold change of 1. Genes that were identified as hypothetical are not included in this list.

Gene ID	Gene Name	Log-fold Change	Expression Change
HI914_04859	Velvet complex subunit 2	1.32	Upregulation
HI914_01636	Oleate hydroxylase FAH12	1.25	Upregulation
HI914_06764	Spore development regulator RYP2	1.21	Upregulation
HI914_04730	putative glycosyl	1.12	Upregulation
HI914_01388	Diphosphoinositol polyphosphate phosphohydrolase aps1	1.10	Upregulation
HI914_05073	putative inorganic phosphate transporter 1-6	1.09	Upregulation
HI914_03392	putative yippee family protein	1.04	Upregulation
HI914_03138	putative sucrose utilization protein	1.03	Upregulation
HI914_00981	Secreted RxLR effector protein	1.08	Upregulation
HI914_04140	Glutathione transporter	-1.00	downregulation
HI914_06808	Cholinesterase	-1.00	downregulation
HI914_05032	Nicotinate catabolism cluster-specific transcription factor	-1.00	downregulation
HI914_02426	Serine/threonine-protein kinase mph1	-1.013	downregulation
HI914_04931	HMG box-containing protein	-1.05	downregulation
HI914_02516	Pyrroline-5-carboxylate reductase	-1.06	downregulation

Table 3.2. (cont'd)

HI914_07444	Orotate phosphoribosyltransferase	-1.07	Downregulation
HI914_02059	Hexokinase-1	-1.07	downregulation
HI914_00994	Acetylesterase	-1.12	downregulation
HI914_00921	O-acetyltransferase PaAT-1	-1.16	downregulation
HI914_04132	Plasma membrane ATPase	-1.18	downregulation
HI914_03305	Catabolic L-serine/threonine dehydratase	-1.19	downregulation
HI914_02418	putative extracellular matrix protein	-1.2	downregulation
HI914_00897	Global transcription regulator sge1	-1.26	downregulation
HI914_03453	putative rare lipoprotein a -like double-psi beta-barrel domain-containing	-1.32	downregulation
HI914_05967	G2/mitotic-specific cyclin-4	-1.33	downregulation
HI914_00736	Transcription factor vib-1	-1.37	downregulation
HI914_03875	putative endo-beta-1%2C4-glucanase D	-1.44	downregulation
HI914_00681	Cell wall mannoprotein CIS3	-1.46	downregulation
HI914_05416	Glucan 1%2C3-beta-glucosidase	-1.46	downregulation
HI914_05905	Gamma-glutamylputrescine oxidoreductase	-1.73	downregulation
HI914_05943	Catalase-peroxidase	-1.77	downregulation
HI914_07067	Agglutinin	-3.81	downregulation

Table 3.3. Log-fold changes in uniquely upregulated and downregulated genes in *Erysiphe necator* conidia treated with quinoxifen compared to control at 6-hour exposure. Genes were classified as up- and down- regulated using an adjusted P value of 0.05 with a log-fold change of 1. Genes that were identified as hypothetical are not included in this list.

Gene ID	Gene Name	LogFold Change	Regulation
HI914_05108	putative ppe family protein	2.28	upregulation
HI914_04743	heat shock protein	1.79	upregulation
HI914_03968	heat shock protein	1.64	upregulation
HI914_03415	Clock-controlled protein	1.64	upregulation
HI914_05697	ABC multidrug transporter	1.59	upregulation
HI914_04741	heat shock protein	1.49	upregulation
HI914_04859	Velvet complex subunit 2	1.44	upregulation
HI914_04746	heat shock protein	1.42	upregulation
HI914_01636	Oleate hydroxylase FAH12	1.40	upregulation
HI914_01388	Diphosphoinositol polyphosphate phosphohydrolase aps1	1.33	upregulation
HI914_04217	heat shock protein	1.307	upregulation
HI914_04980	NADP-dependent malic enzyme	1.25	upregulation
HI914_04568	Secondary metabolism regulator LAE1	1.20	upregulation
HI914_07478	Trichothecene C-4 hydroxylase	1.18	upregulation
HI914_05519	Cytochrome P450 monooxygenase	1.18	upregulation
HI914_02641	Malate synthase%2C glyoxysomal	1.18	upregulation

Table 3.3. (cont'd)

HI914_02627	3-oxoacyl-[acyl-carrier-protein] reductase FabG	1.17	Upregulation
HI914_02814	NADH-ubiquinone oxidoreductase	1.17	upregulation
HI914_06032	Eukaryotic translation initiation factor 4E type 3	1.15	upregulation
HI914_03811	Queuine tRNA-ribosyltransferase catalytic subunit	1.14	upregulation
HI914_01640	putative secreted beta-glucosidase	1.1	upregulation
HI914_05131	Mechanosensitive ion channel protein Msy1	1.1	upregulation
HI914_00716	Glucose-repressible protein	1.091	upregulation
HI914_00322	Glucan 1%2C3-beta-glucosidase	1.07	upregulation
HI914_03302	Serine/threonine-protein kinase KIN28	1.07	upregulation
HI914_00838	Enhancer of polycomb-like protein 1	1.07	upregulation
HI914_07477	Cytochrome P450 monooxygenase acIL	1.07	upregulation
HI914_02337	Iron transport multicopper oxidase fetC	1.06	upregulation
HI914_02873	Mannan endo-1%2C6-alpha-mannosidase DCW1	1.09	upregulation
HI914_03499	Protein N-terminal amidase	1.05	upregulation
HI914_01146	General transcription and DNA repair factor IIH subunit TFB5	1.04	upregulation
HI914_02561	Very-long-chain 3-oxoacyl-CoA reductase	1.03	upregulation
HI914_00771	Secondary metabolism regulator LAE1	1.09	upregulation
HI914_05760	Cytochrome c oxidase assembly protein COX19	1.01	upregulation
HI914_02488	putative peptide transporter ptr2	-1.01	downregulation
HI914_02252	Low affinity vacuolar monovalent cation/H(+) antiporter	-1.01	downregulation

Table 3.3. (cont'd)

HI914_02394	Chitin synthase export chaperone	-1.03	Downregulation
HI914_02048	Receptor expression-enhancing protein 2	-1.03	downregulation
HI914_00117	IQ domain-containing protein IQM6	-1.04	downregulation
HI914_07225	DNA topoisomerase 2	-1.05	downregulation
HI914_07287	Peptidase S41 family protein ustP	-1.06	downregulation
HI914_04670	Histone H4	-1.06	downregulation
HI914_02487	putative peptide transporter ptr2	-1.07	downregulation
HI914_01895	Tyrosine-protein phosphatase cdcA	-1.07	downregulation
HI914_06863	Iron-sulfur clusters transporter atm1%2C mitochondrial	-1.07	downregulation
HI914_00620	Sexual differentiation process protein isp4	-1.13	downregulation
HI914_02608	Serine/threonine-protein kinase sid2	-1.15	downregulation
HI914_00580	Transcriptional activator hac1	-1.17	downregulation
HI914_01231	DNA replication licensing factor mcm2	-1.16	downregulation
HI914_03093	Vesicular-fusion protein sec18	-1.16	downregulation
HI914_03141	Endothelin-converting enzyme	-1.17	downregulation
HI914_00053	Carboxypeptidase S1	-1.19	downregulation
HI914_00845	Serine/threonine-protein kinase STE11	-1.19	downregulation
HI914_04032	DNA polymerase zeta processivity subunit	-1.21	downregulation
HI914_03735	Ras guanine nucleotide exchange factor A	-1.22	downregulation
HI914_03792	Vacuolar calcium ion transporter	-1.22	downregulation
HI914_05663	DNA polymerase lambda	-1.22	downregulation

Table 3.3. (cont'd)

HI914_03671	Ingression protein fic1	-1.23	Downregulation
HI914_05438	Carboxypeptidase Y A	-1.25	downregulation
HI914_01676	Transcriptional regulatory protein pro1	-1.26	downregulation
HI914_02422	Chanoclavine-I aldehyde reductase fgaOx3	-1.26	downregulation
HI914_07433	putative cardiolipin-specific deacylase 1%2C mitochondrial	-1.26	downregulation
HI914_04132	Plasma membrane ATPase	-1.27	downregulation
HI914_02088	Kinesin-like motor protein 9	-1.29	downregulation
HI914_05102	Serine/threonine-protein kinase ark1	-1.30	downregulation
HI914_01062	Amino-acid permease	-1.31	downregulation
HI914_06808	Cholinesterase	-1.32	downregulation
HI914_01891	Cell surface Cu-only superoxide dismutase	-1.33	downregulation
HI914_06405	Bud site selection protein BUD4	-1.34	downregulation
HI914_03895	Chitin synthase 2	-1.35	downregulation
HI914_03419	Major facilitator-type transporter ecdD	-1.355	downregulation
HI914_02876	G2-specific protein kinase nim-1	-1.35	downregulation
HI914_04140	Glutathione transporter	-1.38	downregulation
HI914_00921	O-acetyltransferase PaAT-1	-1.38	downregulation
HI914_01840	G2/mitotic-specific cyclin-B	-1.41	downregulation
HI914_00205	Vacuolar calcium ion transporter	-1.43	downregulation
HI914_04441	Homoserine kinase	-1.45	downregulation
HI914_02516	Pyrroline-5-carboxylate reductase	-1.46	downregulation

Table 3.3. (cont'd)

HI914_06898	Metallothionein expression activator	-1.47	Downregulation
HI914_06615	putative Na(+)/H(+) antiporter	-1.59	downregulation
HI914_03910	Aquaporin	-1.67	downregulation
HI914_03875	putative endo-beta-1%2C4-glucanase D	-1.63	downregulation
HI914_07567	Aspercryptin biosynthesis cluster-specific transcription regulator atnN	-1.65	downregulation
HI914_04931	HMG box-containing protein	-1.68	downregulation
HI914_05905	Gamma-glutamylputrescine oxidoreductase	-1.71	downregulation
HI914_07444	Orotate phosphoribosyltransferase	-1.81	downregulation
HI914_06070	Anaphase spindle elongation protein 1	-1.82	downregulation
HI914_02426	Serine/threonine-protein kinase mph1	-1.92	downregulation
HI914_00736	Transcription factor vib-1	-1.96	downregulation
HI914_05967	G2/mitotic-specific cyclin-4	-2.03	downregulation
HI914_07584	ATP-dependent RNA helicase dbp-4	-2.05	downregulation
HI914_06793	putative GPI-anchored cupredoxin	-2.10	downregulation
HI914_03305	Catabolic L-serine/threonine dehydratase	-2.16	downregulation
HI914_00897	Global transcription regulator sge1	-2.16	downregulation
HI914_05943	Catalase-peroxidase	-2.29	downregulation
HI914_06111	Beta-1%2C2-xylosyltransferase 1	-2.33	downregulation
HI914_00240	WD repeat-containing protein slp1	-2.34	downregulation
HI914_05416	Glucan 1%2C3-beta-glucosidase	-2.50	downregulation

Table 3.3. (cont'd)

HI914_06303	Aquaporin-3	-2.66	Downregulation
HI914_04388	Oxalate--CoA ligase	-2.77	downregulation
HI914_01795	putative gpi anchored serine-threonine rich protein	-2.80	downregulation
HI914_06607	Ribonucleoside-diphosphate reductase small chain	-2.91	downregulation
HI914_02770	Galactitol 2-dehydrogenase	-3.77	downregulation

Table 3.4. Log-fold changes in uniquely upregulated and downregulated genes in *Erysiphe necator* conidia treated with trifloxystrobin or flutianil. Control at 3 and 6-hours were used as baseline to identify differentially expressed genes. Genes were classified as up- and down-regulated using an adjusted P value of 0.05 with a log-fold change of 1. Genes that were identified as hypothetical are not included in this list.

Gene_ID	Gene_Name	Time Duration (hour)	Trifloxystrobin/Control	Flutianil/Control	Expression Change
HI914_00115	NADP-dependent oxidoreductase RED1	3	1.75	-	Upregulated
HI914_07478	Trichothecene C-4 hydroxylase	3	1.12	-	Upregulated
HI914_07477	Cytochrome P450 monooxygenase acIL	3	1.09	-	Upregulated
HI914_00987	O-methyltransferase VdtC	3	-1.13	-	Downregulated
HI914_05456	Vacuolar membrane amino acid uptake transporter fnx2	3	-1.22	-	Downregulated
HI914_05987	Potassium transport protein 1	3	-1.35	-	Downregulated
HI914_05902	Chitinase	6	-	1.01	Upregulated

Table 3.5. Log-fold changes in commonly upregulated and downregulated genes in *Erysiphe necator* conidia treated with trifloxystrobin, quinoxyfen, and/or flutianil compared to control at 3 and 6-hours exposure. Control at 3 and 6-hours were used as baseline to identify differentially expressed genes. Genes were classified as up- and down- regulated using an adjusted P value of 0.05 with a log-fold change of 1. Genes that were identified as hypothetical are not included in this list.

Gene ID	Gene Name	Time Duration (hour)	Trifloxystrobin/ Control	Flutianil/ Control	Quinoxyfen/ Control	Expression Change
HI914_05519	Cytochrome P450 monooxygenase	3.0	1.01	1.04	1.41	Upregulated
HI914_01187	putative ppe family protein	3.0	1.14		1.2	Upregulated
HI914_00719	Maltose permease MAL31	3.0	1.44	1.34		Upregulated
HI914_04666	putative f-box domain containing protein	3.0		1.28	1.06	Upregulated
HI914_03920	Thioredoxin-1	3.0	-1.21		-1.03	Downregulated
HI914_00730	protein kinase family protein	3.0	-1.33		-1.12	Downregulated
HI914_07334	class I SAM-dependent methyltransferase	3.0	-1.47		-1.39	Downregulated
HI914_01057	Demethyl-4-deoxygadusol synthase	3.0	-1.88		-1.65	Downregulated
HI914_05904	Chitinase	3.0	-2.54		-2.29	Downregulated
HI914_00719	Maltose permease MAL31	6.0	1.25	1.07	1.48	Upregulated
HI914_05871	Sphingolipid long chain base-responsive protein LSP1	6.0	1.08	1.01	1.56	Upregulated
HI914_00115	NADP-dependent oxidoreductase RED1	6.0	1.66		1.16	Upregulated
HI914_04831	MFS transporter	6.0		1.45	1.91	Upregulated

Table 3.5. (cont'd)

HI914_06944	KCH domain-containing protein	6.0	1.36	1.64	Upregulated
HI914_02452	Rifampicin monooxygenase	6.0	1.17	1.48	Upregulated
HI914_02682	Enoyl-CoA delta isomerase 3	6.0	1.08	1.8	Upregulated

LITERATURE CITED

- Bachhawat, A. K., Thakur, A., Kaur, J., and Zulkifli, M. 2013. Glutathione transporters. *Biochim. Biophys. Acta* 1830:3154-3164.
- Bartlett, D. W., Clough, J. M., Godwin, J. R., Hall, A. A., Hamer, M., and Parr-Dobrzanski, B. 2002. The strobilurin fungicides. *Pest Manag. Sci.* 58:649-662.
- Baudoin, A., Olaya, G., Delmotte, F., Colcol, J. F., and Sierotzki, H. 2008. QoI resistance of *Plasmopara viticola* and *Erysiphe necator* in the Mid-Atlantic United States. *Plant Health Prog.* 9.
- Chen, S., Zhou, Y., Chen, Y., and Gu, J. 2018. Fastp: An ultra-fast all-in-one FASTQ preprocessor. *Bioinformatics* 34
- Cools, H. J., and Hammond-Kosack, K. E. 2013. Exploitation of genomics in fungicide research: current status and future perspectives. *Mol. Plant Pathol.* 14:197-210.
- Cox, A. D., Fesik, S. W., Kimmelman, A. C., Luo, J., and Der, C. J. 2014. Drugging the undruggable RAS: Mission possible? *Nat. Rev. Drug Discov.* 13:828-851.
- da Silva Dantas, A., Patterson, M. J., Smith, D. A., MacCallum, D. M., Erwig, L. P., Morgan, B. A., and Quinn, J. 2010. Thioredoxin regulates multiple hydrogen peroxide-induced signaling pathways in *Candida albicans*. *Mol. Cell. Biol.* 30:4550-4563.
- Del Sorbo, G., Schoonbeek, H. J., and De Waard, M. A. 2000. Fungal transporters involved in efflux of natural toxic compounds and fungicides. *Fungal Genet. Biol.* 30:1-15.
- Dufour, M.-C., Fontaine, S., Montarry, J., and Corio-Costet, M.-F. 2011. Assessment of fungicide resistance and pathogen diversity in *Erysiphe necator* using quantitative real-time PCR assays. *Pest Manag. Sci.* 67:60-69.
- Ewels, P., Magnusson, M., Lundin, S., and Käller, M. 2016. MultiQC: Summarize analysis results for multiple tools and samples in a single report. *Bioinformatics* 32:3047-3048.
- Fuller, K. B., Alston, J. M., and Sambucci, O. S. 2014. The value of powdery mildew resistance in grapes: Evidence from California. *Wine Econ. Pol.* 3:90-107.
- Feng, X., Nita, M., and Baudoin, A. B. 2018. Evaluation of quinoxifen resistance of *Erysiphe necator* (grape powdery mildew) in a single Virginia vineyard. *Plant Dis.* 102:2586-2591.
- Gadoury, D. M., Cadle-Davidson, L., Wilcox, W. F., Dry, I. B., Seem, R. C., and Milgroom, M. G. 2012. Grapevine powdery mildew (*Erysiphe necator*): A fascinating system for the study of the biology, ecology, and epidemiology of an obligate biotroph. *Mol. Plant Pathol.* 13:1-16.

- Genet, J. L., and Jaworska, G. 2009. Baseline sensitivity to proquinazid in *Blumeria graminis* f. sp. *tritici* and *Erysiphe necator* and cross-resistance with other fungicides. *Pest Manag. Sci.* 65:878-884.
- Graf, S. 2017. Characterization of metrafenone and succinate dehydrogenase inhibitor resistant isolates of the grapevine powdery mildew *Erysiphe necator*. Ph.D. thesis. Technische Universität Kaiserslautern, Kaiserslautern, Germany.
- Haramoto, M., Hamamura, H., Sano, S., Felsenstein, F. G., and Otani, H. 2006. Sensitivity monitoring of powdery mildew pathogens to cyflufenamid and the evaluation of resistance risk. *J. Pestic. Sci.* 31:397-404.
- Ishii, H. 2009. QoI fungicide resistance: Current status and the problems associated with DNA-based monitoring. In: *Recent Developments in Management of Plant Diseases*. U. Gisi, I. Chet, and M. L. Gullino, eds. Springer, Dordrecht, The Netherlands. Pages 37-45.
- Kim, D., Paggi, J. M., Park, C., Bennett, C., and Salzberg, S. L. 2019. Graph-based genome alignment and genotyping with HISAT2 and HISAT-genotype. *Nat. Biotechnol.* 37:907-915.
- Kimura, S., Komura, T., Yamaoka, N., and Oka, H. 2020. Biological properties of flutianil as a novel fungicide against powdery mildew. *J. Pestic. Sci.* 45:206-215.
- Kimura, S., Shibata, Y., Oi, T., Kawakita, K., and Takemoto, D. 2021. Effect of flutianil on the morphology and gene expression of powdery mildew. *J. Pestic. Sci.* 46:206-213.
- Kunova, A., Pizzatti, C., Bonaldi, M., and Cortesi, P. 2016. Metrafenone resistance in a population of *Erysiphe necator* in northern Italy. *Pest Manag. Sci.* 72:398-404.
- Lee, S., Gustafson, G., Skamnioti, P., Baloch, R., and Gurr, S. 2008. Host perception and signal transduction studies in wild-type *Blumeria graminis* f. sp. *hordei* and a quinoxifen-resistant mutant implicate quinoxifen in the inhibition of serine esterase activity. *Pest Manag. Sci.* 64:544-555.
- Li, H., Handsaker, B., Wysoker, A., Fennell, T., Ruan, J., Homer, N., Marth, G., Abecasis, G., Durbin, R., and 1000 Genome Project Data Processing Subgroup. 2009. The sequence alignment/map format and SAMtools. *Bioinformatics* 25:2078-2079.
- Liao, Y., Smyth, G. K., and Shi, W. 2014. featureCounts: An efficient general purpose program for assigning sequence reads to genomic features. *Bioinformatics* 30:923-930.
- Ma, Z., and Michailides, T. J. 2005. Advances in understanding molecular mechanisms of fungicide resistance and molecular detection of resistant genotypes in phytopathogenic fungi. *Crop Prot.* 24:853-863.

- Medintz, I., Jiang, H., Han, E. K., Cui, W., and Michels, C. A. 1996. Characterization of the glucose-induced inactivation of maltose permease in *Saccharomyces cerevisiae*. J. Bacteriol. 178:2245-2254.
- Miles, L. A., Miles, T. D., Kirk, W. W., and Schilder, A. M. C. 2012. Strobilurin (QoI) resistance in populations of *Erysiphe necator* on grapes in Michigan. Plant Dis. 96:1621-1628.
- Miles, T. D., Neill, T. M., Colle, M., Warneke, B., Robinson, G., Stergiopoulos, I., and Mahaffee, W. F. 2021. Allele-specific detection methods for QoI fungicide-resistant *Erysiphe necator* in vineyards. Plant Dis. 105:175-182.
- Munro, A. W., McLean, K. J., Grant, J. L., and Makris, T. M. 2018. Structure and function of the cytochrome P450 peroxygenase enzymes. Biochem. Soc. Trans. 46:183-196.
- Opalski, K. S., Tresch, S., Kogel, K. H., Grossmann, K., Köhle, H., and Hückelhoven, R. 2006. Metrafenone: Studies on the mode of action of a novel cereal powdery mildew fungicide
- Rallos, L. E. E., Johnson, N. G., Schmale, D. G., Prussin, A. J., and Baudoin, A. B. 2014. Fitness of *Erysiphe necator* with G143A-based resistance to quinone outside inhibitors. Plant Dis. 98:1494-1502. doi: 10.1094/PDIS-12-13-1202-RE.
- Robinson, M. D., McCarthy, D. J., and Smyth, G. K. 2010. edgeR: a Bioconductor package for differential expression analysis of digital gene expression data. Bioinformatics 26:139-140.
- Sambucci, O., Alston, J. M., Fuller, K. B., and Lusk, J. 2019. The pecuniary and nonpecuniary costs of powdery mildew and the potential value of resistant grape varieties in California. Am. J. Enol. Vitic. 70:177-187.
- Sharma, N., Heger, L., Neill, T., Mahaffee, W., Gold, K. M., Combs, D., Brannen, P. M., Oliver, C., Moyer, M. M., Holland, L. A., and McFadden-Smith, W. 2022. Investigating QoI and CAA resistance in grape powdery mildew and downy mildew populations in vineyards of the eastern United States and Canada. Phytopathology 112:97-98.
- Sharma, N., Neill, T., Yang, H. C., Oliver, C. L., Mahaffee, W. F., Naegele, R., Moyer, M. M., and Miles, T. D. 2023. Development of a PNA-LNA-LAMP assay to detect an SNP associated with QoI resistance in *Erysiphe necator*. Plant Dis. 107:3238-3247.
- Turrà, D., Segorbe, D., and Di Pietro, A. 2014. Protein kinases in plant-pathogenic fungi: conserved regulators of infection. Annu. Rev. Phytopathol. 52:267-288.
- Wheeler, I., Hollomon, D., Longhurst, C., and Green, E. 2000. Quinoxifen signals a stop to infection by powdery mildews. Pages 841-846 in: The BCPC Conference: Pests and Diseases, Volume 3.

- Wheeler, I., Hollomon, D. W., Gustafson, G., Mitchell, J. C., Longhurst, C., Zhang, Z., and Gurr, S. J. 2003. Quinoxifen perturbs signal transduction in barley powdery mildew (*Blumeria graminis* f. sp. hordei). *Mol. Plant Pathol.* 4:177-186.
- Wittinghofer, A., Scheffzek, K., and Ahmadian, M. R. 1997. The interaction of Ras with GTPase-activating proteins. *FEBS Lett.* 410:63-67.
- Xin, F., Dang, W., Chang, Y., Wang, R., Yuan, H., Xie, Z., Zhang, C., Li, S., Mohamed, H., Zhang, H., and Song, Y. 2022. Transcriptomic analysis revealed the differences in lipid accumulation between spores and mycelia of *Mucor circinelloides* WJ11 under solid-state fermentation. *Fermentation* 8:667.
- Yang, L. B., Dai, X. M., Zheng, Z. Y., Zhu, L., Zhan, X. B., and Lin, C. C. 2015. Proteomic analysis of erythritol-producing *Yarrowia lipolytica* from glycerol in response to osmotic pressure. *J. Microbiol. Biotechnol.* 25:1056-1069.
- Zaccaron, A. Z., Neill, T., Corcoran, J., Mahaffee, W. F., and Stergiopoulos, I. 2023. A chromosome-scale genome assembly of the grape powdery mildew pathogen *Erysiphe necator* reveals its genomic architecture and previously unknown features of its biology. *MBio* 14.
- Zhang, Y., Parmigiani, G., and Johnson, W. E. 2020. ComBat-seq: batch effect adjustment for RNA-seq count data. *NAR Genom. Bioinform.* 2

CHAPTER 4: PREVALENCE OF MUTATIONS ASSOCIATED WITH QOI, QIL, QIOSI AND CAA FUNGICIDE RESISTANCE WITHIN *PLASMOPARA VITICOLA* IN NORTH AMERICA AND A TOOL TO DETECT CAA RESISTANT ISOLATES

Abstract

Grape downy mildew, caused by *Plasmopara viticola*, poses a significant threat to grape cultivation globally. Early detection of fungicide resistance is critical for effective management. This study aimed to assess the prevalence and distribution of mutations associated with resistance to Quinone outside inhibitor (QoI, FRAC 11), Quinone inside inhibitor (QiIs, FRAC 21), Carboxylic acid amide (CAA, FRAC 41), and Quinone inside and outside inhibitor, stigmatellin binding mode (QioSI, FRAC 45) fungicides in *P. viticola* populations in the eastern United States and Canada and to evaluate whether these mutations are linked to fungicide resistance correlated with specific *P. viticola* clades. A total of 658 *P. viticola* samples were collected from commercial vineyards across different states and years in the eastern United States and Canada and sequenced for *PvCesA3* and *Cytb* genes and the ITS1 region. Results showed *P. viticola* clades *aestivalis*, *vinifera*, and *riparia* were prevalent in the eastern United States and Canada. QoI resistance was widespread, and the A-143 resistant genotype was prevalent in *P. viticola* clades *aestivalis* and *vinifera*. The G143A mutation did not show specificity based on clade differentiation. CAA resistance, associated with the G1105S mutation, was mainly identified in *P. viticola* clade *aestivalis* from Georgia, New York, and Ontario. G1105-S1105 mixed-genotype samples observed in *P. viticola* clades *vinifera* and *riparia* from Wisconsin, Michigan and New York. However, mutations associated with QioSI and QiI fungicides were not detected. A TaqMan-probe based assay was developed to detect the G1105S mutation in *P. viticola* conferring CAA fungicide resistance. The TaqMan assay demonstrated

sensitivity at low DNA concentrations and specificity in distinguishing between sensitive and resistant genotypes. The assay accurately distinguished the G1105S mutation in leaf and air samples. This study provides insight into the geographic distribution of fungicide resistance in *P. viticola* populations and presents a reliable method for detecting CAA resistance in *P. viticola*. These findings can be utilized to implement effective fungicide resistance management strategies in viticulture.

Introduction

Grape downy mildew, caused by the oomycete pathogen *Plasmopara viticola* (Berk. & M. A. Curtis) Berl. & De Toni, devastates grape production in 90+ countries worldwide (CABI 2018; Emmett et al. 1992b). In northeastern America, the native range of *P. viticola* includes *Vitis vinifera*, *V. labrusca* L., *V. aestivalis* Michx., *V. riparia* Michx., *V. vulpina*, *V. cinerea*, and *Parthenocissus quinquefolia* L. Planch (Rouxel et al. 2013). Since the 1950s, scientists have speculated that *P. viticola* has host specificity within the Vitaceae family based on spore morphology (Savulescu and Savulescu, 1951, Golovina, 1955). However, morphological characteristics alone could not provide clear evidence for species delineation. In more recent times, a lack of agreement across studies using different *P. viticola* isolates to screen *Vitis* germplasm for disease resistance to *P. viticola* has added evidence to the case for race specificity (Cadle-Davidson, 2008; Rouxel et al. 2013). Furthermore, a small-scale genetic study conducted with 14 *P. viticola* isolates proposed the presence of several lineages (Schröder et al. 2011).

Previously, Rouxel et al. (2013), described four independent cryptic species of *P. viticola* based on multiple genealogies, spore morphology and host plant specialization. However, an expansion upon this work with more samples from diverse host species sourced across a larger geographical region identified five cryptic species, or clades, within the *P. viticola* species

complex with variable degrees of host plant specialization (Rouxel et al. 2014). These cryptic species were identified using phylogenetic concordance of multiple genes and morphological characteristics (Rouxel et al. 2014). Rouxel et al. (2014) provided a provisional nomenclature for *P. viticola* cryptic species as clades. Three *P. viticola* clades, *vinifera*, *riparia* and *aestivalis*, exhibited a wide host range that included both, including wild and cultivated grapes; however, *vulpina* and *quinquefolia* clades, were specialized exclusively to wild grapes (Rouxel et al. 2014). *P. viticola* clade diversification and host specialization may have important implications for grape downy mildew management and resistance breeding.

Grape downy mildew is a polycyclic disease and most *Vitis vinifera* cultivars are highly susceptible to this disease (Huang et al. 2020). Management relies heavily on chemical control (Campbell et al. 2021; Huang et al. 2020; Santos et al. 2020). Regions with favorable disease conditions often require prophylactic fungicide applications from mid-April to mid-September made on either 7-10 or 10-14 day intervals based on wet or dry weather conditions, respectively (Campbell et al. 2021). Along with contact fungicides such as copper, captan and mancozeb, several single-site fungicides are labeled for grape downy mildew management. Some widely used single-site fungicides include famoxadone and fenamidone (Quinone outside inhibitors [QoIs], FRAC 11), cyazofamid (Quinone inside inhibitors [QiIs], FRAC 21) and ametoctracadin (Quinone inside outside inhibitors [QioSIs], FRAC 45) inhibit mitochondrial respiration. The QoI fungicides target complex III, specifically cytochrome bc1 (ubiquinol oxidase), at the Qo site. Similarly, QiI fungicides target the complex III cytochrome bc1 (ubiquinone reductase) at the Qi site, while QioSI fungicides interact with both the Qi and Qo sites of complex III by a stigmatellin binding mode (Cherrad et al. 2018; Cherrad et al. 2023; Fontaine et al. 2019; FRAC 2024; Mounkoro et al. 2019; Sierotzki et al. 2005). Mandipropamid and dimethomorph (FRAC

40, Carboxylic acid amides [CAAs] targeting cellulose synthase) inhibit cell wall biosynthesis (Gisi et al. 2007; Blum et al. 2010). While effective at providing disease control, single-site fungicides have greater risk of fungicide resistance development than multi-site inhibitors if proper resistant management strategies are not followed.

Single-site fungicide active ingredients are assigned as low- to high-based on their intrinsic risk of resistance development as judged by Fungicide Resistance Action Committee (FRAC 2024). The CAA (FRAC 40), QiI (FRAC 21)/QioSI (FRAC 45), and QoI (FRAC 11) fungicides are classified as low- to medium-risk, medium- to high-risk, and high-risk are of resistance development, respectively. The QoI fungicide resistance in *P. viticola* isolates has been reported from various grape-growing regions around the world (Baudoin et al. 2008; Chen et al. 2007; Furuya *et al.* 2010; Genet et al. 2006; Gisi et al. 2002; Gullino et al. 2004; Santos et al. 2020; Sawant et al. 2016; Sierotzki et al. 2005). QoI fungicide resistance in *P. viticola* mainly occurs due to a single nucleotide polymorphism (SNP) at codon 143 conferring an amino acid change from glycine to alanine (G143A) (Chen et al. 2007; Gisi et al. 2002). Another resistance-associated SNP conferring substitution from phenylalanine to leucine (F129L) at codon 129 has also been observed to confer fungicide resistance, however only at very low frequencies (<2%) in French *P. viticola* field populations (Sierotzki et al. 2005). There have been a few reports indicating that QioSI and QiI fungicide resistance in *P. viticola* populations. The QioSI fungicide resistance involves a change in the amino acid sequence from serine to leucine at codon 35 (S34L) in the Cyt b gene, while QiI fungicide resistance involves either an insertion of two amino acids between codons 203 and 204 (E203-DE-V204) or an amino acid change from leucine to serine at codon 201 (L201S) in the Qi site (Cherrad et al. 2018; Cherrad et al. 2023; Fontaine et al. 2019; Sagar et al. 2023). Resistance to CAA fungicides has been attributed to a

SNP resulting in an amino acid substitution from glycine to serine, or rarely to valine, at codon 1105 (G1105S/V) in the *PvCesA3* gene of *P. viticola* (Blum et al. 2010). The CAA fungicide resistance has been detected at several locations, including Brazil (Santos et al. 2020), China (Zhang et al., 2017), Europe (Blum et al., 2010), India (Sawant et al., 2017), Japan (Aoki et al., 2013), and North Carolina and Virginia, United States (Feng and Baudoin, 2018). Resistance to CAA fungicide has also been observed in other oomycete plant pathogens (Blum et al. 2012). In *Phytophthora infestans*, this resistance is attributed to an amino acid change at codon 1105 from glycine to alanine or valine (G1105A/V), or at codon 1109 from valine to leucine (V1109L) (Blum et al. 2012). Similarly, in *Pseudoperonospora cubensis*, resistance is due to an amino acid change at codon 1105 from glycine to valine or tryptophan (G1105V/W) (Blum et al. 2012). For *Phytophthora capsici*, resistance results from amino acid change either at codon 1105 from glycine to alanine (G1105A) or at codon 1109 from valine to leucine or methionine (V1109L/M) (Blum et al. 2012). The development of resistance in *P. viticola* to the above-mentioned at-risk fungicides can lead to reduced efficacy in managing grape downy mildew.

Downy mildew causing organisms are obligate biotrophs, so they cannot be traditionally cultured, which has historically hampered our ability to study resistance development mechanisms. Molecular resistance detection strategies are to be thus instructive and lead to more improving disease and resistance management, as traditional fungicide resistance testing assays are laborious and difficult to accomplish with obligate biotrophs. Molecular assays can be utilized to discriminate and identify specific alleles linked to resistance, sidestepping this bottleneck. This approach has been widely deployed to detect SNP-based fungicide resistance in other obligate pathogens. For example, several rapid molecular assays such as PNA-LNA-LAMP assays, TaqMan-probe based assay, and digital droplet PCR (ddPCR) are used to monitor G143A

based QoI resistance in grape powdery mildew caused by *Erysiphe necator* (Miles et al. 2021; Sharma et al. 2019; Sharma et al. 2023). Molecular assay techniques have been previously developed to detect QoI and CAA fungicide resistance in *P. viticola* – including nested PCR-restriction fragment length polymorphism (RFLP), real-time PCR, and multiplex allele-specific primer PCR (ASP-PCR) (Aoki et al. 2011; Aoki et al. 2013; Furuya et al. 2009). However, these techniques are quite time consuming compared to TaqMan-probe based assay. Moreover, in the case of G1105S mutations conferring CAA resistance, ASP-PCR cannot distinguish between a resistant homozygote and susceptible heterozygote (mixed sample) (Aoki et al. 2013).

Early detection of fungicide resistance is vital to deploy timely fungicide resistance management strategies. Therefore, rapid molecular techniques that can accurately distinguish among fungicide resistant, sensitive and mixed genotypes are crucial, particularly in case of obligate pathogens such as *P. viticola*. In this study, we focused on: (i) determining the geographical prevalence and distribution of the G1105S mutation associated with CAA resistance, the G143A mutation associated with QoI resistance, the S34L mutations associated with QioSI resistance, and the E203-DE-V204 duplication associated with QiI in *P. viticola* populations in the vineyards of the eastern United States and Canada; (ii) evaluating whether the mutations conferring CAA and QoI resistance are associated with specific *P. viticola* clades; (iii) developing a robust TaqMan-probe based assay to detect G1105 mutations conferring CAA resistance in *P. viticola*.

Materials and Methods

P. viticola sample collection

A total of 658 *P. viticola* samples were collected from commercial vineyards located in various regions including Georgia, Indiana, Michigan, New York, and Wisconsin from the

United States, and Ontario from Canada. Out of these, 61 *P. viticola* samples were collected in 2019 from across Michigan and New York; and 64 *P. viticola* samples were gathered from commercial vineyards from Michigan and New York in 2020. Additionally, 359 *P. viticola* samples were collected from vineyards in Georgia, Michigan, New York, and Wisconsin and Ontario in 2021; and 174 samples were collected in 2022 from commercial vineyards in New York and Ontario. *Plasmopara viticola* samples were collected from infected grape leaves throughout the growing season. Four infected leaves were collected per vineyard site for each variety, and if a site consisted of multiple varieties, multiple collections were made. From these infected leaves, single downy mildew colonies were collected using Tough-Spots (Diversified Biotech, Inc., Dedham, MA, USA). These Tough-Spots were placed in 2mL microcentrifuge tubes and transported in a cooler back to the laboratory. Samples were kept at -20°C until DNA extractions were conducted.

DNA extraction

Crude DNA extractions were conducted on the field samples using a modified version of the tape DNA extraction method described by Brewer and Milgroom (2010) and Thiessen et al. (2019). The 2mL microcentrifuge sample tubes were centrifuged at 16,000 g for 1 minute to settle the Tough-Spots at the bottom of the tubes. A suspension of 200 µL of 5% (w/v) Chelex (Sigma-Aldrich, Saint Louis, MO, USA) in molecular-grade water was added to each sample tube. For five minutes, the tubes were vortexed horizontally at 3200 RPM, followed by 20 s of centrifugation at 16000 x g to settle the content at the bottom of the tube. Tubes were kept on a heat block at 95°C for 10 min, followed by vortexing for 5 s and centrifugation of 20 s at 16000 x g. Tubes were again incubated for 10 min at 95°C. To cool down the samples, each tube was kept at 22°C for 20 min. Each tube was centrifuged at 16000 x g for 2 min after cooling, and the

supernatant was transferred to a sterile 1.5-mL microcentrifuge tube. Extracted crude DNA samples were stored at -20°C until they were utilized for resistance detection experiments.

Primer design for determination of Cytb, PvCesA3 genes, and ITS1 sequence polymorphism

A DNA consensus sequence of the *PvCesA3* reference gene of *P. viticola* (accession number: GQ258975) and three other closely related oomycetes including *Pseudoperonospora cubensis* (accession number: JF799098), *Phytophthora capsici* (accession number: JN561772), and *Pseudoperonospora humuli* (accession number: NQFO01001774) were downloaded from the National Center for Biotechnology Information (NCBI) database and were aligned using Geneious R9 (Biomatters Ltd., New Zealand) to design forward and reverse primers for amplification of the G1105S mutation conferring CAA resistance (Table 4.1). The PvPCR_1F_CAA (forward) and PvPCR_1R_CAA (reverse) primers were designed to amplify the *PvCesA3* gene of *P. viticola* (Table 4.1). Another multiple alignment was conducted using Geneious R9 to design amplification primers for detecting G143A; S34L; and E203-DE-V204 duplication/L201S mutations conferring resistance to QoI; QioSI; and Qil fungicides, respectively (Fig. 4.1). The consensus sequence of the *Cytb* reference gene of *P. viticola* (accession number: Pv-NC045922), along with two other oomycetes including *Peronospora tabacina* (accession number: NC028331) and *P. cubensis* (accession number: NC027859) were downloaded from NCBI and used in the multiple alignments. The PV_COB Fwd 1(forward) and PV_COB Rev2 (reverse) primers were designed to amplify the *Cytb* gene of *P. viticola*. ITS1-O and ITS2 primers were used to determine ITS1 sequence polymorphisms in the collected *P. viticola* samples (Rouxel et al. 2013).

Polymerase chain reactions (PCR) were performed independently to amplify the *PvCesA3*, *Cytb* genes, and ITS1 sequence. The optimized reactions had a final volume of 25 µl,

containing 1X Perfecta ToughMix, 200nM each of the forward and reverse primers, 2 ng DNA, and 9.5 µLddH₂O (Table 4.6). The reaction conditions included an initial denaturation at 95°C for 3 min, followed by 45 cycles of 95°C for 15 s, 55°C for 30 s, and 68°C for 30 s, and a final extension of 68°C for 5 min using a C1000 Touch thermal cycler (BioRad Laboratories, Hercules, CA) (Table 4.6). The same reaction conditions were used to amplify the *PvCesA3* and *Cytb* genes, and the ITS1 sequence. The size of the PCR amplicons was examined on a 1% agarose gel with gel Red nucleic acid stain (BioRad Laboratories, Hercules, CA). PCR amplicons that amplified appropriately were purified using the DNA Clean & Concentrator kit (Zymo Research, Irvine, CA). Purified PCR products were sequenced using PV_COB Fwd 1 and PV_COB Rev2 primers for the *Cytb* gene, PvPCR_1F_CAA and PvPCR_1R_CAA primers for the *PvCesA3* gene, and ITS1-O and ITS2 primers for the ITS1 sequence at the Research Technology Support Facility (RTSF) Genomics Core at MSU.

CesA3, Cytb genes, and ITS1 region sequence alignment

All of the sample consensus sequences for the *PvCesA3* and *Cytb* genes were aligned to the *PVCESA3* GQ258975 (Blum et al. 2012) and *Cytb* Pv-NC045922 reference genes, respectively. All of the sample consensus for ITS1 region were aligned to ITS1 reference sequence AY742739, ITS1 reference sequence for *P. viticola* clade *riparia* JF897779 (Rouxel et al. 2014), ITS1 reference sequence for *P. viticola* clade *aestivalis* JF897780 (Rouxel et al. 2014), and the ITS1 reference sequence for *P. viticola* clade *vinifera* JF897781 (Rouxel et al. 2014) downloaded from NCBI. Analyses of sequences was conducted using Geneious software 10.2.6. Sequence alignment for each sample was visually checked for errors and examined for the presence of the G1105S mutation in the *PvCesA3* gene associated with resistance to CAA fungicides. The S34L, G143A mutations, and E203-DE-V204 duplication/L201S mutation in

Cytb gene associated with QioSI, QoI, and QiI fungicides, respectively, and SNPs that differentiate *P. viticola* clades in ITS1 region were also examined.

Development of TaqMan assay to detect G1105S mutation for CAA resistance in P. viticola

Multiple sets of primers and probes were manually designed to target different regions of the *PvCesA3* gene of *P. viticola* based on an alignment developed using Geneious R9. The alignment involved the nuclear DNA sequence of *PvCesA3* gene of *P. viticola* (accession number: GQ258975, previously described by Blum et al. 2011), and three other oomycete species including *Pseudoperonospora cubensis* (accession number: JF799098, previously described by Blum et al. 2011), *Phytophthora capsici* (accession number: JN561772, previously described by Blum et al. 2012), and *Pseudoperonospora humuli* (accession number: NQFO01001774, previously described by Rahman et al. 2017). All primer and probe sets were tested on crude DNA of *P. viticola* isolates (with a known genotype profile based on sequencing) for their ability to discriminate G-1105 (wild-type) and S-1105 (mutant-type) alleles. The selected primer set amplifies a 145 bp amplicon of *PvCesA3* gene and probes were targeted to specifically bind to the wild-type allele (G) and mutant-type alleles (S) at amino acid position 1105 (Table 4.1). Probes specific to G-1105 and S-1105 alleles were labelled at 5' end with FAM and HEX fluorescence, respectively.

To determine the optimal reaction conditions, three primer concentrations (100, 200, and 400 nM) in combination with an annealing temperature gradient ranging from 59 to 68°C was tested. Water was used as a negative control. Three reactions were conducted for each reaction condition and the experiment was repeated once. A primer concentration of 400 nM with annealing temperature at 67°C provided highest specificity. Final reactions had a total volume of 25 µL consisting of 1X Perfecta qPCR ToughMix (Quanta Biosciences, Gaithersburg, MD), 2 ng

of DNA, 400 nM of forward and reverse primers, 100 nM of G-1105 (wild-type), and S-1105 (mutant-type) allele-specific probes, and 8 μ L of ddH₂O (Table 4.6). Reactions were performed at an initial denaturation at 95°C for 2 min, followed by 40 cycles of 95°C for 15 s, and 67°C for 1 min using Bio-Rad CFX96 machine (Bio-Rad Laboratories, Hercules, CA, USA).

Sensitivity and specificity of TaqMan assay

The limit of detection of the TaqMan assay to distinguish the G1105S mutation in the *PvCesA3* gene conferring CAA resistance was determined by analyzing known DNA concentrations of *P. viticola*. Purified DNA of a G-1105 sensitive genotype (CAA-sensitive) and S-1105 resistant genotype (CAA-resistant) isolates were serially diluted from 1 ng/ μ L to 1 pg/ μ L and loaded separately into a reaction. Reactions were conducted in triplicate for each DNA concentration and genotype. Water was used as a negative control. Standard curve plots of log₁₀ DNA concentration and cycle threshold (Ct) values were created using serial dilutions for each genotype. The qPCR software (CFX96 Touch Real-Time System; Bio-Rad Laboratories) was used to determine the slope and efficiency of the standard curve plots.

The specificity of the TaqMan assay to discriminate between G-1105 (wild-type) and S-1105 (mutant-type) alleles of *P. viticola* as well as its specificity when testing other closely related oomycetes was verified using two approaches. First, purified DNA of sixteen *P. viticola* isolates, including eight CAA-sensitive and eight CAA-resistant isolates, were tested using the TaqMan assay. A region of the *PvCesA3* gene of these isolates was partially sequenced using the PCR amplification primers listed in Table 4.1 and the protocol listed above to determine the genotype. The genotype determined based on sequencing was assumed as accurate and treated as a gold standard. Results obtained from the TaqMan assay and sequencing were compared using receiver operating characteristic (ROC) analyses (Turechek and Wilcox 2005). Second, DNA

samples from closely related oomycetes and outgroup fungi that infect cucurbits (*Pseudoperonospora cubensis*), hops (*Pseudoperonospora humuli*), raspberries (*Phytophthora rubi*), azaleas (*Phytophthora foliorum*), peppers (*Phytophthora capsici*) and avocado (*P. cinnamomi*) collected from Monterey County, California (Miles et al. 2021) were tested using the TaqMan assay to determine potential cross reaction with non-target species. Sixteen isolates were tested (two isolates from each species), and each reaction had three technical replicates.

Validation of TaqMan assay using field and air samples

The ability of the TaqMan assay to distinguish between G-1105 sensitive and S-1105 resistant genotypes was tested using *P. viticola* samples collected from vineyards in Michigan, Georgia, Wisconsin, New York, and Ontario. The TaqMan assay was validated on samples collected with two different approaches including leaf samples using Tough-spots and air samples using sampling rods. First, crude DNA (*see DNA isolation*) from 100 *P. viticola* samples collected from diseased leaves using Tough spot were evaluated for G1105S mutation conferring CAA resistance. Second, twenty-four air samples of *P. viticola* were obtained using vacuum grease coated rods of rotating-arm impaction samplers at the Clarksville Research Station of MSU (Clarksville, MI) in 2021. Grease-coated rod samples were collected from three heights (0.6 m (2 ft), 1.3 m (4.5 ft), and 1.8 m (6 ft)) from the ground within a Vitis hybrid cv. ‘Vignoles’ plot. Rods were collected every 3 or 4 days (as denoted as in Table X). Purified DNA of air samples was extracted using the Macherey-Nagel Plant Nucleospin II kit (modified protocol from Klosterman et al. 2016) and tested for the G1105S mutation. Water was used as a negative control. All samples were also sequenced for the *PvCesA3* gene using PCR amplification primers as above to verify the results obtained from the TaqMan assay. All

reactions of the TaqMan assay had three technical replicates and the experiment was repeated once.

Comparison of the SNP distinguishing TaqMan assay with previously developed P. viticola qPCR detection tool

Crude DNA of thirty field samples of *P. viticola*, including ten CAA-sensitive, ten CAA-resistant, and ten CAA-mixed (both alleles were present in a sample), were tested using the TaqMan assay developed in this study and the *P. viticola* quantitative real time-PCR (qPCR) detection tool developed by Valsesia et al. (2005). The Ct values from both assays while detecting *P. viticola* were compared. The genotype of the samples was known based on the sequencing of *PvCesA3* gene conducted. Each reaction had three technical replicates, and water was used as negative control. The *P. viticola* qPCR detection tool was conducted at 95°C for 1 min followed by repeat of 40 cycles of 95°C for 15 s and 60°C for 30 s (Si Ammour et al. 2020) using Bio-Rad CFX96 qPCR machine. The experiment was repeated once.

Statistical Analyses and Data Interpretation

The experiment setup and data generation were conducted using CFX Manager 3.1 software (Bio-Rad Laboratories). The data analyses were conducted using Microsoft Excel (Redmond, WA, USA), SigmaPlot 11 (Systat Software, Inc., San Jose, CA, USA) and R Statistical Software (version 3.3.0; R Foundation for Statistical Computing, Vienna, Austria). In this study, accuracy is described as the capability of the assay to discriminate between true negative and true positive and is calculated using the formula $(\text{True Positive} + \text{True Negative}) / (\text{Total no. of samples})$ (Baratloo et al. 2015). Regression analysis was done using SigmaPlot 11 (Systat Software, Inc., San Jose, CA, USA).

Results

P. viticola clades *aestivalis*, *vinifera*, and *riparia* were prevalent in the eastern United States and Canada

When examining the *P. viticola* samples collected over sampling years from the eastern United States and Canada for the clade differentiation, we found that most *P. viticola* samples belonged to *P. viticola* clade *aestivalis* (Table 4.2; Fig. 4.2). The *P. viticola* clades *aestivalis*, *vinifera*, and *riparia* were observed in 87.5%, 8.0%, and 5.2% of *P. viticola* samples (N=664), respectively, collected from the eastern United States and Canada over the sampling period (Fig. 4.2). Most samples collected from New York (99.3%), Indiana (100%), Georgia (100%), and Ontario (100%) were confirmed as *P. viticola* clade *aestivalis* (Table 4.2). All samples from WI were confirmed as *P. viticola* clade *vinifera* (16/16). However, samples collected from Michigan showed the greatest clade diversity with the presence of *P. viticola* clades *aestivalis* (61.1%), *vinifera* (22.1%), and *riparia* (16.8%) (Table 4.2).

CAA resistance was identified in P. viticola clade aestivalis in specific locations

The G1105S mutation associated with CAA resistance in *P. viticola* was detected for the first time in several states of the eastern United States and Canada over the course of sampling years. The S-1105 resistant genotype was found in more than 48.1% of *P. viticola* samples collected from New York in 2020 and onwards, 25% of samples from Georgia in 2021, and 7.0% of samples from Ontario in 2022 (Table 4.2; Fig. 4.2A). In 2022, the greatest percentage of the S-1105 resistant genotype was observed in New York (76.7%); however, 100% prevalence of the G-1105 sensitive genotype was found in *P. viticola* samples in the samples collected from Indiana and New York in 2019, Michigan in 2019 and 2020, and Ontario in 2021. The S-1105 resistant genotype was not detected in Michigan and Wisconsin, but the G1105-S1105 mixed

genotype was detected in Michigan (7.7%) and Wisconsin (6.3%) in 2021. The G1105-S1105 mixed genotype was most prevalent in Georgia (29.1%) in 2021 (Fig. 4.2A).

The G1105S mutation associated with CAA resistance did not show any specificity based on *P. viticola* clades during the sampling periods (Fig. 4.2). The S-1105 resistant genotype was detected in *P. viticola* clade *aestivalis*, and the G1105-S1105 mixed genotype was detected in *P. viticola* clades *vinifera* and *riparia* (Fig. 4.2). Based on all samples across states and sampling years, 31.82% of the *P. viticola* clade *aestivalis* samples were identified as S-1105 resistant genotype. The S-1105 resistant genotype within *P. viticola* clade *aestivalis* samples increased over the time during the growing season in New York and Ontario (Fig. 4.3). Increase in incidence of resistant isolates in Ontario was also the result of expanding the sampling area in 2022 than 2021. Combined prevalence of S-1105 resistant genotype and G1105-S1105 mixed genotype within *P. viticola* clade *aestivalis* samples increased from 0% in 2019 to 93.3% in 2022 in New York; and 0% in 2021 to 11.4% in 2022 (Fig. 4.3).

QoI resistance was prevalent in P. viticola clades aestivalis and vinifera

QoI-resistance mutations were prevalent across the states sampled during the sampling years (Table 4.2; Fig. 4.2B; Fig. 4.4). The A-143 resistant genotype was observed in more than 50% of all samples collected across states and years, except samples from Michigan in 2021 (Fig. 4.2B; Fig. 4.4). The greatest number of A-143 resistant genotype was observed in Ontario (93.8%) in 2021 and New York (93.3%) in 2022, while samples from Michigan in 2021 showed the greatest amount of the G-143 (sensitive) genotype (58.9%) (Table 4.2; Fig. 4.2B). The G143-A143 mixed genotype was the most prevalent in Georgia in 2021, while no G143-A143 mixed genotype was detected from Indiana in 2019, and Wisconsin and Ontario in 2021 (Table 4.2).

The G143A mutation associated with QoI resistance did not show any specificity based on *P. viticola* clade (Fig. 4.2B). The A-143 resistant genotype was consistently present in *P. viticola* clades *aestivalis*, *vinifera*, and *riparia*. Overall samples across states and sampling years, *P. viticola* clade *aestivalis* had the most frequent A-143 resistant genotype (81.8%), while *P. viticola* clade *riparia* had the least (10%) (Table 4.2). The A-143 resistant genotype within *P. viticola* clade *aestivalis* samples increased over the duration of sample collection trips in New York (Fig. 4.4). However, there was no discernible trend of an increase in the A-143 resistant genotype over time within the *P. viticola* clade *aestivalis* samples collected from Michigan and Ontario (Fig. 4.4). The prevalence of A-143 resistant genotype within *P. viticola* clade *aestivalis* samples increased from 88.2% in 2019 to 93.1% in 2022 in New York (Fig. 4.4).

Resistance mutations associated with FRAC 21 and 45 were not identified

A total of 654 *P. viticola* samples collected over sampling years were tested for the presence for S34L mutation associated with *P. viticola* resistance to ametoctradin, and E203-DE-V204 duplication and L201S mutation associated with resistance to cyazofamid. Among all the *P. viticola* samples analyzed, neither the S34L mutation nor the E203-DE-V204 duplication/L201S mutation were detected in any of the *P. viticola* samples (Table 4.2). was not found Overall, the *P. viticola* samples collected from the eastern United States and Canada showed 100% prevalence of sensitive genotypes to ametoctradin and cyazofamid (Table 4.2).

The TaqMan assay for CAA resistance was sensitive at low DNA concentrations

The TaqMan assay was able to successfully distinguish between the G-1105 sensitive genotype and the S-1105 resistant genotype at even low DNA concentrations (Fig. 4.5). The limit of detection of the G-1105 and S-1105 alleles using TaqMan assay when tested on five-fold

dilutions of purified DNA was 10pg/μL (Fig. 4.5). The reactions with DNA concentrations of 10 pg/μL amplified at approximately 35 Ct (Cycle threshold). The water control did not amplify.

The TaqMan assay for CAA resistance was specific

Approach one: Results showed that the TaqMan assay was accurate and consistent in discriminating G-1105 sensitive genotype and S-1105 resistant genotype in purified DNA for all tested isolates. On an average, all tested G-1105 sensitive genotype isolates and S-1105 resistant genotype isolates amplified at approximately 27.8 and 26.8 Ct values. The TaqMan assay showed 100% accuracy when confirmed with the genotype identity provided from sequencing.

Approach two: The TaqMan assay did not cross react when tested using the genomic DNA of closely related oomycetes and outgroup fungi. No real-time amplification was detected for *Pseudoperonospora cubensis* isolates, *Pseudoperonospora humuli* isolates, *Phytophthora rubi* isolates, *Phytophthora foliorum* isolates, *Phytophthora cinnamomi* isolates, *Rhizoctonia solani* AG-I and *R. solani* AG-G isolates. However, one of the three replicates of a *Phytophthora capsici* isolate showed very late amplification (approximately 39 Ct value). The actual status of fungicide resistance of these oomycete and fungal species was unknown.

The assay was validated on several leaf and air samples from multiple locations

For the tested leaf samples collected using Tough spots, the TaqMan assay showed 100% agreement with the results obtained from sequencing when samples either had G-1105 sensitive or G1105-S1105 mixed genotypes (Table 4.3). In samples with S-1105 resistant genotype, the TaqMan assay was able to accurately detect 97.1% (33/34) of the S-1105 resistant genotype samples; it misclassified only 2.9% (1/34) of the S-1105 resistant genotype samples as G1105-S1105 mixed genotypes (Table 4.3). The TaqMan assay demonstrated 100% concordance in

detecting all air samples as G-1105 sensitive genotype, consistent with the results obtained through sequencing (Table 4.4). The water control did not amplify in both experiments.

The SNP distinguishing TaqMan assay was compared with a previously developed P. viticola qPCR detection tool

All *P. viticola* samples tested using the *P. viticola* qPCR detection tool and the SNP distinguishing TaqMan assay amplified consistently between both assays. The *P. viticola* qPCR detection developed by Valsesia et al. (2005) detected all samples earlier than the SNP distinguishing TaqMan assay with a Ct difference of approximately between 8.3 to 11.8 Ct (Table. 5). All the samples tested, amplified at ³13.3 Ct value for *P. viticola* qPCR detection tool (Valsesia et al. 2005) and ³23.3 Ct value for TaqMan assay (Table 4.5). The negative control did not amplify in either assay.

Discussion

In the United States and Canada, QoI fungicides are widely used to manage grape downy mildew. Although QoI resistance in *P. viticola* has been reported in several European countries since 2000, the presence of QoI resistance in *P. viticola* in the United States was first confirmed in 2008 in Virginia (Baudoin et al. 2008). Our study found high occurrence of G143A mutations in the *Cytb* gene in the *P. viticola* samples collected across several states and Ontario, Canada, indicating widespread QoI resistance in *P. viticola* populations of the eastern United States and Canada. These results coincide with the previous findings in Georgia in 2017 and 2018 (Campbell et al. 2020). However, a trend change can be observed in samples from New York, as Gee et al. (2013) found low frequencies of QoI resistance in samples collected from New York and Pennsylvania in 2009 and 2010, while the current findings in this study show high prevalence of QoI resistance in samples collected from 2019 to 2022. Interestingly, *P. viticola*

samples collected from Michigan demonstrate lower A-143 genotype frequencies in 2021 as compared to 2019-2020 samples. This could be due to increased grower awareness from extension talks on the prevalence of QoI resistance in the state leading to reduced usage of QoI fungicides. Increased *P. viticola* samples were collected from wild grapes (*Vitis riparia*) across Michigan in 2021 which contained only the G-143 sensitive genotype, possibly due to low or no direct exposure of the QoI fungicides.

The mutations associated with fungicide resistance to QiI (FRAC 21) and QioSI (FRAC 45) were not discovered from the *P. viticola* samples collected in the eastern United States and Canada over the span of four years from 2019 to 2022. There are only a few brief studies from Europe that confirm the presence of the mutation L201S or the insertions of two amino acids (E203 DE V204) conferring QiI resistance (Cherrad et al. 2018; Cherrad et al. 2023; Nanni et al. 2019). Therefore, these mutations should be investigated on a larger sample size for further insight. Recently, S34L mutations associated with QioSI fungicide resistance have been detected in India, with control failures also reported due to a potential loss of sensitivity to the fungicide (Sagar et al. 2023). Furthermore, low frequencies of the S34L mutation have been found in a study conducted using a large sample size from *P. viticola* populations in France (Fontaine et al. 2019). The low frequencies of S34L mutations can be potentially associated with a fitness cost, as potential adverse effect on growth and complex III cytochrome bc1 activity has also been found in strains of mutant yeasts containing S34L mutations (Mounkoro et al. 2019). In future studies, sampling throughout the season for detection of the S34L mutation in *P. viticola* populations is suggested to understand the seasonal effect.

Recently, control failures due to loss of sensitivity to CAA fungicides in *P. viticola* populations have been reported in Brazil, China and India (Huang et al. 2020; Santos et al. 2020;

Sawant et al. 2017). In the United States, CAA resistance associated with the G1105S mutation was first reported in vineyards of Virginia and North Carolina in 2018 (Feng et al. 2018). Our study was performed on a large scale in the eastern United States and Canada to confirm the geographic prevalence of mutations associated with CAA resistance in *P. viticola* populations. Along with the G1105S mutation, the G1105V mutation at the same codon (1105) of the *PvCesA3* gene, has been associated with CAA resistance in *P. viticola* at low frequencies (Blum et al. 2010; Sierotzki et al. 2011; Zhang et al. 2017). We did not find this mutation (G1105V) in any samples collected in our survey. The G1105S mutation predominates in the eastern United States and Canada, a finding consistent with reports from China (Huang et al. 2020), Japan (Aoki et al. 2015), Europe (Blum et al. 2010; Sierotzki et al. 2011), and India (Sawant et al. 2017). This is the first report to confirm the presence of the G1105S mutation conferring CAA resistance in *P. viticola* populations in several states including Georgia, New York, Wisconsin, Michigan, across the eastern United States and Ontario Canada. An increased percentage of the G1105S mutation in *P. viticola* populations over time can be observed in states where samples were collected for multiple years (New York and Michigan). The G1105S mutation was also detected in Ontario in 2022 when the sampling region was broadened compared to 2021. This trend is alarming in some states. For instance, the increase from no detection of the G1105S mutation (2019) to 93.3% being either the S-1105 resistant genotype or mixed (containing both G-1105 sensitive and S-1105 resistant genotype in the sample) (2022) shows significant resistance development. Campbell et al. (2020) found that the G1105S mutation was not detected in samples collected from vineyards in Georgia between 2015 and 2018; however, in this study, *P. viticola* samples collected from Georgia in 2021 showed that 54.1% of samples were either the S-1105 resistant genotype or a mixed genotype. This pattern is consistent with Michigan and

Ontario, where the G1105S mutation was first detected in the most recent sampling years, specifically in 2021 and 2022. Studies from Brazil and China demonstrated that the frequency of CAA-resistant *P. viticola* populations was significantly correlated with exposure to CAA fungicides (Santos et al. 2020; Huang et al. 2020). Increased resistance might be occurring due to strong selection of S-1105 resistant genotype. Therefore, there is a high chance of potential expansion of CAA fungicide resistance in vineyards in the eastern United States and Canada in the future if proper fungicide resistance management strategies are not applied.

Fungicide resistance is widespread in other major fungal pathogens infecting grapes such as *Erysiphe necator*, causing powdery mildew, and *Botrytis cinerea*, causing botrytis bunch rot. Fungicide resistance has been already reported in major FRAC codes (FRAC 1, 2, 3, 7, 9, 11, 13, 17) that are actively used to manage either powdery mildew or botrytis bunch rot in grapes (Alzohairy et al. 2021; Feng et al. 2018; Miles et al. 2012; Miles et al. 2021). Moreover, *B. cinerea* isolates have shown resistance to multiple fungicides used to manage gray mold in grapes, worldwide (Alzohairy et al. 2021; Hahn 2021). Continuous monitoring for fungicide resistance is an important step to determine abundance of fungicide-resistant isolates in pathogen populations. Several sampling strategies such as air sampling using active air sampling devices, glove sampling, and leaf sampling using Tough spots can be deployed for rapid and simple sample collection (Lowder et al. 2023; Miles et al. 2021; Sharma et al. 2022). These sampling techniques can be easily combined with crude DNA extraction methods such as Chelex extractions, making the process of molecular detection more robust and effective (Miles et al. 2021; Sharma et al. 2023). Furthermore, sampling time should also be considered as an important factor while developing monitoring strategies. A significant increase in chemical class resistance of *B. cinerea* isolates in strawberry was observed from the isolates collected late in the growing

season compared to the early in California (Cosseboom et al. 2019). Hence, factors such as sampling timing and collection method should be considered while planning for fungicide resistance monitoring.

Previously, phylogenetic studies of *P. viticola* found five different cryptic species with varying host range, geographic distribution, and size of sporangia in the eastern North America¹⁴). In our survey, *P. viticola* clades *aestivalis* and *vulpina* were the most and least abundant species, respectively (Rouxel et al. 2014). Similarly, Hong et al. (2019) found that the *P. viticola* clade *aestivalis* was the most abundant and widely distributed clade, followed by *P. viticola* clade *vinifera*, as the second most prevalent among the samples collected from cultivated grapes in Georgia and Florida. Similar clade dynamics were also observed in our study, where three *P. viticola* clades (*aestivalis*, *vinifera* and *riparia*) were found in the samples collected. Consistent with previous studies, *P. viticola* clade *aestivalis* was the dominant clade with widespread distribution across the eastern United States and Ontario, Canada. Interestingly, Hong et al. (2019) also detected *P. viticola* clades *vinifera* and *vulpina* (in very low frequencies) in coastal regions of Georgia, while Rouxel et al. (2014) found *P. viticola* clade *riparia* in the eastern United States and Quebec, Canada. In Georgia, temporal shifts in clade composition were observed in the coastal regions, with *P. viticola* clade *vinifera* increasing from 0% in 2015 to 90.2% in 2016, followed by a decline to 42.4% in 2017 (Hong et al. 2019). Moreover, *P. viticola* clade *vinifera* was not detected in our samples collected from Georgia in 2021. In Quebec, Canada, a trend was observed where *P. viticola* clade *riparia* was detected in the early season, while *P. viticola* clade *aestivalis* dominated in the mid- to late-growing season in air samples collected from multi-variety vineyards (Carisse et al. 2021). However, only *P. viticola* clade *riparia* was detected through-out the growing season in one of the sites planted with the hybrid

grape variety Chancellor (Carisse et al. 2021). Timing of sample collection along with vineyard composition and size could influence clade composition. In the present study, we observed that different *P. viticola* clades based on different vineyard plantation composition within Michigan, where only *P. viticola* clade *aestivalis* was found in southwest Michigan (mostly *V. labrusca*), while *P. viticola* clade *vinifera* and *riparia* were mostly found in northwest Michigan (mostly *V. vinifera* or interspecific hybrids). This distribution of the *P. viticola* clades in Michigan based on cultivars planted in the vineyards agrees with the already established host range of each clade and host plant distribution throughout the state.

Clade specific occurrence of fungicide resistance mutations has been reported in *Pseudoperenospora cubensis* clades causing cucurbit downy mildew (D’Arcangelo et al. 2023). The G1105W mutation associated with CAA resistance in cucurbits was primarily found in *P. cubensis* clade 2, while G1105V resistant and sensitive genotypes were most common in *P. cubensis* clade 1 (D’Arcangelo et al. 2023). However, our results suggests that G1105S mutations conferring CAA resistance in *P. viticola* is not associated with specific *P. viticola* clades. The S-1105 resistant genotype was widely prevalent in *P. viticola* clade *aestivalis*, while G1105-S1105 mixed genotype was also observed in *P. viticola* clades *vinifera* and *riparia*. The presence of G1105-S1105 mixed genotype in *P. viticola* clades *vinifera* and *riparia* has been mainly observed in the Michigan, Wisconsin and New York vineyards where downy mildew management heavily relies on CAA fungicides.

Interestingly, QoI resistance was widely distributed in both clades of *P. cubensis* (D’Arcangelo et al. 2023). Similar findings were observed in the *P. viticola* clades, as the G-143 resistant genotype is the most prevalent mutation across the *P. viticola* clades found in this study. The *P. cubensis* clade 2 (on cucumbers) is extensively managed with fungicides and undergoes

heavy selection pressure for the resistance genotype, that can quickly disperse long distances (D’Arcangelo et al. 2023). In contrast, *P. viticola* overwinters as oospores in leaf litter in vineyard soil (Wong et al. 2001); hence, the genotype in the vineyard from the previous growing season can influence occurrence of fungicide resistance alleles in the upcoming growing season’s *P. viticola* populations. The findings in our study indicate that QoI and CAA resistance in *P. viticola* is mainly affected by fungicide use strategies rather than clades.

In this study, tsamples were considered as “mixed” in a case where two nucleotide signals at a SNP site were found when screening was conducted through use of sanger sequencing. This suggests either co-infection with both resistant and sensitive genotypes or heteroplasmy, or heterozygotes. Although, we tried to collect samples from only single colonies, there is still a high probability of the presence of multiple strains within a small collection area. In instances of resistance to QoI fungicides, the *P. viticola* samples may also exhibit heteroplasmy, which refers to the coexistence of multiple types of mitochondrial DNA within a single cell. This phenomenon has been observed in several other plant pathogens including *Venturia inaequalis* (Vielba-Fernandez et al. 2018), *Podosphaera xanthii* (Villani and Cox et al. 2014) and *Botrytis cinerea* (Ishii 2009; Ishii et al. 2009) for the G143A mutation associated with QoI resistance. However, Miles et al. (2021) did not find heteroplasmy in any of their single-spored *E. necator* isolates. Therefore, further investigation would also be required to determine whether the mixed *P. viticola* samples were due to mixed strains of both genotypes or the presence of heteroplasmy. In the case of the G1105S mutation conferring CAA resistance, mixed samples showing two sequencing signals could also be due to the presence of heterozygote *P. viticola* samples. The G1105S mutation occurs in a recessive nuclear gene, hence, both alleles are required to achieve a CAA resistant phenotype (Blum et al. 2010). In other words, the

phenotype of a CAA mixed sample will be sensitive if it is a heterozygote sample instead of sample containing mixed *P. viticola* strains. Therefore, it is difficult to confirm the phenotype of these mixed samples from our results until further investigation is done. However, the presence of the sensitive heterozygote samples indicates the potential risk of development of full resistance to CAA fungicides based on ability of the pathogen to reproduce sexually and asexually (Aoki et al. 2015).

When dealing with challenging obligate pathogens such as *P. viticola*, the need for a rapid, sensitive, and specific allele-discriminating molecular tool cannot be overlooked. Isothermal diagnostic tools such as recombinase polymerase amplification (RPA) and the loop mediated isothermal amplification assay (LAMP) are novel and highly sought after techniques used to diagnose plant pathogens. Various species-specific RPA tools have been developed to detect *Banana bunchy top virus* (BBTV), *Clavibacter michiganensis* subsp. *michiganensis*, *C. michiganensis* subsp. *sepedonicus*, and *Xylella fastidiosa* (Agdia Inc. Elkhart, IN, U.S.A.). This technique is rapid, easy to develop, and can efficiently tolerate PCR inhibitors and background DNA. However, this technique has a high likelihood for mismatches (9 nucleotides), which is a major disadvantage in the case of single nucleotide polymorphism identification (SNP) associated with fungicide resistance (Daher et al. 2015; Sharma et al. 2023). Sharma et al. (2023) showed that an RPA assay failed to detect the G143A mutation in *E. necator* isolates.

When compared to RPA, the LAMP technique is more promising for detecting SNPs in plant pathogens. Several LAMP assays have been deployed to detect mutations in plant pathogens, such as the F167Y mutation in carbendazim-resistant *F. graminearum* and the H272R mutation in succinate dehydrogenase inhibitor (SDHI)-resistant isolates of *B. cinerea* (Duan et al. 2014; Fan et al. 2018). Sharma et al. (2023) developed a modified PNA-LNA-LAMP assay to

detect the G143A mutation in *E. necator* isolates that showed 100% detection when a single allele was present. However, this LAMP assay had some difficulty in discriminating mixed samples. Hence, LAMP tools can be used to designed as allele-discriminating assays, however, these are difficult to design, may have contamination issues and struggle to discriminate mixed samples. Other approaches such as TaqMan qPCR based techniques and ddPCR can also be used to detect SNPs. Miles et al. (2021) developed a TaqMan assay and ddPCR assay to detect G143A detection in *E. necator*. Both techniques discriminated alleles well, even in mixed samples, however ddPCR had higher resolution. The ddPCR has its own disadvantage as it is not high-throughput and requires more time to set up than TaqMan assay, as well as different technology and buffers (Miles et al. 2021). Future molecular tools that are high-throughput, highly quantitative and can detect SNPs rapidly in mixed samples will be required to detect mutations associated with fungicide resistance in. a timely manner.

In conclusion, widespread QoI and first detections of CAA fungicide resistance in *P. viticola* in various states of the eastern United States and Canada has been reported in this study. These results emphasize the need to employ fungicide resistance management strategies in grape downy mildew management. The 2024 FRAC recommendations for managing resistance in *Plasmopara viticola* suggest: (a) limiting the number of fungicide applications to a maximum of three QoI (Quinone Outside Inhibitors) and three to four CAA fungicides (based on resistance level) per vine cycle, and using them preventively in combination with effective partner fungicides like multisite or non-cross-resistant options, (b) applying the full recommended dosage, and (c) alternating between different modes of action in fungicide treatments. These recommendations should be followed to reduce the selection pressure and maintain the efficacy of the fungicides for a longer period. Continuous monitoring for QoI, QiI, QioSI and CAA

fungicides is needed to make effective and timely management strategies for grape downy mildew.

Acknowledgements

The authors would like to acknowledge all the grape growers that allowed us to sample their vineyards throughout this project. Additionally, we would like to acknowledge funding support from the Michigan State Horticultural Society and New York Farm Viability Foundation through Specialty Crop Block grant programs. This project was supported by a Michigan State University Hatch project: MICL02617.

Figures

Figure 4.1. Alignment of A) PvCesA3 and B) CytbB as well as the location of critical amino acid changes and primers and probes developed for confirming the presence of the mutations. Yellow denotes a previously identified amino acid change. Arrows denote amplification primers.

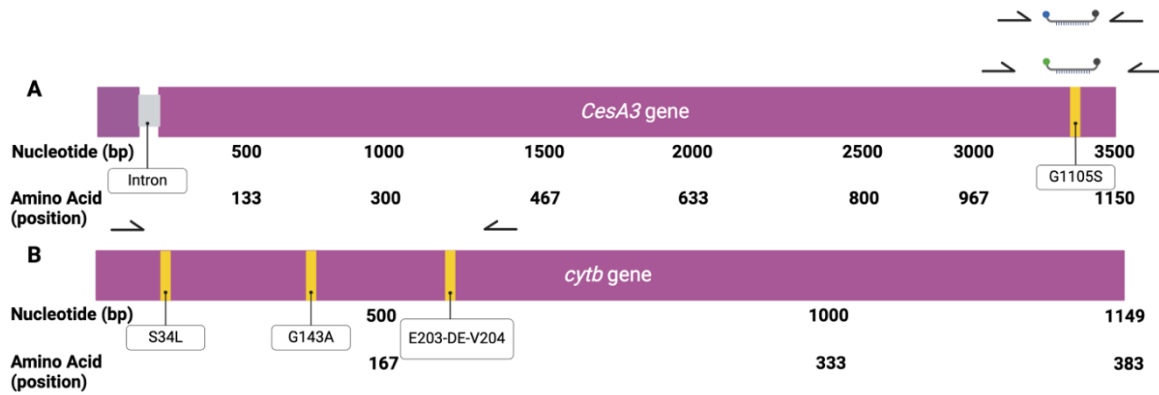


Figure 4.2. A) Geographical distribution of the G1105S mutation conferring CAA resistance within *Plasmopara viticola* species complex/clades across the eastern United States and Ontario, Canada. B) Geographical distribution of the G143A mutation conferring QoI resistance within *P. viticola* species complex/clades across the eastern United States and Ontario, Canada. The Letters above circles represents *P. viticola* clade differentiation; Letter A represents *P. viticola* clade *aestivalis*; letter V represents *P. viticola* clade *vinifera*; and letter R represents *P. viticola* clade *riparia*.

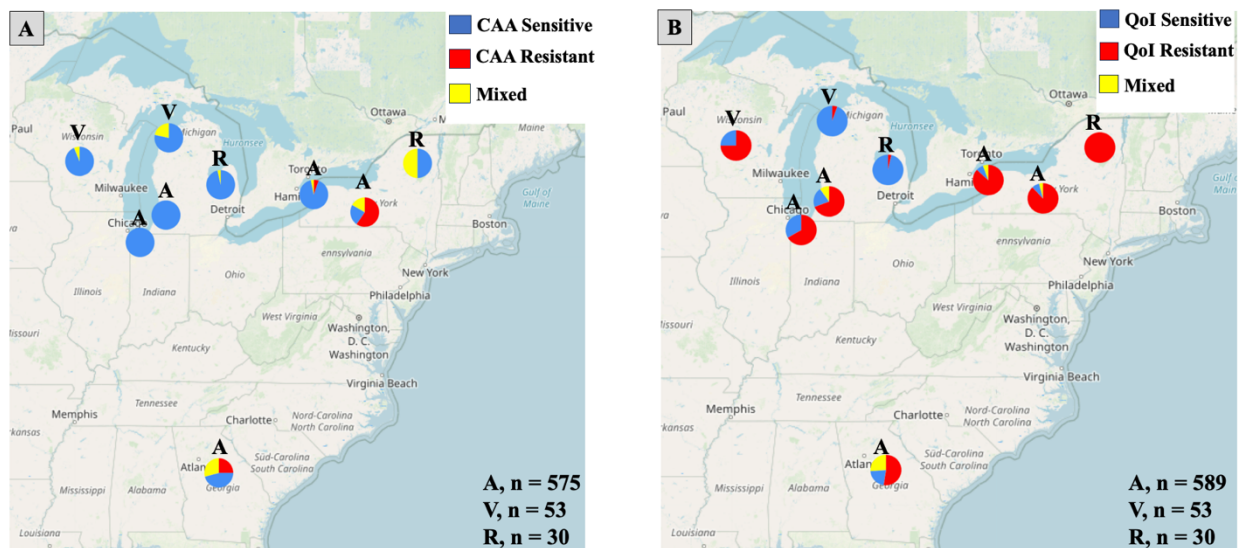


Figure 4.3. Temporal distribution of the *Plasmopara viticola* clade *aestivalis* samples containing the G1105S mutation associated with CAA resistance collected from the eastern United States and Ontario, Canada in 2019 to 2022. A) *P. viticola* samples collected from Michigan in 2019, 2020, and 2021. B) *P. viticola* samples collected from New York in 2019, 2020, 2021 and 2022. C) *P. viticola* samples collected from Ontario, Canada in 2021 and 2022. D) *P. viticola* samples collected from Indiana in 2019 and Georgia in 2021.

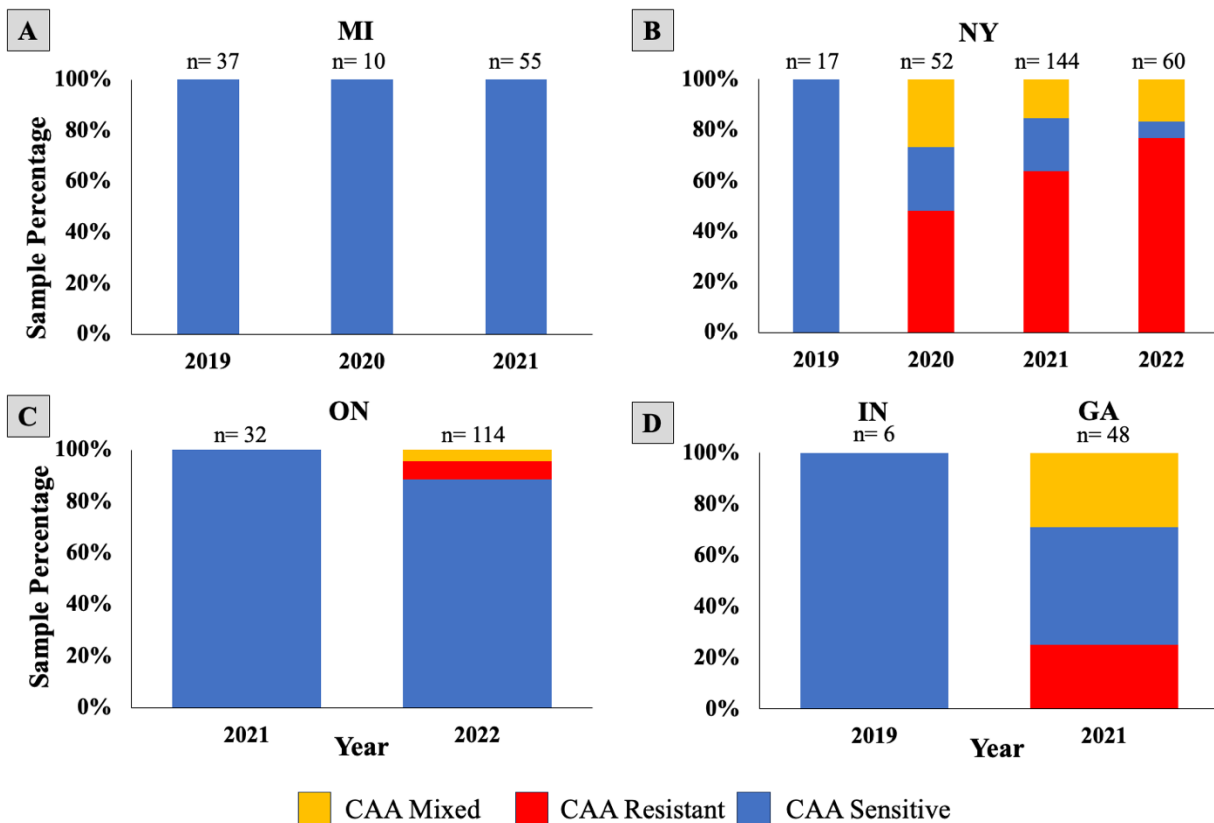


Figure 4.4. Temporal distribution of the *Plasmopara viticola* clade *aestivalis* samples containing the G143A mutation associated with QoI resistance collected from the eastern United States and Ontario, Canada in 2019 to 2022. A) *P. viticola* samples collected from Michigan in 2019, 2020, and 2021. B) *P. viticola* samples collected from New York in 2019, 2020, 2021 and 2022. C) *P. viticola* samples collected from Ontario, Canada in 2021 and 2022. D) *P. viticola* samples collected from Indiana in 2019 and Georgia in 2021.

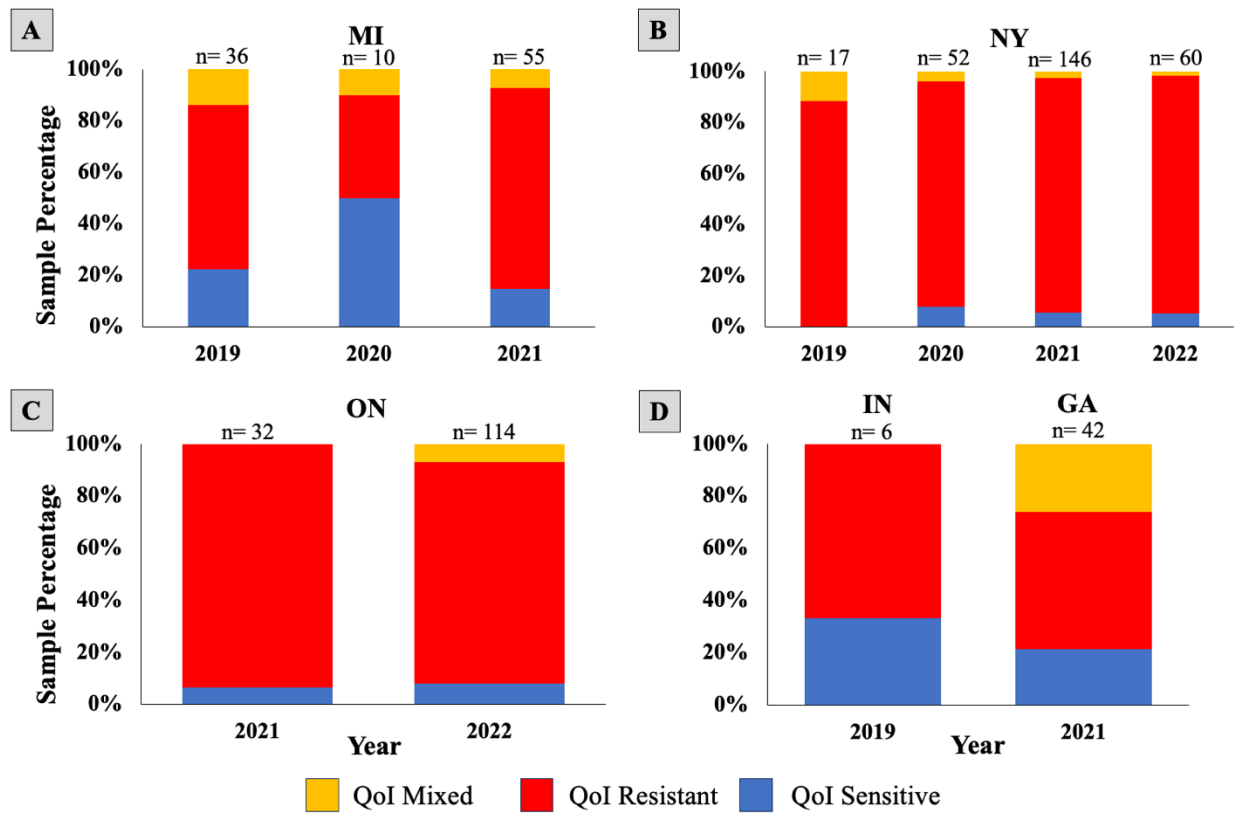
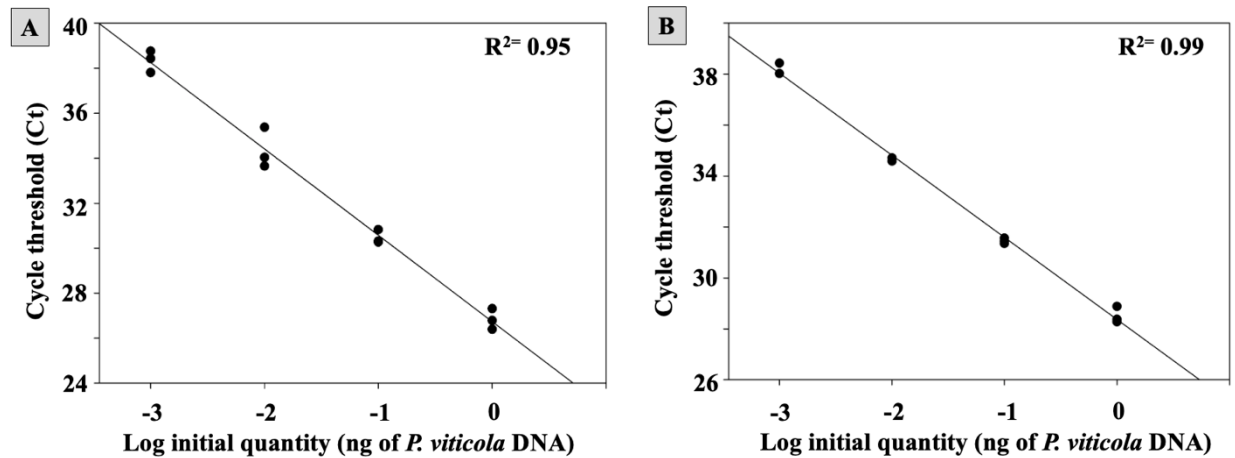


Figure 4.5. Sensitivity of TaqMan probe-based assay using varying DNA concentrations to detect CAA resistance in *Plasmopara viticola*. A) Various DNA concentrations (ng) of the G-1105 sensitive genotype (CAA-sensitive) isolate were compared with cycle threshold (Ct) values of the TaqMan probe-based assay. B) Various DNA concentrations (ng) of the S-1105 sensitive genotype (CAA-resistant) isolate were compared with cycle threshold (Ct) values of the TaqMan probe-based assay. The CAA-sensitive (MI-21-35) containing the G-1105 allele and the CAA-resistant isolate (NY-21-155) containing S-1105 allele were compared at various concentrations from 1 ng/mL to 1 pg/mL and tested to determine the limit of detection of the assay.



Tables

Table 4.1. Primers and probes used in this study to amplify *PvCesA3*, *Cyrb*, and the ITS region and detect G1105S, S34L, L201S, E203 and E204 mutations associated with fungicide resistance in *Plasmopara viticola*.

Diagnostic assay	Sequence 5'-3'	Length	T _m (°C) ^b	GC (%)	5' label	3' quencher
1. <u>TaqMan assay for G1105S mutation</u>						
Amplification primers						
qPCR_CAA Fwd	ACACGGCTGCTACCTTTA	18	55.5	50		
qPCR_CAA Rev	CCAGTTTCGGCATTGCC	17	56.6	58.8		
Designed Probes						
G-1105 Pvit ^a	GTGTT C <u>GGCT</u> CGTTGCTGGT	20	63.6	60	FAM	BHQ-1
A-1105 Pvit ^a	GTGTT C <u>AGC</u> TCGTTGCTGGT	20	63.5	55	HEX	BHQ-1
2. <u>PCR amplification for G1105S mutation</u>						
Amplification primers						
PvPCR_1F_CAA	CGTTTATCACGATGATGGCTATTGT	25	59.8	40		
PvPCR_1R_CAA	CTACGTCACAGTCGTGGCA	19	59.7	57.9		
3. <u>PCR amplification for G143A, S34L, L201S and E203 and E204 mutation</u>						
Amplification primers						
PV_COB Fwd 1	TCATTTAATTGATTATCCTACACCT	25	54.1	28		
PV_COB Rev2	ACGATTAAACCAAATAAATCTTTTGT	26	55.0	23.1		
4. <u>PCR amplification for ITS1 sequence polymorphism</u>						
Amplification primers						
ITS1-O	CGGAAGGATCATTACC					
ITS2	GCTGCGTTCTTCATCGATGC					

^aBold and underlined indicates SNP position in probes in the TaqMan assay.

^bT_m = annealing temperature.

Table 4.2. The *P. viticola* genotype (mutations associated with fungicide resistance and clade differentiation) frequencies among sampling years from 2019 to 2022, where samples were collected from vineyards of the eastern United States and Canada.

Genotype	Number of locations											
	<u>2019^a</u>			<u>2020^a</u>		<u>2021^a</u>					<u>2022^a</u>	
	MI ^b	NY ^b	IN ^b	MI ^b	NY ^b	MI ^b	NY ^b	WI ^b	ON ^b	GA ^b	ON ^b	NY ^b
<u><i>Cytb</i> gene^c</u>												
G-143 allele	8	-	2	5	4	69	8	4	2	9	9	3
A-143 allele	25	15	4	6	46	44	136	12	30	22	97	56
Mixed (G-143 & A-143 alleles)	5	2	-	1	2	4	4	-	-	11	8	1
S-34 allele	38	17	6	12	52	117	148	16	32	42	114	60
L-34 allele	-	-	-	-	-	-	-	-	-	-	-	-
E203-DE-V204 duplication	-	-	-	-	-	-	-	-	-	-	-	-
<u><i>PvCesA3</i> gene^c</u>												
G-1105 allele	38	17	6	12	13	108	31	15	32	22	101	4
S-1105 allele	-	-	-	-	25	-	92	-	-	12	8	46

Table 4.2. (cont'd)

Mixed (G-1105 & S-1105 alleles)	-	-	-	-	14	9	23	1	-	14	-	10
--	---	---	---	---	----	---	----	---	---	----	---	----

ITS gene^c

Clade Aestivalis	37	17	6	10	52	55	146	-	32	52	114	60
Clade Vinifera	1	-	-	2	-	34	-	16	-	-	-	-
Clade Riparia	-	-	-	-	-	28	2	-	-	-	-	-

^aThe number of samples was 61, 64, 359 and 174 collected in 2019, 2020, 2021 and 2022, respectively using Toughspots.

^b Abbreviations used for States from where *P. viticola* samples were collected. MI = Michigan, NY = New York, IN = Indiana, WI = Wisconsin, GA = Georgia, ON = Ontario, Canada.

^cThe *P. viticola* genotypes were based on *Cytb*, *PvCesA3* or *ITS* gene confirmed by sequencing.

Table 4.3. Validation of the TaqMan probe-based qPCR assay for detecting G1105S mutation in the *PvCesA3* gene associated with CAA resistance in *P. viticola* using crude DNA samples collected from the eastern United States and Canada by comparing outcome with sequencing.

Sample CAA sensitivity status ^a (Sequencing)	Number of samples with CAA sensitivity status	TaqMan probe-based assay results			Accuracy of TaqMan assay relative to sanger sequencing ^b
		Sensitive	Resistant	Mixed	
Sensitive	33	33	-	-	100
Resistant	34	-	33	1	97.1
Mixed	33	-	-	33	100

^a*P. viticola* samples on leaves were collected from Michigan, Georgia, New York, and Wisconsin in 2021 using the Tough-Spots method.

^bAccuracy of the assay was calculated using formula: ((True Positive + True Negative)/(Total no. of cases)).

Table 4.4. Comparison of the TaqMan probe-based qPCR assay with sequencing in detecting the G1105S mutation in the *PvCesA3* gene associated with CAA resistance in *P. viticola* air samples collected from Michigan using rotating arm air samplers.

Sample Name ^a	TaqMan ^b		Sequencing ^c
	G-1105 Ct ^d	S-1105 Ct ^d	
11.4.B	27.0025203	nd ^e	+ ^f
13.4.A	28.9045514	nd	+
9.5.B	27.023	nd	+
10.12.B	31.04	nd	+
10.10.B	28.98	nd	+
10.7.B	32.17	nd	+
9.1.A	26.41	nd	+
11.10.B	27.99	nd	+
9.12.A	27.90	nd	+
10.1.B	25.34	nd	+
10.3.B	27.95	nd	+
9.5.A	27.39	nd	+
13.11.A	27.37	nd	+
9.4.A	27.46	nd	+
11.11.B	28.21	nd	+
10.4.B	27.58	nd	+
13.12.A	27.10	nd	+
10.11.B	30.05	nd	+
13.7.B	28.15	nd	+
10.2.B	27.21	nd	+
13.8.A	29.59	nd	+
13.3.A	28.35	nd	+
13.2.A	25.57	nd	+

Table 4.4. (cont'd)

^a DNA from air samples that were collected from Clarksville, Michigan by using rotating-arm air samplers. “A” represents rod samples collected after 4 days, “B” represents samples collected after 3 days.

^b Fluorophores used in TaqMan probe-based assay are fluorescein (FAM) dye for G-1105 allele and hexachlorofluorescein (HEX) dye for S-1105 allele. TaqMan reactions were carried out at 67°C using Bio-Rad CFX96 machine.

^c Sequencing of *PvCesA3* gene was conducted using air samples.

^d Ct= cycle threshold

^e “nd” represents no detection

^f “+” represents detection of G-1105 allele (Wild Type allele)

Table 4.5. Comparison of the TaqMan probe-based qPCR assay capable of distinguishing the G1105S mutation in the *PvCesA3* gene associated with CAA resistance in *P. viticola*, with the *P. viticola* qPCR ITS detection tool (Valsesia et al. 2005; Si Ammour et al. 2020).

Sample Name ^a	TaqMan ^b		qPCR-ITS Ct ^d	Δ Ct ^d	Sequencing ^c
	G-1105 Ct ^d	S-1105 Ct ^d			
GA-001	25.00	nd ^e	14.34	10.65973605	+ ^f
GA-023	nd	23.59	14.04	8.39971688	- ^g
GA-011	24.63	nd	16.23	11.07343163	+
GA-022	28.18	24.36	13.29	11.85589466	+/- ^h
GA-035	27.18	28.59	16.74	10.29	+/-
GA-002	24.01	nd	13.71	8.70	+
GA-012	24.62	nd	15.91	9.54	+
GA-036	25.20	28.00	15.17	10.03	+/-
GA-003	23.28	nd	13.50	9.78	+
GA-013	30.17	30.84	20.29	9.87	+/-
GA-024	nd	26.20	15.01	11.19	+/-
GA-037	28.24	28.82	17.30	10.93	+/-
GA-004	25.63	nd	15.44	10.18	+
GA-014	28.57	29.59	17.64	10.92	+/-
GA-029	nd	25.43	15.37	10.05	-
GA-046	nd	27.81	19.34	8.46	-
GA-005	24.52	nd	13.80	10.71	+

Table 4.5. (cont'd)

GA-015	28.10	nd	17.78	10.31	+
GA-030	nd	25.86	16.53	9.32	-
GA-006	25.48	nd	14.43	11.05	+
GA-019	26.16	28.20	16.31	9.85	+/-
GA-031	nd	26.49	16.54	9.94	-
GA-008	25.12	nd	15.94	9.17	+
GA-020	25.73	32.07	15.68	10.04	+/-
GA-032	nd	25.19	15.14	10.05	-
GA-010	28.26	nd	18.11	10.15	+
GA-021	nd	25.03	16.59	8.44	-
GA-033	26.64	29.52	17.01	9.63	+/-

^a Crude DNA from samples that were collected from Georgia.

^b Flourophores used in TaqMan probe-based assay are fluorescein (FAM) dye for G-1105 allele and hexachlorofluorescein (HEX) dye for S-1105 allele. TaqMan reactions were carried out at 67°C using Bio-Rad CFX96 machine.

^c Sequencing of *PvCesA3* gene was conducted using air samples.

^d Ct= cycle threshold

^e “nd” represents no detection

^f “+” represents detection of G-1105 allele (Wild Type allele) conferring CAA sensitive sample

^g “-” represents detection of S-1105 allele (Mutant Type allele) conferring CAA resistance sample

^h “+/-” represents detection of both G-1105 allele and S-1105 allele conferring mixed sample

Table 4.6. TaqMan and PCR reaction reagents and conditions.

Reagents	Reaction volume (μL)	Final concentration
<u>1. PCR amplification for G1105S mutation</u>		
10uM PvPCR_1F_CAA	0.5	200nM
10uM PvPCR_1R_CAA	0.5	200nM
2X Perfecta ToughMix	12.5	1X
1ng DNA Template	2	
DNase-free water	9.5	
<u>2. PCR amplification for G143A, S34L, and E203 and E204 mutation</u>		
10uM PV_COB Fwd 1	0.5	200nM
10uM PV_COB Rev2	0.5	200nM
2X Perfecta ToughMix	12.5	1X
1ng DNA Template	2	
DNase-free water	9.5	
<u>3. TaqMan assay for G1105S mutation</u>		
10uM qPCR_CAA Fwd	1	400nM
10uM qPCR_CAA Rev	1	400nM
10uM G-1105 Pvit probe	0.25	100nM
10uM A-1105 Pvit probe	0.25	100nM
2X Perfecta ToughMix	12.50	1X
1ng DNA Template	2	
DNase-free water	8	

LITERATURE CITED

- Alzohairy, S. A., Gillett, J., Saito, S., Naegele, R. N., Xiao, C. L., and Miles, T. D. 2021. Fungicide resistance profiles of *Botrytis cinerea* isolates from Michigan vineyards and development of a TaqMan assay for detection of fenhexamid resistance. *Plant Dis.* 105:285-294.
- Aoki, Y., Furuya, S., and Suzuki, S. 2011. Method for rapid detection of *PvCesA3* gene allele conferring resistance to mandipropamid, a carboxylic acid amide fungicide, in *Plasmopara viticola* populations. *Pest Manag. Sci.* 67:1557–1561.
- Aoki, Y., Hada, Y., and Suzuki, S. 2013. Development of a multiplex allele-specific primer PCR assay for simultaneous detection of QoI and CAA fungicide resistance alleles in *Plasmopara viticola* populations. *Pest Manag. Sci.* 69:268-273.
- Aoki, Y., Hashimoto, M., and Suzuki, S. 2013. Emergence of single point mutation in *PvCesA3*, conferring resistance to CAA fungicides, in *Plasmopara viticola* populations in Japan. *Plant Health Prog.* doi: <https://doi.org/10.1094/PHP-2013-0729-01-BR>.
- Baudoin, A., Olaya, G., Delmotte, F., Colcol, J. F., and Sierotzki, H. 2008. QoI Resistance of *Plasmopara viticola* and *Erysiphe necator* in the Mid-Atlantic United States. *Plant Health Prog.* doi:10.1094/PHP-2008-0211-02-RS.
- Blum M., Waldner M., and Gisi U. 2010. A single point mutation in the novel *PvCesA3* gene confers resistance to the carboxylic acid amide fungicide mandipropamid in *Plasmopara viticola*. *Fungal Genet. Biol.* 47:499–510.
- Blum, M., Gamper, H. A., Waldner, M., Sierotzki, H., and Gisi, U. 2012. The cellulose synthase 3 (*CesA3*) gene of oomycetes: Structure, phylogeny and influence on sensitivity to carboxylic acid amide (CAA) fungicides. *Fungal Biol.* 116:529–542.
- CABI. 2018. *Plasmopara viticola*. Crop Protection Compendium. CABI. <https://www.cabi.org/isc/datasheet/41918>
- Cadle-Davidson L. 2008. Variation within and between *Vitis* spp. for foliar resistance to the downy mildew pathogen *Plasmopara viticola*. *Plant Dis.* 92:1577–1584.
- Campbell, S. E., Brannen, P. M., Scherm, H., and Brewer, M. T. 2020. Fungicide sensitivity survey of *Plasmopara viticola* populations in Georgia vineyards. *Plant Health Prog.* 21:256–261.
- Campbell, S. E., Brannen, P. M., Scherm, H., Eason, N., and MacAllister, C. 2021. Efficacy of fungicide treatments for *Plasmopara viticola* control and occurrence of strobilurin field resistance in vineyards in Georgia, USA. *Crop Prot.* 139:105371. <https://doi.org/10.1016/j.cropro.2020.105371>

- Carisse, O., Van der Heyden, H., Tremblay, D. M., Hébert, P. O., and Delmotte, F. 2021. Evidence for differences in the temporal progress of *Plasmopara viticola* clades *riparia* and *aestivalis* airborne inoculum monitored in vineyards in eastern Canada using a specific multiplex quantitative PCR assay. *Plant Dis.* 105:1666-1676.
- Chen, W.J., Delmotte, F., Richard-Cervera, S., Douence, L., Greif, C., and Corio-Costet, M.F. 2007. At least two origins of fungicide resistance in grapevine downy mildew populations. *Appl. Microbiol. Biotechnol.* 73: 5162–5172.
- Cherrad, S., Hernandez, C., Steva, H., and Vacher, S. 2018. Resistance de *Plasmopara viticola* aux inhibiteurs du complexe III: Un point sur la caracterisation phenotypique et genotypique des souches. *Plant Dis.* 7:11–12.
- Cherrad S, Gillet B, Dellinger J, Bellaton L, Roux P, Hernandez C, Steva H, Perrier L, Vacher S, and Hughes S. 2023. New insights from short and long reads sequencing to explore cytochrome b variants in *Plasmopara viticola* populations collected from vineyards and related to resistance to complex III inhibitors. *PLoS One.* 18:e0268385. doi:10.1371/journal.pone.0268385
- Cosseboom, S. D., Ivors, K. L., Schnabel, G., Bryson, P. K., and Holmes, G. J. 2019. Within-season shift in fungicide resistance profiles of *Botrytis cinerea* in California strawberry fields. *Plant Dis.* 103:59-64.
- Daher, R. K., Stewart, G., Boissinot, M., Boudreau, D. K., and Bergeron, M. G. 2015. Influence of sequence mismatches on the specificity of recombinase polymerase amplification technology. *Mol. Cell. Probes.* 29:116-121.
- D’Arcangelo, K. N., Wallace, E. C., Miles, T. D., and Quesada-Ocampo, L. M. 2023. Carboxylic acid amide but not quinone outside inhibitor fungicide resistance mutations show clade-specific occurrence in *Pseudoperonospora cubensis* causing downy mildew in commercial and wild cucurbits. *Phytopathol.* 113:80–89.
- Duan, Y., Zhang, X., Ge, C., Wang, Y., Cao, J., Jia, X., Wang, J., and Zhou, M. 2014. Development and application of loop-mediated isothermal amplification for detection of the F167Y mutation of carbendazim-resistant isolates in *Fusarium graminearum*. *Sci. Rep.* 4:7094-7098.
- Emmett, R., Wicks, T., and Magarey, P. 1992. Downy mildew of grapes. Pages 90-128 in: *Plant Diseases of International Importance. Volume III. Diseases of Fruit Crops*, J. Kumar, H. Chaube, U. Singh, and A. Mukhopadhyay, eds. Prentice Hall, Englewood Cliffs, NJ.
- Fan, F., Yin, W. X., Li, G. Q., Lin, Y., and Luo, C. X. 2018. Development of a LAMP method for detecting SDHI fungicide resistance in *Botrytis cinerea*. *Plant Dis.* 102:1612-1618.

- Feng, X., and Baudoin, A. 2018. First report of carboxylic acid amide fungicide resistance in *Plasmopara viticola* (grapevine downy mildew) in North America. *Plant Health Prog.* 19:139-139.
- Feng, X., Nita, M., and Baudoin, A. B. 2018. Evaluation of quinoxifen resistance of *Erysiphe necator* (grape powdery mildew) in a single Virginia vineyard. *Plant Dis.* 102:2586-2591.
- Fontaine S., Remuson F., Caddoux L., and Barrès B. 2019. Investigation of the sensitivity of *Plasmopara viticola* to amisulbrom and ametoctradin in French vineyards using bioassays and molecular tools. *Pest Manag. Sci.* 75:2115–2123.
- Furuya S., Suzuki S., Kobayashi H., Saito S., and Takayanagi T. 2009. Rapid method for detecting resistance to a QoI fungicide in *Plasmopara viticola* populations. *Pest Manag. Sci.* 65:840-843.
- Furuya, S., Mochizuki, M., Saito, S., Kobayashi, H., Takayanagi, T., and Suzuki, S. 2010. Monitoring of QoI fungicide resistance in *Plasmopara viticola* populations in Japan. *Pest manag. Sci.* 66:1268-1272.
- Gee, C. T., Chestnut, S., Duberow, E., Collins, A., and Shields, M. A. 2013. Downy mildew from Lake Erie vineyards is diverse for the G143A SNP conferring resistance to Quinone Outside Inhibitor Fungicides. *Plant Health Prog.* doi:10.1094/PHP-2013-0422-01- RS.
- Genet, J-L., Jaworska, G., and Deparis, F. 2006. Effect of dose rate and mixtures of fungicides on selection for QoI resistance in populations of *Plasmopara viticola*. *Pest Manag. Sci.* 62:188–194.
- Gisi, U., Sierotzki, H., Cook, A., and McCaffery, A. 2002. Mechanisms influencing the evolution of resistance to Qo inhibitor fungicides. *Pest Manag. Sci.* 58:859-867.
- Gisi U., Waldner M., Kraus N., Dubuis P.H., Sierotzki H. 2007. Inheritance of resistance to carboxylic acid amide (CAA) fungicides in *Plasmopara viticola*. *Plant Pathol.* 56:199–208.
- Gullino, M. L., Gilarda, G., Tinivella, F., and Garibaldi, A. 2004. Observations on the behaviour of different populations of *Plasmopara viticola* resistant to QoI fungicides in Italian vineyards. *Phytopathol. Mediterr.* 43:341-350.
- Hahn, M. 2014. The rising threat of fungicide resistance in plant pathogenic fungi: *Botrytis* as a case study. *J. Chem. Biol.* 7:133-141.
- Hong, C. F., Brewer, M. T., Brannen, P. M., and Scherm, H. 2019. Prevalence, geographic distribution and phylogenetic relationships among cryptic species of *Plasmopara viticola* in grape-producing regions of Georgia and Florida, USA. *J. Phytopathol.* 167:422–429.

- Huang, X., Wang, X., Kong, F., van der Lee, T., Wang, Z., and Zhang, H. 2020. Detection and characterization of carboxylic acid amide-resistant *Plasmopara viticola* in China using a taqman-mgb real-time PCR. *Plant Dis.* 104:2338–2345.
- Ishii, H. 2009. QoI fungicide resistance: current status and the problems associated with DNA-based monitoring. Pages 37-45 in: Recent developments in management of plant diseases. U. Gisi, I. Chet and M. L. Gullino, Eds. Springer, Dordnecht.
- Ishii, H., Fountaine, J., Chung, W. H., Kansako, M., Nishimura, K., Takahashi, K., and Oshima, M. 2009. Characterisation of QoI-resistant field isolates of *Botrytis cinerea* from citrus and strawberry. *Pest Manag Sci* 65:916–922.
- Lowder, S. R., Neill, T. M., Peetz, A. B., Miles, T. D., Moyer, M. M., Oliver, C., Stergiopoulos, I., Ding, S., and Mahaffee, W. F. 2023. A rapid glove-based inoculum sampling technique to monitor *Erysiphe necator* in commercial vineyards. *Plant Dis.* 107: 3096-3105.
- Miles, L. A., Miles, T. D., Kirk, W. W., and Schilder, A. M. C. 2012. Strobilurin (QoI) resistance in populations of *Erysiphe necator* on grapes in Michigan. *Plant Dis.* 96:1621-1628.
- Miles, T. D.; Neill, T.; Colle, M.; Warneke, B.; Robinson, G.; Stergiopoulos, I.; Mahaffee, W. F. 2021. Allele-specific detection methods for QoI fungicide resistant *Erysiphe necator* in vineyards. *Plant Dis.* 105:175–182.
- Mounkoro P., Michel T., Benhachemi R., Surpateanu G., Iorga B.I., Fisher N., Meunier B. 2019. Mitochondrial complex III Qi-site inhibitor resistance mutations found in laboratory selected mutants and field isolates. *Pest Manag. Sci.* 75:2107–2114.
- Nanni, I., Taccioli, M., Burgio, S., and Collina, M. 2019. Sensitivity of *Plasmopara viticola* populations and presence of specific and non-specific resistance mechanisms. Pages 137-138 in: Modern Fungicides and Antifungal Compound, Vol. IX. Deising, H. B; Fraaije, B.; Mehl, A.; Oerke, E. C.; Sierotzki, H.; and Stammler, G., Eds. Deutsche Phytomedizinische Gesellschaft, Braunschweig, Germany.
- Rouxel, M., Mestre, P., Comont, G., Lehman, B. L., Schilder, A., and Delmotte, F. 2013. Phylogenetic and experimental evidence for host-specialized cryptic species in a biotrophic oomycete. *New Phytol.* 197:251-263.
- Turechek, W. W., and Wilcox, W. F. 2005. Evaluating predictors of apple scab with receiver operating characteristic curve analysis. *Phytopathology* 95:679-691.
- Sagar, N., Jamadar, M. M., Reddy, C. N. L., Sayiprathap, B. R., Bharath, M., Shalini, N. H., Jagginavar, S. B., Pattar, P. S., and Basha, C. J. 2023. First report of quinone outside inhibitor stigmatellin binding type (QoSI) resistance in *Plasmopara viticola* in India. *New Dis. Rep.* 48: e12223.

- Santos, R. F., Fraaije, B. A., Garrido, L. da R., Monteiro-Vitorello, C. B., and Amorim, L. 2020. Multiple resistance of *Plasmopara viticola* to QoI and CAA fungicides in Brazil. *Plant Pathol.* 69:1708–1720.
- Sawant, S. D., Ghule, M. R., and Sawant, I. S. 2016. First report of QoI resistance in *Plasmopara viticola* from vineyards of Maharashtra, India. *Plant Dis.* 100:229-229.
- Sharma, N., Colle, M., Neill, T., Mahaffee, W. F., and Miles, T. D. 2019. Development of a rapid isothermal assays to detect QoI resistance in *Erysiphe necator* the causal agent of grape powdery mildew. (Abstr.) *Phytopathology* 109:S2.1. <https://doi.org/10.1094/PHYTO-109-10-S2.1>
- Sharma, N., Heger, L., Neill, T., Mahaffee, W., Gold, K. M., Combs, D., Brannen, P. M., Oliver, C., Moyer, M. M., Holland, L. A., McFadden-Smith, W., and Miles, T. D. 2022. Investigating QoI and CAA resistance in grape powdery mildew and downy mildew populations in vineyards of the eastern United States and Canada. (Abstr.) *Phytopathology* 112:S3.1. <https://doi.org/10.1094/PHYTO-112-11-S3.1>
- Sharma, N., Neill, T., Yang, H. C., Oliver, C. L., Mahaffee, W. F., Naegele, R., Moyer, M., and Miles, T. D. 2023. Development of a PNA-LNA-LAMP assay to detect an SNP associated with QoI resistance in *Erysiphe necator*. *Plant Dis.* 107:3238-3247.
- Si Ammour, M., Bove, F., Toffolatti, S. L., and Rossi, V. 2020. A real-time PCR assay for the quantification of *Plasmopara viticola* oospores in grapevine leaves. *Front Plant Sci.* 11:1202. doi: 10.3389/fpls.2020.01202
- Sierotzki, H., Kraus, N., Assemet, P., Stanger, C., Cleere, S., and Windass, J. 2005. Evolution of resistance to QoI fungicides in *Plasmopara viticola* populations in Europe. Pages 73-80 in: *Modern Fungicides and Antifungal Compounds IV*. Dehne, H. W., Gisi, U., Kuck, K. H., Russell P. E., Lyr, H., eds. BCPC, Alton, UK.
- Sierotzki, H., Blum, M., Olaya, G., Waldner, M., Cohen, Y., and Gisi, U. 2011. Sensitivity to CAA fungicides and frequency of mutations in cellulose synthase 3 (*CesA3*) gene of oomycete pathogen populations. Pages 151-154 in: *Modern Fungicides and Antifungal Compounds*. H. Dehne, H. Deising, U. Gisi, K. Kuck, P. Russell, and H. Lyr, eds. Selbstverlag, Braunschweig, Germany.
- Schröder, S., Telle, S., Nick, P., and Thines, M. 2011. Cryptic diversity of *Plasmopara viticola* (Oomycota, Peronosporaceae) in North America. *Org Divers Evol.* 11:3–7.
- Valsesia, G., Gobbin, D., Patocchi, A., Vecchione, A., Pertot, I., and Gessler, C. 2005. Development of a high-throughput method for quantification of *Plasmopara viticola* DNA in grapevine leaves by means of quantitative real-time polymerase chain reaction. *Phytopathology* 95: 672–678.

- Vielba-Fernandez, A., Bellón-Gómez, D., Tores, J. A., de Vicente, A., Perez-Garcia, A., and Fernandez-Ortuno, D. 2018. Heteroplasmy for the cytochrome b gene in *Podosphaera xanthii* and its role in resistance to QoI fungicides in Spain. *Plant Dis* 102:1599–1605.
- Villani, S. M., and Cox, K. D. 2014. Heteroplasmy of the cytochrome b gene in *Venturia inaequalis* and its involvement in quantitative and practical resistance to trifloxystrobin. *Phytopathology* 104:945–953.
- Wong, F. P., Burr, H. N., and Wilcox, W. F. 2001. Heterothallism in *Plasmopara viticola*. *Plant Pathol.* 50: 427-432.
- Zhang, H., Kong, F., Wang, X., Liang, L., Schoen, C. D., Feng, J., and Wang, Z. 2017. Tetra-primer ARMS PCR for rapid detection and characterisation of *Plasmopara viticola* phenotypes resistant to carboxylic acid amide fungicides. *Pest Manag. Sci.* 73:1655-1660.

CONCLUSION AND FUTURE DIRECTIONS

In summary, this dissertation enhances our understanding of fungicide resistance in *Erysiphe necator* and *Plasmopara viticola*, that are globally considered as major grapevine pathogens. by exploring their prevalence, geographical distribution, and genetic mutations associated with these fungicides across vineyards in the eastern United States and Canada. Development of a PNA-LNA-LAMP assay for the rapid detection of the G143A mutation, associated with QoI resistance in *E. necator*, provides a reliable, cost-effective diagnostic tool for diagnostic laboratories, enabling timely resistance monitoring. To the best of our knowledge, this application of PNA-LNA-LAMP represents the first use of this method for SNP-based detection of fungicide resistance in plant pathology. Investigations into the effects of sublethal dose (EC₅₀) of fungicides revealed that flutianil, trifloxystrobin and quinoxyfen effectively inhibited conidial germination in *E. necator* and triggered distinct changes in gene expression, including the upregulation of genes involved in respiratory pathways. Metrafenone and cyflufenamid does not inhibit conidial germination in *E. necator*. Transcriptomic analyses also showed that quinoxyfen suppresses the expression of various kinase family protein that are important for signal transduction pathways. While some differentially expressed genes showed similarities, flutianil, quinoxyfen, and trifloxystrobin appear to impact distinct pathways in the fungus. The upregulation of sugar and MFS transporters in flutianil-treated samples suggests increased energy demands. Additionally, the upregulation of multidrug transporters (MFS and ABC transporters) with flutianil and quinoxyfen treatments indicates a potential fungicide efflux mechanism, which could contribute to resistance development.

In *P. viticola*, the G1105S mutation linked to CAA resistance was predominantly identified in *P. viticola* clade *aestivalis* clade populations from Georgia, New York, and Ontario, with mixed-genotype samples appearing in *P. viticola* clades *vinifera* and *riparia* from Michigan, New York, and Wisconsin. The QoI resistance was found to widespread in *P. viticola* clades *aestivalis* and *vinifera*. The QoI and CAA fungicide resistance does not appear to be associated with *P. viticola* clade differentiation. Mutations associated with resistance to QioSI and QiI fungicides were not detected in the eastern United States and Canada. TaqMan probe-based assay is capable detecting G1105S mutation associated with

CAA resistance in *P. viticola*. This rapid detection tool is sensitive and specific and will be valuable tool for early detection of CAA resistance. The insights gained from this research provides a foundation for improved SNP-based diagnostic approaches, geographical distribution and prevalence of mutations associated with important fungicides for managing grape downy mildew and some understanding of transcriptomic effects of quinoxifen and flutianil on conidial germination of *E. necator*. This research offers valuable tools and insights to support disease management in grape production in the face of evolving pathogen resistance.

APPENDIX A: MANAGING GRAPEVINE DOWNY MILDEW

Introduction

Grapevine downy mildew caused by *Plasmopara viticola*, is a persistent and destructive disease that poses a significant threat to grape growers. To effectively manage this disease, it is crucial to implement practical strategies and adopt sustainable vineyard practices. By prioritizing sustainability, vineyard owners can protect their grapevines while minimizing the use of fungicides and reducing the risk of resistance development. In this article, we will explore integrated grapevine downy mildew management strategies, encompassing good vineyard practices, biological control, and the avoidance of fungicide resistance.

Disease signs and symptoms

Downy mildew symptoms can be seen on all green parts of the grapevines. Normally, the symptoms are first observed on the leaves following 5 to 17 days after infection. Foliar symptoms include green to yellow circular spots that appear like oil spots (Fig. A.1A). Under optimal disease conditions, several oil spots may develop and merge to cover larger areas of the leaf. Warm and humid nights can lead to white downy fuzzy growth (sporangia) on the underside of the infected leaf or other plant parts (Fig. A.1B; A.1C). Later the lesions turn brown as the infected tissue dies. Severe infections can lead to premature defoliation of the grapevines (Fig. A.2). Also, infected inflorescence can dry up completely and get covered with white sporangia (Fig. A.1D). Young, infected berries changes color to dull green or reddish brown and may either die or become discolored. Eventually, these berries can also be covered with white sporangia. Within 3 weeks after bloom, berries develop resistance to the pathogen. However, rachis remains susceptible for several weeks after bloom.

Disease cycle

To achieve proper downy mildew management, it is essential to understand the disease cycle. This pathogen overwinters as resting spores, known as oospores on fallen leaves or may be released into the soil as leaves decay in vineyards. Rainfall at least 10 mm (0.04 in.) ensuring soil wetness and temperature above 10°C are required for oospore germination. Oospores serve as the primary inoculum and begin germinating after bud break in the spring. Oospores produce a single germ tube, which terminates in a sporangium. Sporangium releases zoospores once they encounter water. Rain-splashed zoospores germinate by producing a germ tube and enter the lower surface of the leaf through stomata. Infections usually occurs in the morning hours as after 5 to 7 hours of sunlight exposure can inactivate sporangia. After infection, sporangia are further produced for secondary infection on the underside of the leaves through stomates and other infected tissues. Disease spreads further through newly produced sporangia that are dispersed by wind or rain onto new shoots, leaves, or clusters. The optimal temperature for disease development is 18 to 25 °C (64 to 76 °F), with minimum temperature 10°C (50 °F) and maximum temperature 30 °C (86 °F). The nights with high humidity and temperature above 13 °C (55 °F) favors disease development and sporangia production.

Regular Scouting and Monitoring of pathogen

Regular scouting and monitoring are essential for early detection of downy mildew symptoms and timely intervention. By following these practical tips, growers can effectively scout for downy mildew and ensure sustainable disease management:

1. **Visual Inspection:** Regularly examine leaves, shoots, and clusters after bloom for symptoms of downy mildew. Look for yellow "oil spots" on the upper surfaces of leaves and the presence of white, cottony spores on the undersides.

2. **Timely Intervention:** If downy mildew symptoms are observed, apply a fungicide with post-infection and anti-sporulant activity as soon as possible. Timely intervention can prevent further disease spread and minimize the need for extensive fungicide applications.

3. **Record-Keeping:** Maintain detailed records of disease severity and location in the vineyard. This information can aid in future decision-making and treatment strategies, leading to more sustainable and targeted management practices.

Integrated Disease Management

Cultural Control

To promote integrated disease management, it is crucial to focus on preventive measures and cultural practices that minimize the reliance on fungicides. Implementing the following practices can reduce the initial inoculum and create an unfavorable environment for the pathogen that will slow down the spread of the disease.

1. **Site Selection:** Choose vineyard sites with well-drained soils, good air circulation and sunlight. Proper site selection contributes to sustainable downy mildew management by reducing the disease pressure.

2. **Dormant Season Practices:** During the dormant season, it is essential to remove plant debris from vineyards in the fall season to minimize the overwintering spores. Shredding, burying, or removing plant debris can significantly reduce the inoculum for the upcoming season.

3. **Vineyard Management:** Implementing proper vineyard management practices can minimize disease development. Positioning shoots properly and practicing leaf pulling can promote vine drying and reduce humidity, which hinders downy mildew development.

Biological Control

Biological control utilizes natural enemies of the pathogen to suppress disease development. Beneficial microorganisms, such as specific strains of bacteria and fungi, can be used to suppress downy mildew. These microorganisms can colonize the grapevine surfaces, competing with the pathogen for resources and inhibiting its growth. Certain antagonistic organisms, such as *Bacillus mycoides*, *Trichoderma* spp. etc. have shown potential in controlling downy mildew. These organisms can directly attack the pathogen, parasitize its structures, or produce compounds that inhibit its growth. Market available bioproducts such as LifeGard can also be used as a preventative measure to manage the disease. Integrating biological control methods into disease management can enhance disease suppression while promoting a more environmentally friendly approach.

Resistant Varieties

Planting grapevine varieties that exhibit natural resistance to downy mildew can provide sustainable long-term management. Resistant varieties can reduce the disease pressure and minimize the need for fungicide applications. Resistant cultivars are not available however, less susceptible cultivars to downy mildew are available (Table A.1).

Chemical Control

While sustainable grapevine downy mildew management aims to minimize fungicide usage, there are instances where fungicides are necessary. Adopting preventative fungicide practices can help reduce the risk of resistance development and promote long-term effectiveness.

Consider the following guidelines:

1. Timing of Fungicide Applications: Initiate protectant fungicide sprays when shoots reach 1 to 2 inches in wet springs or no later than the pre-bloom stage. Early timing can effectively prevent primary infections and reduce disease severity.

2. Recommended Fungicides: Downy mildew can be managed using fungicides in three phases:

Phase 1: Protectants such as Mancozeb, Captan, Ziram, and copper can be used before the symptom appears. Protectant fungicides are required to be applied at regular interval as they provide protection only for short span and do not move inside the plant.

Phase 2: when symptoms are visible, curative fungicides should be used. However, few products have been shown to be curative for downy mildew.

Phase 3: When sporulation is visible, eradicants should be used. Several fungicide classes such as FRAC 4 (mefenoxam), 11 (fenamidone, famoxadone), 21 (Cyazofamid), 27 (Cymoxanil), 33 (phosphite-based fungicides), 40 (mandipropamid), 44 (Biologicals), 45 (Ametoctradin) are labelled for downy mildew management.

To prevent the development of fungicide resistance, it is crucial to rotate fungicides with different modes of action. Do not apply the specific FRAC code consecutively. Also, do not make use a specific FRAC code more than twice in a growing season. Rotate the fungicides with different FRAC codes in a growing season. Fungicide resistance to FRAC 11 and 40 has been detected in MI, therefore these fungicides groups should be carefully used.

By implementing integrated management strategies, growers can effectively manage downy mildew while minimizing the impact on the environment.

Conclusion

Integrated downy mildew management requires a comprehensive approach that combines good vineyard practices, biological control methods, and sustainable fungicide usage. By implementing these strategies and integrating them into vineyard management practices, growers can enhance their downy mildew management efforts while promoting sustainability. It is essential to stay vigilant, adapt to changing conditions, and monitor the effectiveness of management approaches to achieve long-term success in downy mildew control. By prioritizing sustainability, growers can protect their grapevines, reduce environmental impact, and ensure the health and productivity of their vineyards.

Figures

Figure A.1. A plate of infected downy mildew leaves (4 photos). Photos (A & B) taken by Nancy Sharma; Photos (C&D) by Timothy Miles.

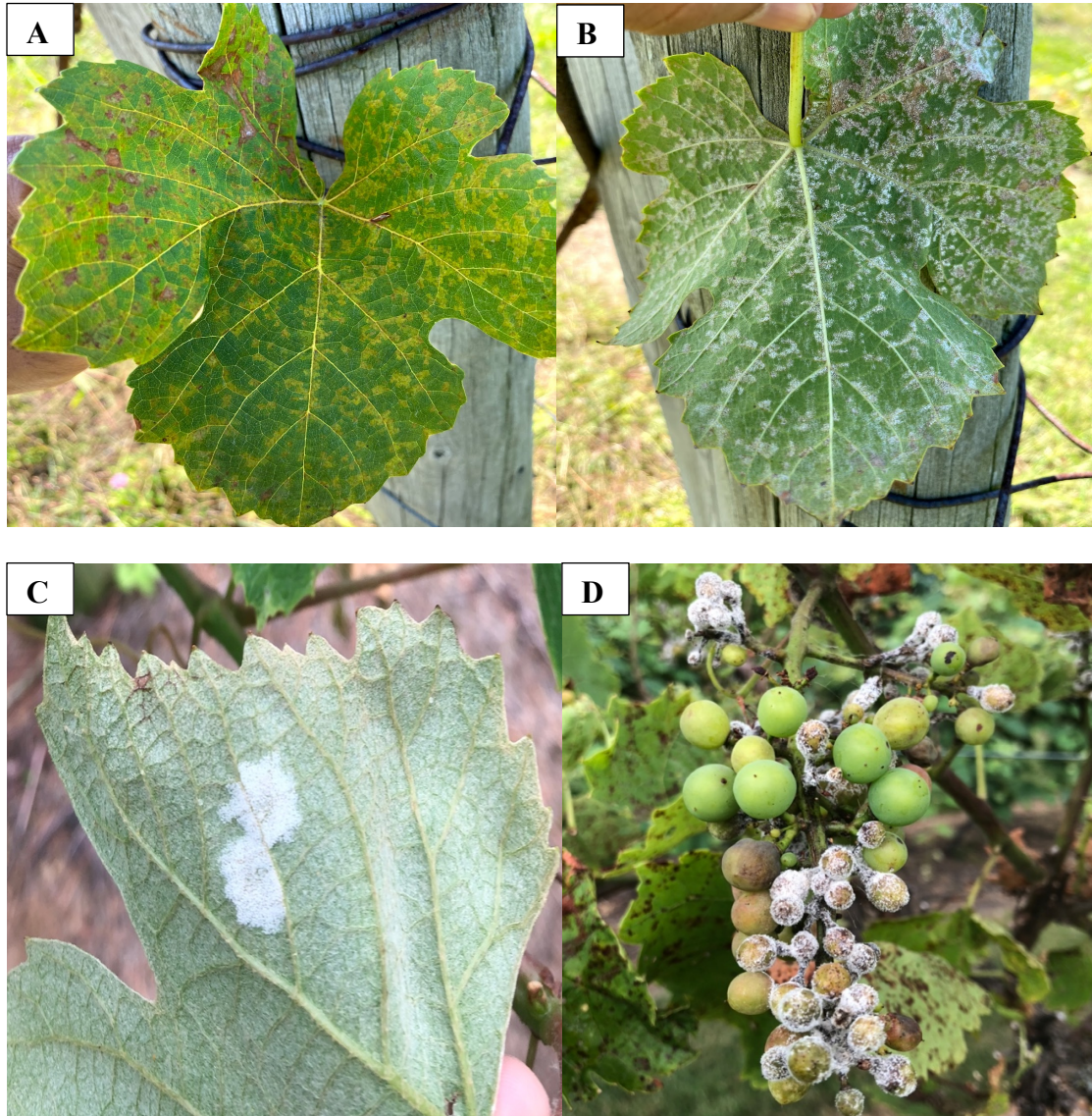
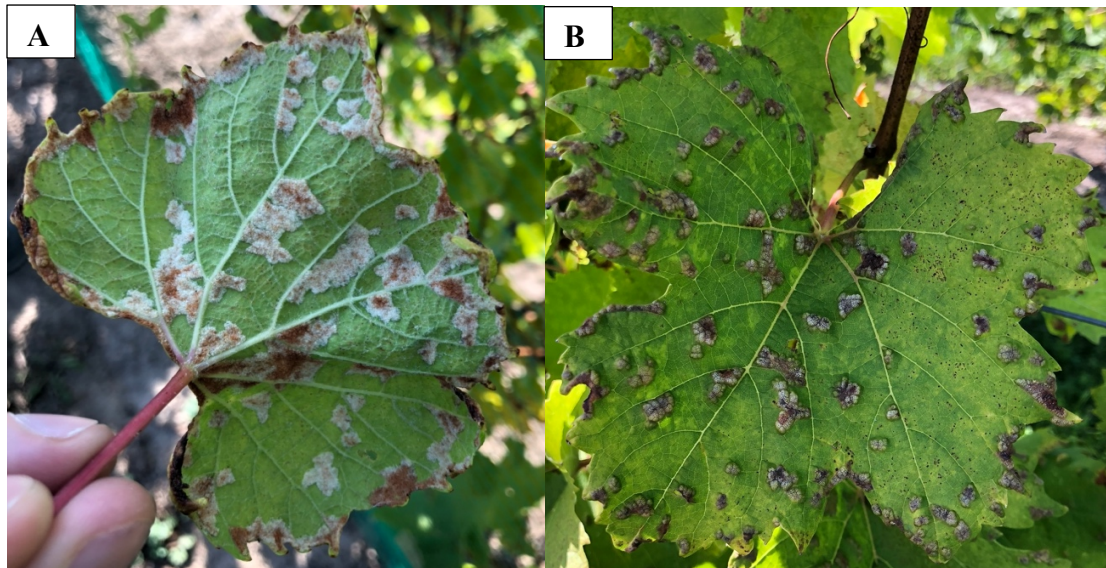


Figure A.2. Heavy defoliation of downy mildew infected leaves (Photos taken by Timothy Miles).



Figure A.3. Lookalike downy mildew infections (Erinium mites) (Photos (A&B) taken by Timothy Miles).



Tables

Table A.1. Tolerance level of various grape cultivars to downy mildew.

Slightly susceptible		Moderately susceptible	
Alden	Alwood	Alpenglow	Aurore
Baco Noir	Bluebell	Buffalo	Canadice
Beta	Brianna	Caco	Chambourcin
Cascade	Chelois	Cayuga White	Cynthiana
Colobel	Concord	Chardonel	Dutchess
Concord Seedless	Edelweiss	DeChaunac	Einset Seedless
Foch	Frontenac	Elvira	Geneva Red-7
Frontenac Gris	Interlaken	Esprit	Golden Muscat
Horizon	Himrod	Glenora	Jupiter
Isabella	Einset Seedless	La Crescent	Leon Millot
Landot 4511	Kay Gray	Landot 4511	Melody
Glenora	King of the North	Louise Swenson	Noiret
Lakemont	La Crosse	Neptune	NY81.0315.17
New York Muscat	Marchal Foch	NY76.0844.24	Seyval
Marquette	Moore's Diamond	Rosette	St. Vincent
Prairie Star	Ravat 34	St. Croix	Traminette
Sangiovese	Seneca	Swenson white	Ventura
Sheridan	St. Pepin	Vanessa	Vignoles
Steuben	Suffolk red	Venus	Villard blanc
Sunbelt	Villard noir	Vidal blanc	
Valvin muscat	Vincent		
Worden	Sabrevois		

APPENDIX B: OTHER PUBLISHED PEER-REVIEWED ARTICLES DURING PH.D. PROGRAM

1. Szymanski, S., Longley, R., Hatlen, R.J., Heger, L., **Sharma, N.**, Bonito, G. and Miles, T.D., 2023. The blueberry fruit mycobiome varies by tissue type and fungicide treatment. *Phytobiomes Journal*, 7(2), pp.208-219.
2. Morris, O.R., Chahal, K., Cregg, B., **Sharma, N.**, Wieferich, J., Sakalidis, M.L. and McCullough, D.G., 2024. Seasonal activity and phoresy rates of Nitidulid beetles (Coleoptera: Nitidulidae) captured in stands with oak wilt infections in northern Michigan, USA. *Environmental Entomology*, p.nvae101
3. **Sharma, N.**, Heger, L., Combs, D., Gold, K. and Miles, T.D., 2022. Assessment of QoI and CAA fungicide resistance of *Plasmopara viticola* populations in vineyards of the Great Lakes region in the United States of America. In *BIO Web of Conferences* (Vol. 50, p. 02011). EDP Sciences.
4. Heger, L., Martin, F., **Sharma, N.** and Miles, T.D., 2022. Advances in molecular and optical detection strategies for grape downy mildew. In *BIO Web of Conferences* (Vol. 50, p. 01005). EDP Sciences.
5. Heger, L., **Sharma, N.**, Martin, F., Miles, L., McCoy, A., Chilvers, M., Naegele, R., and Miles, T.D. 2024. Multiplexed qPCR and dPCR tools to differentiate clades of *Plasmopara viticola* in grapes. Submitted in Plant Disease.